DIRECTIONAL SOLVENT EXTRACTION DESALINATION

By

Anurag Bajpayee

BS in Mechanical Engineering, University of Missouri, 2006
SM in Mechanical Engineering, Massachusetts Institute of Technology, 2008

Submitted to the Department of Mechanical Engineering
In Partial Fulfillment of the Requirements of the Degree of
Doctor of Philosophy in Mechanical Engineering

At the

MASSACHUSETTS INSTITUTE OF TECHNOLOGY

September 2012

Author.....
Department of Mechanical Engineering
August 31, 2012

Certified By.....
Gang Chen
Carl Richard Soderberg Professor of Power Engineering
Thesis Supervisor

Accepted By.....
David E. Hardt
Chairman, Department Committee on Graduate Students

DIRECTIONAL SOLVENT EXTRACTION DESALINATION

By

Anurag Bajpayee

Submitted to the Department of Mechanical Engineering
In Partial Fulfillment of the Requirements of the Degree of
Doctor of Philosophy in Mechanical Engineering

Abstract

World water supply is struggling to meet demand. Production of fresh water from the oceans could supply this demand almost indefinitely. As global energy consumption continues to increase, water and energy resources are getting closely intertwined, especially with regards to the water consumption and contamination in the unconventional oil and gas industry. Development of effective, affordable desalination and water treatment technologies is thus vital to meeting future demand, maintaining economic development, enabling continued growth of energy resources, and preventing regional and international conflict.

We have developed a new low temperature, membrane-free desalination technology using directional solvents capable of extracting pure water from a contaminated solution without themselves dissolving in the recovered water. This method dissolves the water into a directional solvent by increasing its temperature, rejects salts and other contaminants, then recovers pure water by cooling back to ambient temperature, and re-uses the solvent. The directional solvents used here include soybean oil, hexanoic acid, decanoic acid, and octanoic acid with the last two observed to be the most effective. These fatty acids exhibit the required characteristics by having a hydrophilic carboxylic acid end which bonds to water molecules but the hydrophobic chain prevents the dissolution of water soluble salts as well the dissolution of the solvent in water. Directional solvent extraction may be considered a molecular-level desalination approach.

Directional Solvent Extraction circumvents the need for membranes, uses simple, inexpensive machinery, and by operating at low temperatures offers the potential for using waste heat. This technique also lends itself well to treatment of feed waters over a wide range of total dissolved solids (TDS) levels and is one of the very few known techniques to extract water from saturated brines. We demonstrate >95% salt rejection for seawater TDS concentrations (35,000 ppm) as well as for oilfield produced water TDS concentrations (>100,000 ppm) and saturated brines (300,000 ppm) through a benchtop batch process, and recovery ratios as high as 85% for feed TDS of 35,000 ppm through a multi-stage batch process. We have also designed, constructed, and demonstrated a semi-continuous process prototype. The energy and economic analysis suggests that this technique could become an effective, affordable method for seawater desalination and for treatment of produced water from unconventional oil and gas extraction.

Thesis Supervisor: **Gang Chen**
Title: **Carl Richard Soderberg Professor of Power Engineering**
Department of Mechanical Engineering
Massachusetts Institute of Technology

To my family

Acknowledgements

It goes without saying that no doctoral dissertation is the work of just one person. Many have contributed to the completion of this work and one short written section can never be enough to acknowledge all contributions or to express my gratitude.

First of all, I would like to gratefully acknowledge the constant guidance, and mentorship of my advisor Professor Gang Chen without whom this work would not have been possible. I have learned many lessons from Professor Chen, both professionally and personally. His unfettered support throughout my stay at MIT, his inspiring style of supervision, the high level of freedom that he allowed me, and the great faith that he showed in me now seem so critical to the completion of my doctoral work. I hope I can emulate my advisor's humility in the face of success and that my association with him will remain life-long.

I would like to thank my thesis committee member Professor John Lienhard whose expert knowledge and insight in the field of desalination and of the thermal sciences in general was extremely helpful throughout this work. I also learned from Professor Lienhard's excellent command over the art of technical writing and communication. In addition, I would like to thank Professor Alexander Mitsos, another committee member, for his thorough feedback and attention to detail which helped make this work more comprehensive.

Now emeritus professors Bora Mikic and Ernie Cravalho, two great names in heat transfer and thermodynamics, were very helpful with valuable discussions in the early stages of this work. I was also very fortunate to sit through their academic lectures as many generations of MIT graduate students had done before.

Special thanks are due to Professor Mehmet Toner of Harvard Medical School who was my masters advisor and working with whom we discovered the phenomenon of directional solubility of water in soybean oil which first led to the idea that this thesis is based upon. Professor Toner's support and mentorship, even after my graduation from his lab, have been undiminished.

I would also like to acknowledge the contribution of my undergraduate research advisor, Professor Gary Solbrekken of the University of Missouri, who was responsible for giving me my first official research project and for generating in me a predilection for the thermal sciences and engineering.

Many members of Professor Chen's Nanoengineering group at MIT have been helpful directly and indirectly. Andrew Muto and Daniel Kraemer were involved closely in the early stages of this work. Daniel was responsible for finding C.W. Hoerr et al's 1942 publication on the solubility of water in fatty acids which is heavily cited in this thesis. Michael Fowler worked with me as an undergraduate researcher and contributed very significantly. Michael's creativity, resourcefulness, and dedication during construction of the directional solvent extraction prototype were outstanding. Kevin Kleinguetl and Monica Zheng also worked with me and were helpful with conducting early solubility experiments. I would also like to thank Matteo Chiesa, Gregg Radtke, Vincent Berube, Arvind Narayanaswamy, Poetro Sambegoro, Kimberlee Collins, George Ni and many others for their help, support, and friendship.

Other members of the larger Rohsenow-Kendall Heat Transfer Laboratory, especially Prakash Govindan, Karan Mistry, and Maximus St. John helped all along through insightful discussions, generation of ideas, and sometimes direct assistance with experiments or analysis.

The mechanical engineering administrative staff at MIT is an incredible group of people without whom I suspect this great department would cease to function. I would especially like to thank Leslie Regan who has been as much a guide and mentor as she has been an administrator throughout my stay at MIT. Joan Kravit and Sucharita Berger-Ghosh have also been very helpful and a pleasure to work with. I would also like to thank the support staff of Prof. Chen's Nanoengineering group, specifically Edward Jacobson and Mai Hoang whose many small contributions throughout my stay in the group added up very meaningfully.

In addition, I would like to express grateful thanks to the Desphande Center for Technological Innovation at MIT for funding this project. Leon Sandler, the executive director of the mentor has been a mentor and friend.

At MIT one learns at least as much outside the lab as within. I was fortunate to be part of the MIT Global Startup Workshop (GSW), a highlight of my stay at MIT which took me to nine countries and gave me opportunities to work with diverse people from around the world. Specific GSW people whom I have learned from and whom I am very thankful to are Bill Aulet, Nader Darehshori, Marcus Dahlem, Pedro Pinto, Grace Chen, and Nevan Hanumara. Nevan has been one of my longest acquaintances at MIT, a remarkable colleague, and a true friend to have around. I would also like to thank other friends Eerik Hantsoo and Erica Ueda who made my stay at MIT so memorable. I trust that these bonds established here at the Institute will remain eternal.

My first few years at MIT, I lived at Ashdown House whose housemasters Profs. Ann and Terry Orlando helped make a smooth transition to the Institute and created a home away from home. I shall remain thankful for their relentless support and care.

I would also like to take this opportunity to thank my friends from back home and in Missouri, Aakash Prasad, Siddharth Agarwal, Archit Jauhari, and Ankur Shukla who have shown true support and care to this day and who I trust will remain so forever. I am undoubtedly forgetting some friends, both at MIT and back home, who deserve mention but let it be said that I'm truly grateful for having such people in my life.

My family is the strongest force in my life and has been supportive through everything that I have done. No words can express my gratitude towards my parents, Neelu and Dinesh Kumar Bajpayee, who have taught me so much, inspired me, supported me, made several sacrifices, to make me who I am. I have learned from them some of the most fundamental lessons about personal and professional life, honor and respect, relationships, spirituality and practical dealings within the human society.

My aunt and uncle, Sunita and Rakesh Bajpai have been extremely important in my life, in whose care I "grew up" for three years that I spent in mid-Missouri and without whom I would not have been able to come to the United States to pursue education. My cousins Ambar and Ashish Bajpai have been just like brothers and made my transition to the United States so much easier. My aunts and uncles, Meera and Umesh Kumar Bajpayee, and Rohini and Atal Bihari

Mishra have also provided unwavering support and I know have always selflessly wished for my success and well-being.

My grandparents Dhanvanti Devi and Ravi Shanker Bajpayee, and Shanti Mishra and the Late Shashi Shekhar Mishra are examples of simple and well grounded, but truly great people who have been sources of many of life's philosophies that I have acquired and who remain humbling sources of inspiration.

My brother, Abhishek, has been a great partner and friend since childhood to this day. We have spent countless hours planning making grand plans and indeed learned a great deal from each other. I trust we will continue to make those grand plans and give effect to at least some of them at some point in our lives.

Lastly, but perhaps most importantly, I am indebted to my wife Ambika for her friendship, love, and support in everything I do. She not only shares my ambitions but also makes it possible for me to dream. By showing the greatest level of confidence and trust in whatever I wish to pursue, she brings out the best in me and inspires me to do better than I ever thought I could. In addition to being such an ideal personal support she has also been a partner in intellectual discussions and together we have discovered answers to many questions, both scientific and philosophical. I could not have come this far without her and I am truly blessed to have her by my side. And even though many hours dedicated towards this work were taken away from her she has constantly wished for its success.

Table of Contents

List of Figures

Chapter 1 Introduction

The World Water Supply

Water is among the most vital natural resources for sustaining life on earth. Growing human populations and standards of living have created major stresses on the supply on fresh water which is struggling to meet demand. There are already about 2.8 billion people living in water stressed areas [1]. At the current growth rates we will be consuming 90% of the available fresh water by 2025, by which time the population living in water stressed areas is expected to increase to 3.9 billion[2, 3].

The current state of water stress according to a recent study by the International Water Management Institute (IWMI) is illustrated in the map in figure 1 [4]. Regions of physical water scarcity are defined as parts of the world where there is naturally not enough water to support demand. These regions are usually desert areas such as the Arabian Peninsula, Central Asia, and the Southwestern United States. Regions of economic water scarcity are where water is naturally present but cannot be made available to area's population due to lack of water supply and/or treatment infrastructure. This is often the situation in the least developed regions such as sub-Saharan Africa and parts of South Asia and Central America. Furthermore, water scarcity, is not limited to under-developed or developing regions. High water consumption, together with energy consumption, is a characteristic of countries with high standards of living. As such even the more developed regions are expected to experience increasing water shortages in the near future [5].

Figure 1. Map of World Water Stress in 2006 [6]

While fresh water stress is increasing, the oceans contain over 97% of the earth's water [6]. This water, due to high levels of salinity, is unfit for human consumption and most industrial and agricultural use. However, with affordable and effective salt removal techniques, the oceans could supply this demand seemingly indefinitely [6, 7]. Development of desalination technologies to produce fresh water from the ocean has therefore been identified as vital to meeting future demand, maintaining economic development, and preventing regional and international conflict. Techniques to remove salt from water have existed for centuries and the recent years have seen significant advances in desalination technology. While the costs of seawater desalination had reduced from over $\$9/m^3$ in the 1950s to under $\$1/ m^3$ by the early 2000s [8] for large scale plants, desalinated water remains considerably more expensive and

energy intensive than fresh water from existing sources [9]. At small scales (1 – 10 m^3/ day) the cost of seawater desalination may range from \$3/ m^3 to over \$12/ m^3 [10].

The National Research Council roadmap for water desalination sets a target of 50-80% reduction in desalination costs by 2020 which may be difficult to achieve by incremental improvements in existing technologies [9].

1.2 Energy Water Nexus & the Role of Unconventional Oil & Gas

Water and energy have always had a close inter-dependence which has become more evident with increasing demand and supply of both. Energy is required for water extraction, treatment, and transportation, while most energy production requires the use of large amounts of water [11, 12]. Furthermore, as the global energy consumption continues to increase, and energy extraction and production becomes more resource intensive, water and energy are getting further intertwined[11, 12]. This inter-relationship is nowhere more evident than in the unconventional oil and gas industry, where large amounts of water are required for well drilling and hydraulic fracturing operations, which gets contaminated and thus rendered useless for recycling or discharge [13–15].

Unconventional oil and gas is fundamentally changing the current energy landscape, especially in North America [16–18]. The game-changing potential of these reserves has been recently discovered and the North American reserves (Figure 2(a)) alone are estimated to contain over 700 trillion cubic feet (tcf) of recoverable natural gas [19], and over 1.3 trillion barrels of recoverable oil [20], the equivalent of more than 200 years of US and Canada's energy supply at current consumption rates[21]. In the year 2000, shale gas accounted for only 1% of the US

natural gas supply. By 2011, it had risen to 20%. As another example, North Dakota, home of the Bakken formation, one of the largest unconventional oil reserves, increased oil production from 30 million barrels in the year 2004 to almost 200 million barrels in 2011 [22].

Extraction of unconventional oil and gas, however, requires hydraulic fracturing of the deposits, which uses 2-4 million gallons of water per fracturing job [23] . Between 20 and 50% of this water returns to the surface as highly contaminated water that is 2-8 times more saline than seawater and which may contain heavy metals and radioactive isotopes among other solutes. In addition, contaminated water is also "produced" during the lifespan of the well operation and could be as saline as saturated brine. This flowback and produced water is unfit for discharge or re-use in subsequent fracturing operations. Improper disposal of this water may negatively affect the environment by polluting rivers or municipal water supplies. In many states, fracking has met fierce public opposition. New York State currently has a moratorium on shale gas drilling due to water related environmental concerns. Nova Scotia, home to large shale deposits, has also recently banned drilling due to water contamination issues. Furthermore, large volumes of water need to be transported to and from the fracturing sites. This increases traffic levels, pollution, and discomfort of the local population.

Water treatment issues are thus among the greatest barriers gating the growth and expansion of the unconventional oil and gas industry. The ability to treat and recycle flowback water during fracturing and produced water during well operation would reduce the need to transport fresh water to the well sites and contaminated water away from the sites. This would translate into significant cost reduction as well as further reduce public discomfort and opposition to hydraulic fracturing. It must be noted that due to the very high salinity of produced

water, desalination forms the most expensive part of the treatment process. State-of-the-art technologies to treat flowback and produced water are recognized by the industry as being either ineffective, uneconomical, or both. Another desirable characteristic of any produced water treatment process is high recovery ratios. In fact, industry surveys suggest that an effective produced water desalination system would likely be required to demonstrate recoveries greater than 70%.

The alternative to handling this water therefore consists of transporting it away from the well production sites and injecting in deep saltwater injection wells [24]. Contaminated water transportation infrastructure is expensive, complicated, and often consists of transporting the water away from the production sites in certified hazardous waste tankers. Industry surveys revealed that these disposal costs depend on the distance of injection wells from the production sites and can range from \$2-3/ bbl. (\$12-18/ m^3) in North Texas to over \$10/ bbl. (> \$60/ m^3) in Pennsylvania (Figure 2(b)) Development of new desalination technologies is thus critical to enable the continued growth of unconventional oil and gas.

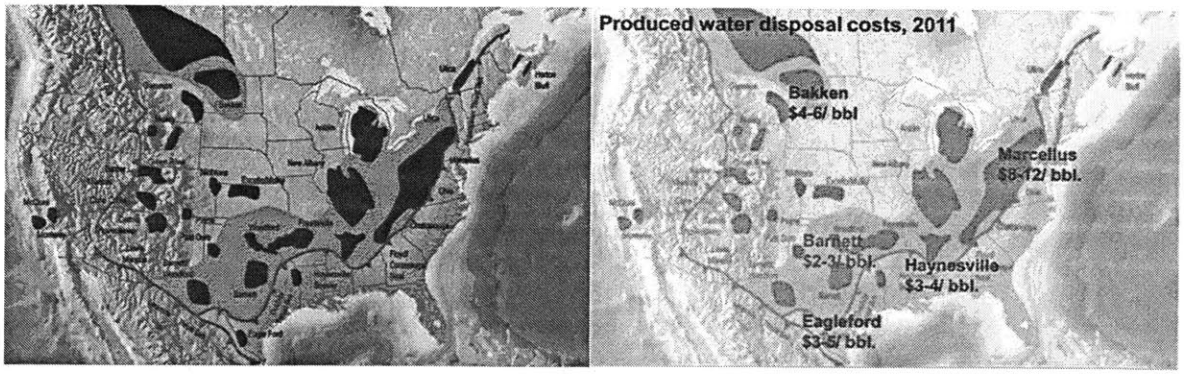

(a) (b)

Figure 2. (a) Map of North American shale basins [25] and (b) produced water handling costs

1.3 Desalination State of the Art

Desalination technologies have witnessed significant advances in the last half a century. As discussed earlier the cost of seawater desalination has reduced by almost nine times between the 1950s and the early 2000s. The total capacity of seawater desalination plants worldwide has also increased almost two hundred and fifty times in this period, from 0.110 million m^3/ day to over 28 million m^3/ day by 2005 [9]. Most of this existing capacity is in reverse osmosis (RO) or multi-stage flash distillation plants, the two most popular desalination technologies [6], [26]. Despite these advances and economic gains, water from desalination remains considerably more expensive than that from freshwater sources [9].

Most desalination technologies can be classified as membrane processes or evaporative processes. Reverse Osmosis (RO) is a membrane-based technique [27–30] which has rapidly gained popularity due to better efficiency than thermal processes, the convenience of operating electrically without heating, and the scale flexibility of operating as small scale units or large scale plants. In the RO process the saline solution is passed through a semi-permeable membrane which allows water to pass through but holds back the salt ions. In order to drive flow against the natural osmotic gradient, a high pressure is required to overcome the osmotic pressure. Energy required to raise this process is supplied electrically. Electricity is high grade energy and in this case accounts for 44% of the process cost [9] for sea water desalination. Seawater RO electricity consumptions have been reported to be between 3 kWh/ m^3 and 8 kWh/ m^3 [31–34]. As a comparison the minimum work required for seawater desalination at about 40% recovery is 1.06 kWh/ m^3 [35]. In addition to the cost of energy, another challenge is that RO membranes are prone to fouling and may require frequent replacement [6]. Furthermore, at very high TDS levels

of produced water and due to the presence of other impurities, RO membranes may foul faster, and may not be able to withstand the higher pressures need to overcome the increased osmotic pressure. These higher pressures would also necessitate much higher energy inputs, thus increasing the overall cost of the process.

Forward osmosis (FO) [36], [37] is a new membrane method which claims to offer better efficiency and lower cost but is yet to be demonstrated to do either; being a membrane based technology, FO may also be ineffective at the high TDS levels. Recent research on high-flux membranes based on carbon nanotubes [38] can potentially reduce the energy consumption, and on alternative electrical-based desalination technology such as ion concentration polarization in nano-devices [39] can potentially avoid the fouling.

Electrodialysis (ED) is another electricity drive membrane-based technique wherein an electrical potential difference is used to transport charged particles (salt ions) across an ion-exchange membrane from saline water to relatively pure water [31], [32]. In ED, however, the energy consumption rises quickly with increasing salt concentrations, and the process is therefore limited to desalination of brackish waters (TDS <0.5%) [40].

Multistage flash distillation (MSF) is a thermal desalination process based on evaporating water and condensing the vapor back into pure water [9, 10] . Evaporation requires large amounts of energy to overcome the latent heat of water [12]. Energy consumptions of MSF processes have been reported to be between 60 kWh/ m^3 and 90 kWh/ m^3 [31], [33], [34], [41–43]. In an MSF process, heat released during condensation is re-used in the next stage, which is at a lower vapor pressure, partially offsetting the large amount of energy required in the evaporation process. The temperatures required are usually above 90 °C which are energy

intensive to attain and the thermal energy accounts for almost half of the process cost [9]. All evaporative systems may suffer from scaling caused by evaporation of water and the resulting crystallization of scaling agents such as calcium. This scaling can increase greatly when high TDS water is involved and significantly reduce the system lifetime. In addition, MSF systems, are large due to the many evacuated stages, and cannot be scaled down for produced water treatment volume requirements.

A similar process is Multi-effect distillation (MED) [44], often regarded as the oldest desalination process other than simple distillation [45]. MED is also an evaporative process that operates at slightly lower temperatures (about 70°C) than MSF. The main difference between MED and MSF is that in MED, the seawater evaporates at the heat transfer surface, whereas in MSF the water is only preheated within the heat exchanger and evaporates from a flow of brine in each stage [46]. Another evaporation-based technique is to condense the vapor by mechanical vapor compression and to use the latent heat of condensation to pre-heat a part of the feed water (MVC/ MVR) [47]. MVC systems are mostly small-scale and industry interviews suggest that this is the only evaporation technology that is being tested for produced water treatment. Vapor compressors, however, require electrical energy input and their costs can be prohibitive for most applications.

Humidification-dehumidification (HDH) is a promising thermal desalination technology which mimics the natural rain cycle. HDH has witnessed considerable development and progress recently especially for small scale and solar driven systems [48–50]. This technology, however, is yet to be demonstrated at a significant scale outside the laboratory.

1.4 Thesis Outline

This thesis describes the conception, design, demonstration of concept, and further development of Directional Solvent Extraction (DSE), a new low temperature, membrane-free method of water desalination. Directional solvent extraction works by dissolving water from a saline or otherwise contaminated solution into a directional solvent by increasing its temperature. The directional solvents extract the water phase but rejects salts and other contaminants. These salts are then separated and removed. Upon cooling back down the water precipitates out of the solvent, is recovered as purified water, and the solvent is reused. Importantly the solvent does not itself dissolve into water and the recovered water therefore contains a negligible amount of residual solvent.

Chapter 2 describes the basic concept of directional solubility, introduces the directional solvents and lays down the fundamentals of the proposed technology development. Chapter 3 explains in detail the proof of concept through a bench-top batch process demonstrating effective desalination and accompanying calculations which show the energy and exergy consumption of the process. Chapter 4 furthers the understanding of directional solvent extraction by describing experiments to characterize process parameters and assessing their effects on the performance through observations and analyses. Chapter 5 introduces a potential improvement upon the basic process by describing the demonstration of a multi-stage directional solvent extraction method which shows increased recovery ratios. Chapter 6 describes the design, construction, and testing of a semi-continuous process prototype which is imperative to bringing this technology closer to field application. Chapter 7 discusses a detailed economic analysis which suggests that directional solvent extraction could be an economically viable technology to treat produced

water. Chapter 8 summarizes the work, outlines major conclusions, highlights outstanding questions, and identifies potential future directions.

Chapter 2 Fundamentals of Directional Solvent Extraction

2.1 Directional solubility

Ideas of solvent extraction for desalination were explored by Hood and coworkers in the 1950s who used secondary and tertiary amines as solvents [51], [52]. These solvents, however, were limited to treatment of water with low salinities of up to 5000 ppm (seawater is about 35000 ppm, produced water can be up to 300,000 ppm) [52]. Most importantly, these were discounted due to significant residual presence of solvents in the recovered water [53], i.e. while the solvents dissolved water they were themselves found to dissolve in water in significant amounts (e.g. 3-13% by weight). Furthermore, no significant understanding of the molecular interactions of water, solvent, and salt was developed, and the progress on this subject remained marginal for almost half a century. Lazare and the Puraq Company attempted to commercialize solvent based desalination for two decades from the 1960s through the 1980s [54–57]. Lazare's process, however, involved synthetic solvents (such as a copolymer of vinyl pyrrolidone and vinyl acetate), which necessitated high costs, and also required the use of membranes to prevent salt from mixing with the solvents. Significant development was impeded due to these factors as well as the lack of investment and market interest [58].

The mutual solubility as discussed above is the generally expected behavior. However, in some rare cases pairs of materials do exhibit directional solubilities where one substance dissolves the other but without dissolving in the other. This thesis reports directional solvents

that dissolve water while rejecting water soluble salts, and, are themselves insoluble in water. Certain edible oils such as soybean oil and medium to long chained carboxylic acids possess this unusual ability to dissolve water while rejecting other water soluble substances such as sodium chloride. This solubility of water in the carboxylic acid has also been seen to increase with temperature [59–62], another required quality for the proposed thermally driven directional solvent extraction to function.

Carboxylic acids dissolve water due to the presence of the carboxylic acid group (-COOH) at their chain ends. The highly polar C=O and O-H groups facilitate the formation of hydrogen bonds with water molecules. While this chain end is hydrophilic the rest of the fatty acid molecule is hydrophobic. As such, the reduction of chain length results in higher solubility of water in the acid but also higher solubility of the acid in the water. The lowest carboxylic acids, such as formic and acetic acid, are miscible with water, but as the chain length increases the solubility of both substances in each other decreases significantly. In addition, salts such as sodium chloride exist in solution in ionized form. A polar solvent is therefore likely to dissolve salt ions. As the carboxylic acid chain length increases, its non-polar nature also increases, thus reducing the solubility of salts in the acid.

Stephan Kress [63] and Tengfei Luo [64] have further investigated the theoretical aspect and provided explanations for such directional solubility behavior. An illustration of hydrogen bond formation between water and decanoic acid is shown in figure 3.

One way to describe the solubility behavior is by considering the solvation free energies of water in a solvent, solvent in water, and salt in solvent and water. Solvation free energy is equivalent to the work required to transfer a molecule from its bulk phase into a solution.

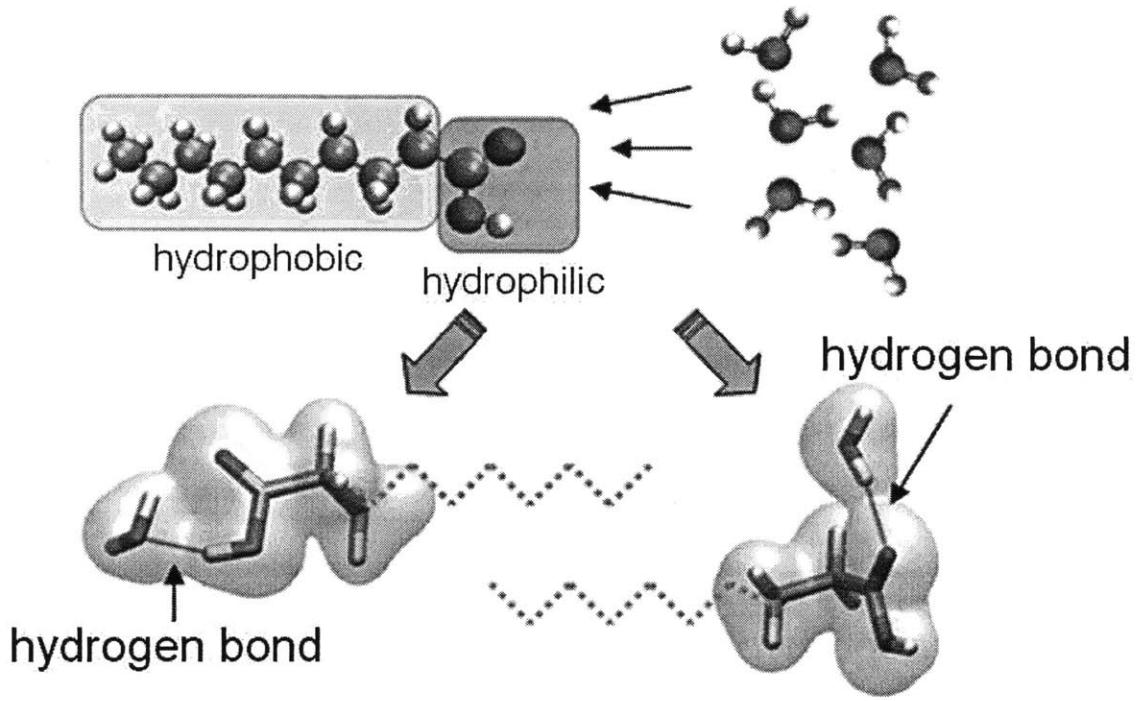

Figure 3. Illustration of hydrogen bond formation between water and decanoic acid; carbon is depicted by blue color, oxygen by red, and hydrogen by white

To describe solubility from this thermodynamic point of view, the free of energy of solvation was calculated using molecular dynamics simulation and the thermodynamics integration (TI) [64], [65] method for water-decanoic acid-sodium ion interaction and the results are shown in Figure 4. As may be seen the solvation free energy of water decreases as it goes from water among other water molecules to water in decanoic acid, i.e. a water molecule is more stable in a decanoic acid solution (-8.46 Kcal/mol) than in its bulk phase (-6.33 Kcal/mol), suggesting that water is likely to dissolve into decanoic acid. However, as the concentration of water in the acid increases, it becomes difficult for successive water molecules to dissolve as

seen from the increasing free energy values (4% water in acid: -7.44 Kcal/mol and 6% water in acid: -6.03 Kcal/mol).

A water molecule in saline solution (3.5% NaCl w/w) has lower solvation free energy (-7.13 Kcal/mol) than in pure water (-6.33 Kcal/mol) due to the extra Coulombic interaction with salt ions. As a result, water molecules from saline droplets are expected to dissolve into decanoic acid until equilibrium is attained when the free energy of water in saline solution becomes equal to that of water in decanoic acid. This equilibrium state corresponds to the solubility limit of water in decanoic acid, beyond which additional energy is required to dissolve more water. An increase in temperature could supply this energy and allow further dissolution of water.

A decanoic acid molecule, however, is much less stable when dissolved in water (-9.82 Kcal/mol) than in its amorphous bulk phase (-16.04 Kcal/mol), suggesting that decanoic acid is unlikely to dissolve in water. Furthermore, salt ions are unlikely to diffuse into decanoic acid from the saline water due to the large free energy barrier (e.g. -99.60 Kcal/mol [66] for a sodium ion in water compared to -72.44 Kcal/mol for a sodium ion in decanoic acid).

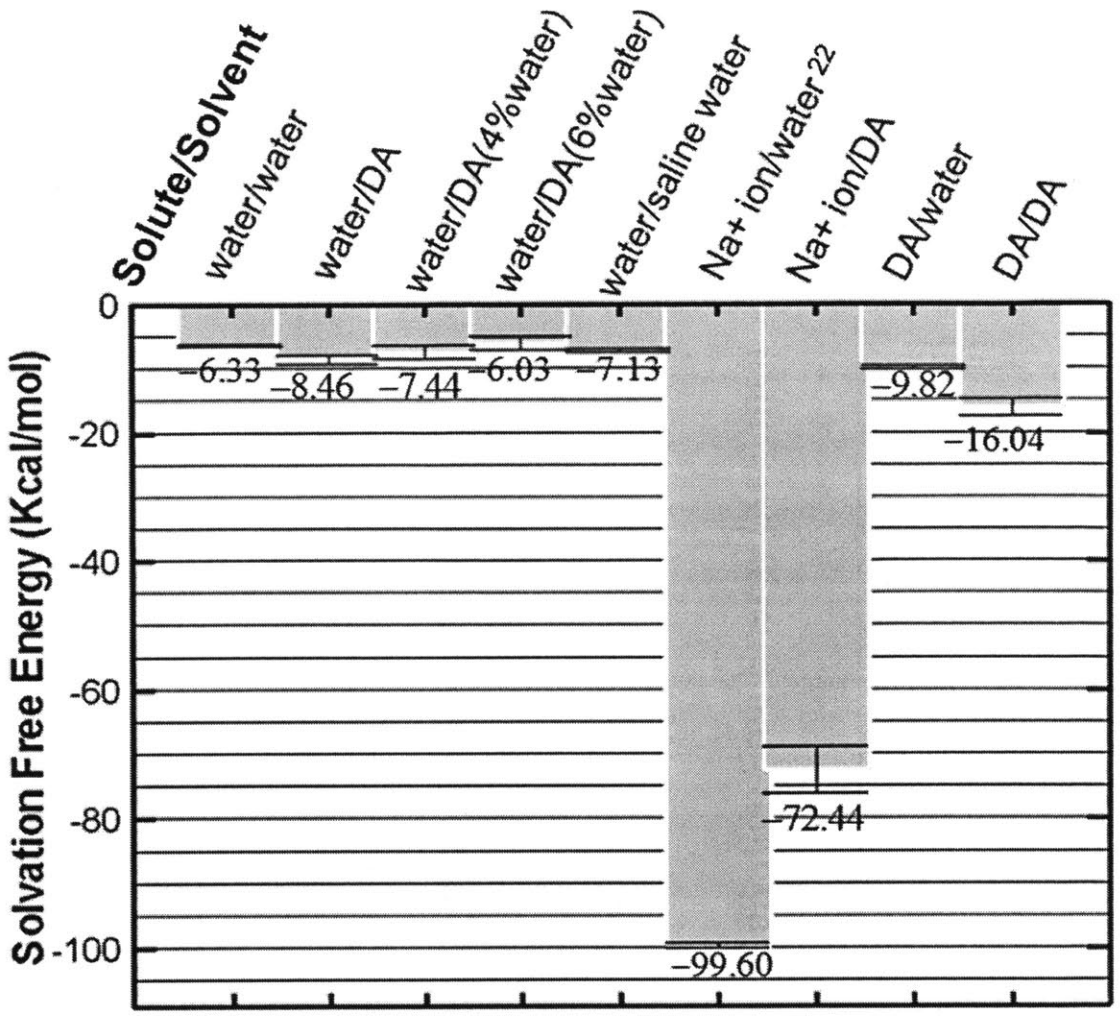

Figure 4. Free energy of solvation of various solute-solvent pairs calculated by the thermodynamic integration (TI) method. (DA = decanoic acid)

2.2 Directional solvents

In summary, to be an effective candidate for this process a solvent must possess the following characteristics:

Water is soluble in the solvent

Water solubility in the solvent is a function of temperature

Salts do not dissolve in the solvent

The solvent does not dissolve in water

In addition, it is ideal if the directional solvent is also non-toxic, naturally occurring, inexpensive, and abundant.

Our first directional solvent was in fact soybean oil. Soybean oil dissolves water while being insoluble in water [61], [62]. Soybean oil is also inexpensive, abundant, and edible. The solubility of water in soybean oil, however, is extremely low (0.3% v/v or 0.33% w/w at 25 °C) [61], [62]. Therefore, while soybean oil does behave as a directional solvent and an effective desalination can be demonstrated with it, the low solubility of water, necessitates large volumes of soybean oil to be used, thus leading to large system sizes and heating energy requirements. Soybean oil is mainly a mixture of oleic acid ($CH_3(CH_2)_7CH{=}CH(CH_2)_7COOH$), alpha-linoleic acid ($C_{18}H_{30}O_2$), linoleic acid ($C_{18}H_{32}O_2$) and palmitic acid ($CH_3(CH_2)_{14}CO_2H$) [67].

In search of a better solvent, experiments were then conducted on hexanoic acid ($C_5H_{11}COOH$) which dissolves about 5.5% w/w water at 20 °C and almost 10% w/w at 55°C

[60]. Hexanoic acid, however, dissolves in water to a non-negligible extent (968 ppm w/w [68]) and is more corrosive and foul-smelling than desirable. Furthermore, hexanoic may dissolve some salts as well due to its shorter chain length, as will be discussed in the experimental section. Hexanoic acid thus lies at the lower end, in terms of chain length, of carboxylic acids that form effective directional solvents.

Moving up the carboxylic acid chain, we found decanoic acid ($CH_3(CH_2)_8COOH$) to dissolve a maximum of about 3.8% w/w water at 34 °C, increasing to 5.9% at 80 °C. Earlier estimation by Hoerr et. al. [60] suggests the same trend and similar solubility values. Yet the solubility of decanoic acid in water is negligible, with a theoretically predicted value of 28 ppm at 27 °C, as described in the chapter 3.2 and reported values between 30 ppm [69] and 150 ppm [70] at 25 °C. The batch process experiments, as discussed in the chapter 3.2, confirmed these ranges by measuring a residual decanoic acid content of 36 ppm in the recovered water. To put this in perspective, whole milk contains about 1300 ppm of decanoic acid [71]. Decanoic acid is also used as a food preservative, and is relatively inexpensive, characteristics which make it an effective directional solvent.

Another effective directional solvent is octanoic acid ($CH_3(CH_2)_6COOH$), on which extensive experimentation was conducted, and which was found to dissolve 1.8% w/w water at 25 °C increasing to almost 5.2% at 80 °C. The solubility of octanoic acid in water, however, is only 680 ppm [68]. This level is considered non-toxic as whole milk contains over 1080 ppm of octanoic acid [71]. Octanoic acid is also used as a food preservative and is inexpensive and readily available. Having been found to be the most suitable for this application, decanoic acid and octanoic acid were used as the primary directional solvents in this work.

Thermophysical properties of water, decanoic acid, and octanoic acid are used extensively in this work and are listed for reference in Table 1.

Table 1. Thermophysical properties of water, decanoic acid, and octanoic acid (Data from Yaw [68] and Verschueren [72])

	Density* (kg/m^3)	Viscosity (cP) @ 25 °C	Specific heat* (J/ kg K)	Molecular weight (g/ mol.)
Water	1000	0.89	4180	18.02
Decanoic acid	893	5.86**	2351	172.26
Octanoic acid	910	5.25	2200	144.21

*Density and specific heat change only slightly with temperature and are assumed to be constant
**Viscosity at 33 °C as decanoic acid solidifies at about 29 °C

2.3 Design of the Directional Solvent Extraction process

In order to accomplish effective salt removal from saline water using directional solvents the process cycle must consist of (1) forming a saline water-in-solvent emulsion (2) heating the emulsion to a temperature greater than ambient so that pure water is dissolved into the solvent (3) brine-phase settling and removal (4) cooling down the solvent to ambient temperature to precipitate out pure water. Based on this concept an experimental directional solvent extraction batch process was designed as illustrated in Figure 5:

(a) A directional solvent is heated in a beaker and maintained at 40 – 95 °C and the saline solution is added while stirring. Care is taken to ensure that the temperature is higher than ambient to facilitate recovery of water but less than 100 °C to prevent vaporization of

water. Phase change could lead to undesired evaporation and loss of water as well as cause excessively high energy consumption.

(b) Upon mixing the beaker turns cloudy indicating emulsion formation. The water droplets formed within the solvent scatter light and give the contents a cloudy appearance.

(c) Upon mixing for some time, the cloudiness in the beaker reduces indicating dissolution of some water. This is due to the water droplet sizes and numbers reducing resulting in the reduced light scattering.

(d) After stirring is stopped, the remaining brine settles gravitationally, leaving clear solvent and the dissolved water above. At this stage the solvent has dissolved the pure water phase and separated it from the salts.

(e) The clear contents are decanted into conical tubes maintained at room temperature. Care is taken to ensure that the brine or crystallized salts do not get transferred to the conical tubes and get mixed with the pure water.

(f) Cloudiness reappears in the conical tubes as the contents cool and pure water precipitates out resulting in the re-appearance of water-in-solvent emulsion droplets.

(g) Pure water separates gravitationally leaving clear the clear solvent above a forming a clear water layer at the bottom.

(h) This purified water is separated from the bottom of the tube and the solvent is reused. Again, care is taken to ensure that solvent is not lost or gets collected together with the recovered water sample.

The mixing and separation times throughout the process can be critical and are discussed in chapter 4. Description of this design may also be found in peer reviewed publications [64], [73] and US and international patents [74].

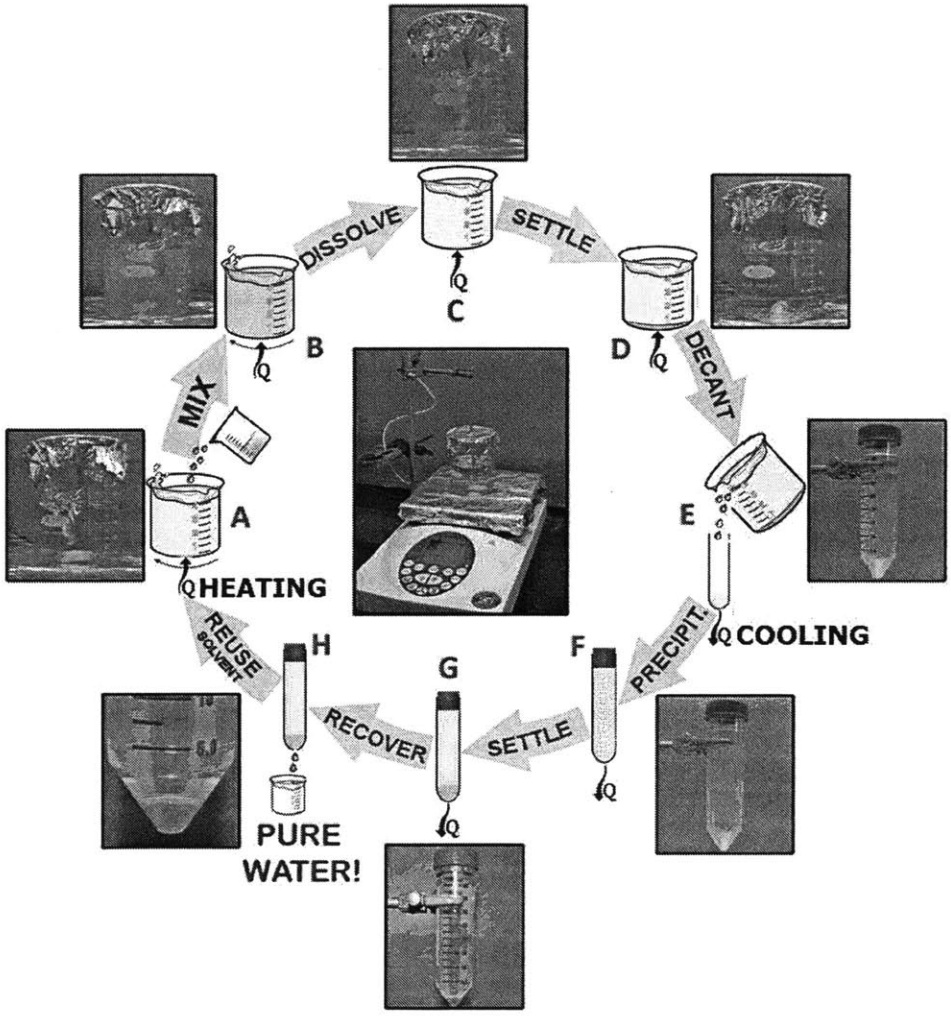

Figure 5. Illustration of the cyclic directional solvent extraction experimental batch process

2.4 Advantages of Directional Solvent Extraction

Motivation for deeper understanding of directional solvent extraction (DSE), its laboratory demonstration, and further development as a continuous, commercially viable process stems from its apparent advantages as seawater desalination and produced water treatment technology.

Membrane-free operation: By being a membrane-free process, DSE eliminates a source of capital and maintenance cost. Membrane-based methods are also unsuitable for produced water treatment where high TDS feed water is encountered. By circumventing the use of membranes DSE promises to become one of the very few currently known techniques to handle a wide TDS range up to and including saturated brines.

Low temperature thermal process: By operating at low temperatures, DSE paves way for utilization of low grade waste heat which may reduce or eliminate the energy costs involved with desalination. In fact, as discussed in the rest of this thesis, DSE has been shown to function effectively with a heat source of temperature as low as 40 ℃, lower than any known thermal desalination process. It must be noted, however, that the nature of DSE does not restrict its use to low temperatures. In case of produced water treatment on oil and gas drilling or operating sites, where waste heat might be difficult to scavenge, DSE can be fueled by a natural gas heat source which is often readily available.

Simple, inexpensive machinery: Perhaps the most significant advantage of DSE stems from its simplicity as a desalination process. The concept is easy to understand, develop, and operate. The batch process design discussed and the continuous process prototype discussed later

in this thesis do not require the use of require the use of expensive or complicated machine. Most the equipment needed is readily available or manufacturable using inexpensive material. These characteristics could lead to low capital costs as well as low operation and maintenance overhead.

Chapter 3 Technology Demonstration

3.1 Experimental Demonstration of Directional Solvent Extraction

After iterations with soybean oil and hexanoic acid, decanoic acid was selected for the first demonstration of concept of directional solvent extraction. Decanoic acid, as mentioned earlier, possesses the required characteristics of a directional solvent and is inexpensive, non-toxic, and readily available. The following section describes the experimental procedure.

Directional Solvent preparation: It is important that the solvent (decanoic acid) is saturated with water at the lower process temperature. If pure solvent is used, water will dissolve into the solvent upon heating, but when the solvent is cooled back down not all the earlier dissolved water will be precipitated as some water will remain dissolved in the solvent according to water solubility in solvent at the lower process temperature. Therefore, pure decanoic acid was first mixed, by stirring, with excess distilled water in a beaker maintained at the lower process temperature (34 ℃ in this case). Some water dissolved into the decanoic acid and the un-dissolved water was allowed to settle to the bottom of the beaker gravitationally. The decanoic acid was carefully decanted off the top and now, being saturated with water at 34 ℃, was set aside for use in the experiment.

Feed-water sample preparation: Seawater contains 3.5% (35,000 ppm) of total dissolved solids (TDS) of which over 85% is formed by sodium (Na^+) and chloride (Cl^-) ions [75]. In addition, seawater also contains smaller amounts of biological matter. To replicate seawater artificially to a first degree a 3.5% w/w solution of sodium chloride (Morton ® table-

salt non-iodized) was made in distilled water by adding measured amount of salt and water and mixing in a beaker using a magnetic stir bar.

Experimental run: 200 g of decanoic acid [CH3(CH2)8COOH, >98% Kosher, Sigma Aldrich, St. Louis, MO] were taken in a beaker and heated on a digital heating and stirring plate (HS 40, Torrey Pines ® Scientific, Carlsbad, CA), as shown in Figure 6.

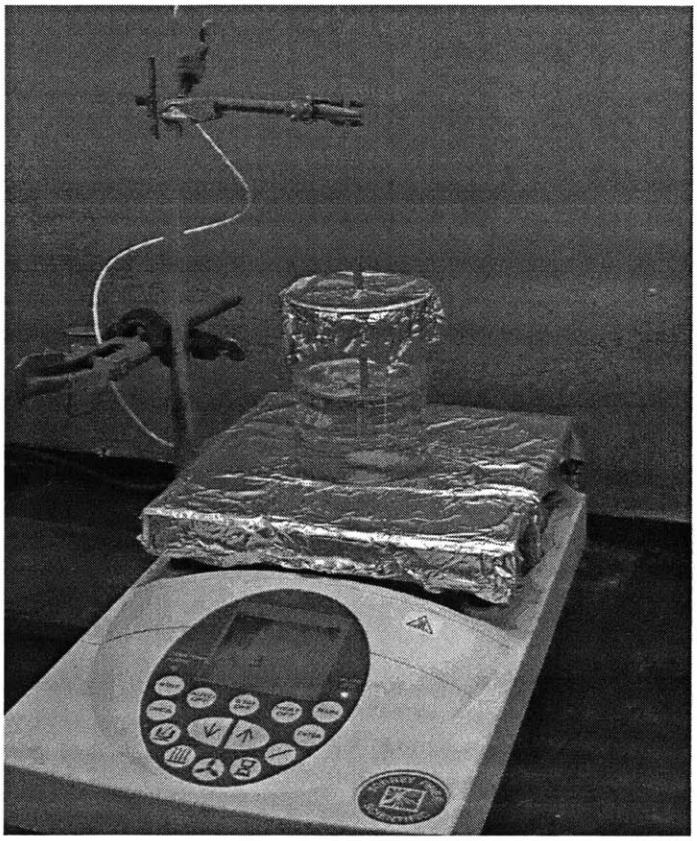

Figure 6. Heating decanoic acid on a heating and stirring plate with feedback temperature control

Over different runs decanoic acid was heated to temperatures between 40 and 80 °C (Fig. 4A). Once the temperature of the decanoic acid became steady, 10 g of the prepared salt solution were added to the beaker and mixed with the solvent by stirring using a magnetic stir bar rotating

at 600 rpm. An emulsion was observed to form immediately and the clear beaker contents turned cloudy (Fig. 4B). In this first instance, stirring was continued at the elevated temperature for 60 minutes. During this time some water dissolved into the solvent, leaving behind smaller water droplets highly concentrated with salt. This dissolution and droplet shrinking was visually evident as the emulsion becomes clearer (Fig. 4C).

Upon stopping the stirrer, the un-dissolved water droplets (brine), being denser than decanoic acid (density: 893 kg/ m^3), gravitationally separated to form a layer of brine at the bottom of the beaker, leaving a clear layer of decanoic acid containing dissolved water above (Fig. 4D). The brine droplets were allowed to settle over 60 minutes in this instance, even though visual appearance suggested that the separation only took a few seconds.

The clear upper layer in the beaker was then decanted by carefully pouring off into conical tubes maintained at 34 °C in a water bath (Fig. 4E). It must be noted at this point that decanoic acid has a freezing point of about 30 °C [76] and the lowest process temperature was maintained at 34 °C to stay clear of phase change issues. This freezing point in the ambient may be considered to be a drawback of using decanoic acid as a solvent.

The cooling of decanoic acid reduces the solubility of water in it facilitating the precipitation of pure water droplets. The contents of the conical tubes appeared to turn cloudy again providing visual evidence of this precipitation (Fig. 4F). These tubes were allowed to stand at 34 °C for 72 hours to allow for complete gravitational separation of the water from the acid. Droplets of the precipitated water are expected to be on the order of 10 μm diameter in size as shown by Kress [63]. Kress' experiments were conducted with octanoic acid as the solvent

which has similar properties as decanoic acid. The significance of these droplet sizes and their effect on separation time is discussed in chapters 4 and 6.

When most of the precipitated water had separated, two clear layers made of water (bottom) and decanoic acid (top) were observed (Fig. 4G). This separated, presumably desalinated water was recovered by piercing a hole in the bottom of the conical tubes and carefully draining into another tube (Fig. 4H). Care was taken to ensure that no solvent was collected along with the precipitated water.

The salinity of the recovered water was measured using an ATAGO® salt meter (Atago USA Inc., Bellevue, WA). This salt meter measures salinity by actually measuring the conductivity of the solution which varies with ionic TDS content. The weights of the recovered water,W_p, and of the decanoic acid (solvent), W_s, in the conical tubes were also recorded to calculate yield of pure water per unit volume of decanoic acid used.

To determine the effect of TDS on water yield from the process, the saline solution was replaced with distilled water and the above steps, except salinity measurement were repeated.

Measurement of solubility of water in decanoic acid: To obtain a baseline estimate of solubility of water in decanoic acid at the lower process temperature (34 °C), 10 g of decanoic acid was maintained at 34 °C and while stirring distilled water was added to it in increments of 0.2 g, 0.1, and several increments of 0.01 g until no more water dissolved after stirring for 180 minutes. The solubility of pure water at higher temperatures was calculated by adding the yield at a given temperature to the solubility limit at 34 °C.

Measurement of residual solvent content: Samples of water recovered from the process were collected and allowed to stand for 72 hours. These samples contained residual salt content as well as some residual solvent. Their salt content was measured and the absolute weight of the salt present in a given weight of the sample was thus calculated. In order to check whether any residual decanoic acid was left in the recovered water, a small sample (137.595 mg) of water was weighed on a UMT 2 scale (Mettler Toledo, Columbus, OH) and heated on a VWR 575 Hot Plate (VWR Scientific, Westchester, PA) to 120 °C. This was done to boil off the water until a brownish white residue was left behind. The remaining sample contents were weighed again. After evaporation the remaining contents must be the residual decanoic acid and the residual salt. Since the amount had been measured previously, the total weight of residual decanoic acid and its fraction in the water sample was calculated. The same process was repeated with a small sample (504 mg) of water recovered from octanoic acid and the residual octanoic acid content was recorded.

Experiments with octanoic acid: Upon successful demonstration with decanoic acid, as discussed in the results section, octanoic acid was tested as a directional solvent. Octanoic acid has the advantages of having a higher solubility of water in solvent, greater change in solubility with temperature, as well as a lower freezing point of about 15 °C. Its disadvantages include the higher amounts in which it dissolves in water as well as slightly higher toxicity as compared to decanoic acid. Such issues, however, may not be important if the desalination process is for treating produced water which will be reused for drilling or other industrial uses. The experimental procedure described for decanoic acid was repeated with octanoic acid, except that the lowest process temperature was the lab ambient temperature of about 25 °C, and highest

temperature was taken to 90 °C. The amount of solvent (octanoic acid) used was reduced to 100g per run while the feed water was kept the same at 10g, thus the feed to solvent ratio increased to 10% in the case of octanoic acid. This was done because octanoic acid dissolves more water than decanoic acid.

A slight experimental improvement over decanoic acid runs was made by replacing the experimental beaker covered by aluminum foil, with a conical flask capped by a rubber stopper, as shown in Figure 7. This was done to prevent any evaporation of water which might result in loss of water that would otherwise be recovered as product at the end of the process. It is recommended that this setup be used if these experiments are repeated or added on to.

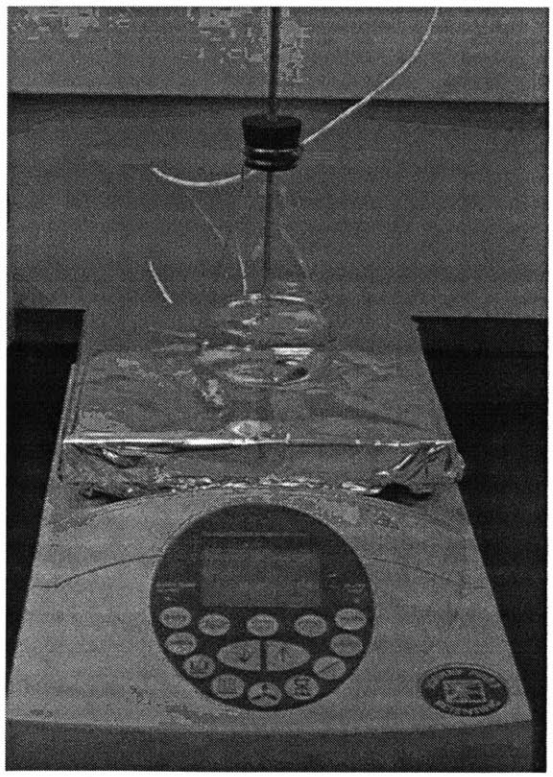

Figure 7. Conical flask with cork stopper used for stirring and mixing to prevent water loss due to evaporation

Process characterization (discussed in chapter 4) revealed that the mixing and brine separation times used for decanoic acid were too long and they were thus reduced to one minute each. Furthermore the gravitational separation was replaced by separation using a lab centrifuge (Fisher Scientific ® Marathon 21000). The samples were centrifuged for 60s at relative centrifugal force of 5000 g. The samples were centrifuged after they were allowed 60 minutes to cool to ambient temperature. As expected, the centrifugation drastically enhanced the speed of separation of the recovered water from the solvent. All experimental runs were repeated three times.

Experiments with high TDS water: In order to test the effectiveness of Directional Solvent Extraction as a method to treat produced and flowback water from unconventional oil and gas extraction, it became imperative to use high TDS water as feed samples. Produced water from unconventional oil and gas operations often contains TDS levels of between 60000 ppm and 300,000 ppm, of which over 80% could be dissolved sodium and chlorides [77]. A 10% w/w (100,000 ppm) solution of sodium chloride in de-ionized water was prepared to simulate produced water. It must be noted that produced water may contain organics as well as residual oils which might need to be removed in a pre-treatment process. Using these high TDS samples, experiments were conducted with octanoic acid as the directional solvent and using the protocol described in the preceding text.

Additionally, to test the limits of feed TDS levels that the DSE process can handle, a saturated brine was prepared (>29%, 290000 ppm NaCl w/w), and used as feed for the experimental process. Saturated brines were not treated experimentally in as much detail as the other feed samples, but a first order evidence for DSE's ability to extract water from them was

sought by looking for salt crystallization upon addition of the saturated brine to octanoic acid at 90 °C.

Experiments with field samples of flowback water: To further verify the efficacy of DSE, actual field samples were obtained from flowback water ponds in Kennetcook, Nova Scotia with the help of Dillon Consulting, London, Ontario. These samples were measured for starting TDS, run through the DSE process with octanoic acid, and the recovered product water was measured for final TDS content.

3.2 Experimental results & analysis

Product salinity: A primary process performance parameter is the salinity or total dissolved solids (TDS) content of the product water. This product salinity for a starting feed TDS of 3.5% (seawater) and 10% (produced water) was measured for all samples and is depicted in Figure 8, as a function of highest process temperature for both decanoic acid and octanoic acid. Salinity of recovered water varied between 0.07% (700 ppm) and 0.11% (1100 ppm) for decanoic acid. Experiments with octanoic acid resulted in higher product salinities of between 0.17% (1700 ppm) and 0.32% (3200 ppm). Experiments with octanoic acid and 10% TDS feed water resulted in even higher product salinities of between 0.37% (3700 ppm) and 0.51% (5100 ppm). According to WHO standards drinking water must not have more than 0.1% (1000 ppm) [9] salinity while EPA standards define drinkable water as containing less than 0.05% salt (500 ppm) [78]. Other standards define up to 0.14% (1400 ppm) salinity as acceptable [53]. In theory, given that no salt is expected to dissolve in the solvent, the final salinity of the recovered water should be zero. The remaining salt is attributed to the possibility that not all the un-dissolved

brine salt had separated before decantation and eventually mixed with precipitated water. The higher degree of salinity in the product water from octanoic acid trials may be attributed to the shorter brine separation times used in those experiments (1 min vs. 60 min). Salinities greater than the drinking water limits may not be an issue for produced water application. Industry surveys suggest that operators may be able to use water with salinity as 1% (10000 ppm) for reuse and water with salinity up to 0.3% (3000 ppm) may be stored in open ponds or transported without treating them as hazardous waste.

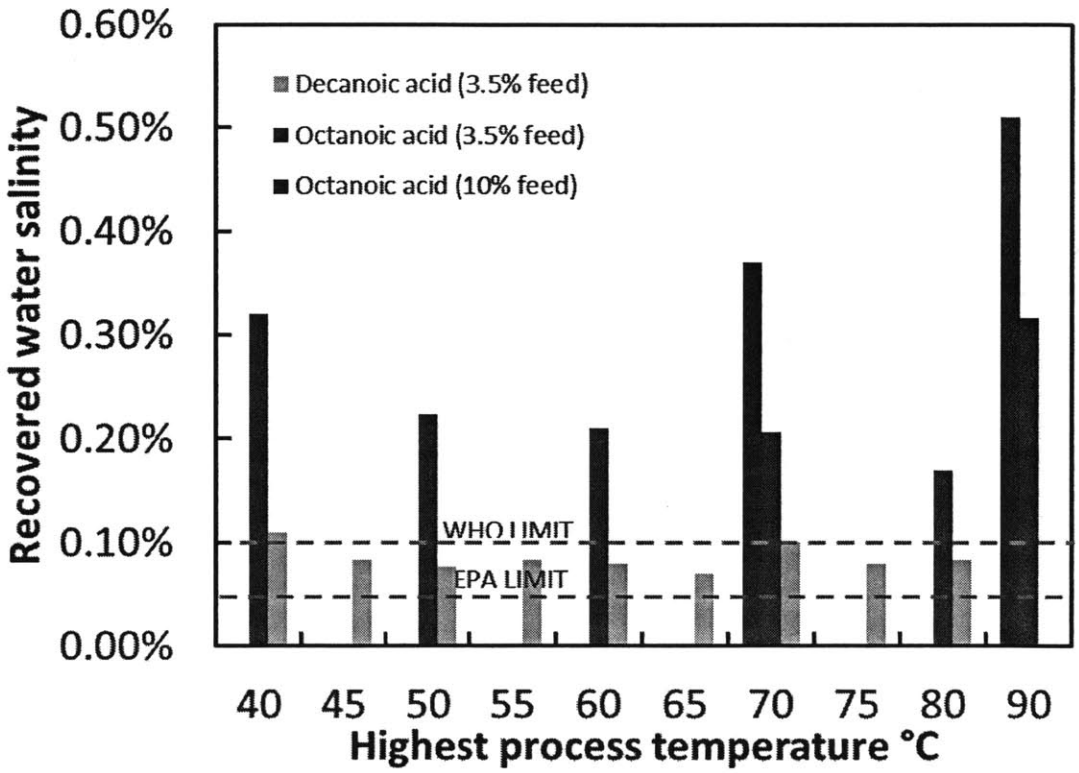

Figure 8. Salinity of product water from experimental runs with Decanoic acid and Octanoic acid for feed salinity of 3.5% and 10% (only with Octanoic)

Water yield: Water yield for this process refers to the weight of purified product water obtained at the end of the cycle per unit weight of the solvent used. In mathematical terms,

$$Y = \frac{W_p}{W_s} \tag{1}$$

Yield is thus a measure of system energy efficiency and the economics. A higher water yield per volume of solvent implies lower energy consumption due to the smaller amount of solvent requiring heating. In addition, higher water yield would also mean smaller system sizes thus reducing capital costs. Water yield, however, should not be confused with the recovery ratio,

$$R = \frac{W_p}{W_f} \tag{2}$$

which is the weight of water recovered, W_p at the end of the cycle per unit weight of the input feed water, W_f.

From the weights of product water and the solvent used the yield was calculated for the experimental runs at different temperatures. The product water yield from decanoic acid experiments is depicted in Figure 9. The experimental yield for both saline water and pure water is superimposed with the yield calculated from Hoerr et al.'s solubility estimations [60]. The lower yield for saline water (3.5% TDS) as compared to pure water are due to the strong interactions of water with the dissolved salt and the resulting difficulty of extracting water from a salt-water solution. As represented by the calculations depicted in Figure 4, the solvation free energy of water in a 3.5% aqueous salt solution (-7.13 kcal/ mol) is lower than that of water in bulk pure water (-6.33 kcal/ mol) and therefore if the water salinity is increased the yield would

be expected to reduce further. As may also be noted, the experimental yield for pure water conforms to that the theoretically expected yield.

The product water yield was similarly calculated for experiments with octanoic acid and is depicted in Figure 10. In this plot the yields from 10% TDS feed water are also depicted. The yields at various temperatures are compared with those expected from solubility measurements done by Kress [63] as well the solubility predicted by Hoerr [60]. The data point of pure water yield at 90 °C was not presented by Kress and was added by conducting further experiments. Similar to results from decanoic acid experiments the yields for 3.5% TDS water are lower than those from pure water. The yields for 10% TDS water are even lower due to even more salt concentration in the solution. The yields from decanoic acid are also superimposed in the plot for comparison. Octanoic acid dissolves more water and has greater absolute change in the solubility of water in acid for a given temperature increase. Thus, as expected, it may be noted that the product water yield from octanoic acid are almost twice of those from decanoic acid.

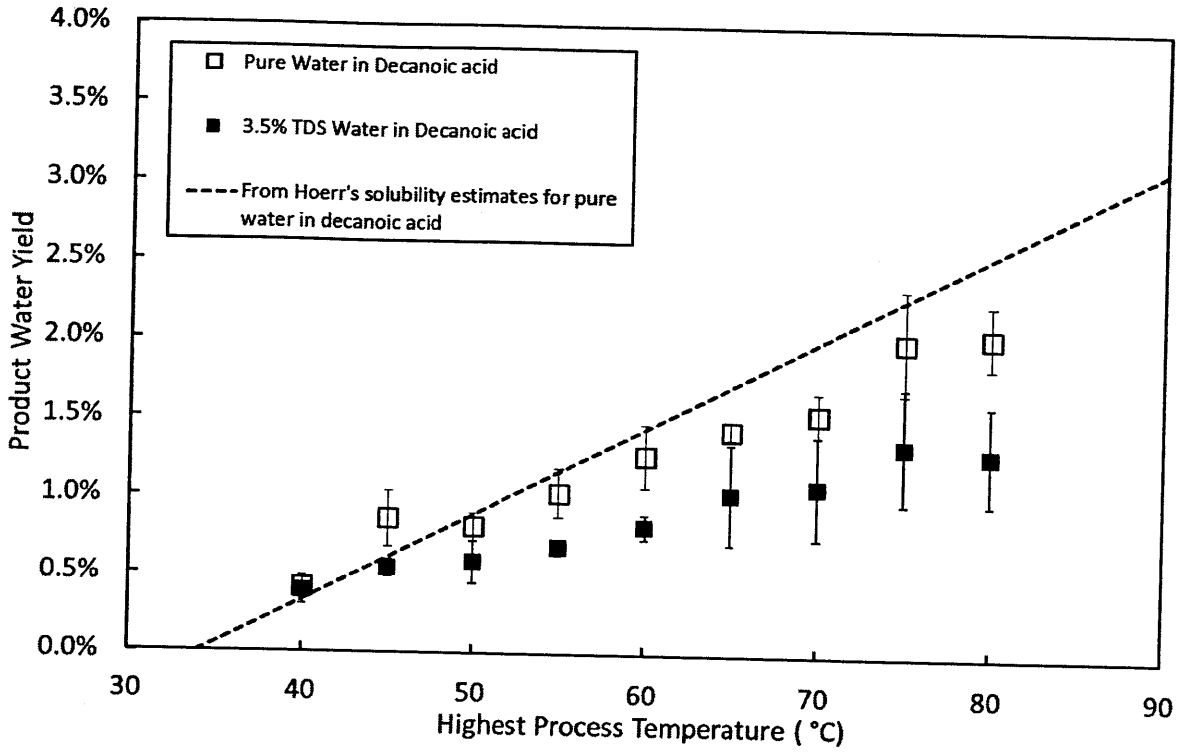

Figure 9. Product water yield as function of temperature for when pure water is dissolved in decanoic acid and recovered upon cooling (open square), 3.5% TDS water is dissolved in decanoic acid and pure water is recovered (filled circle), and calculated from Hoerr's solubility estimates [60] of pure water in decanoic acid (broken line)

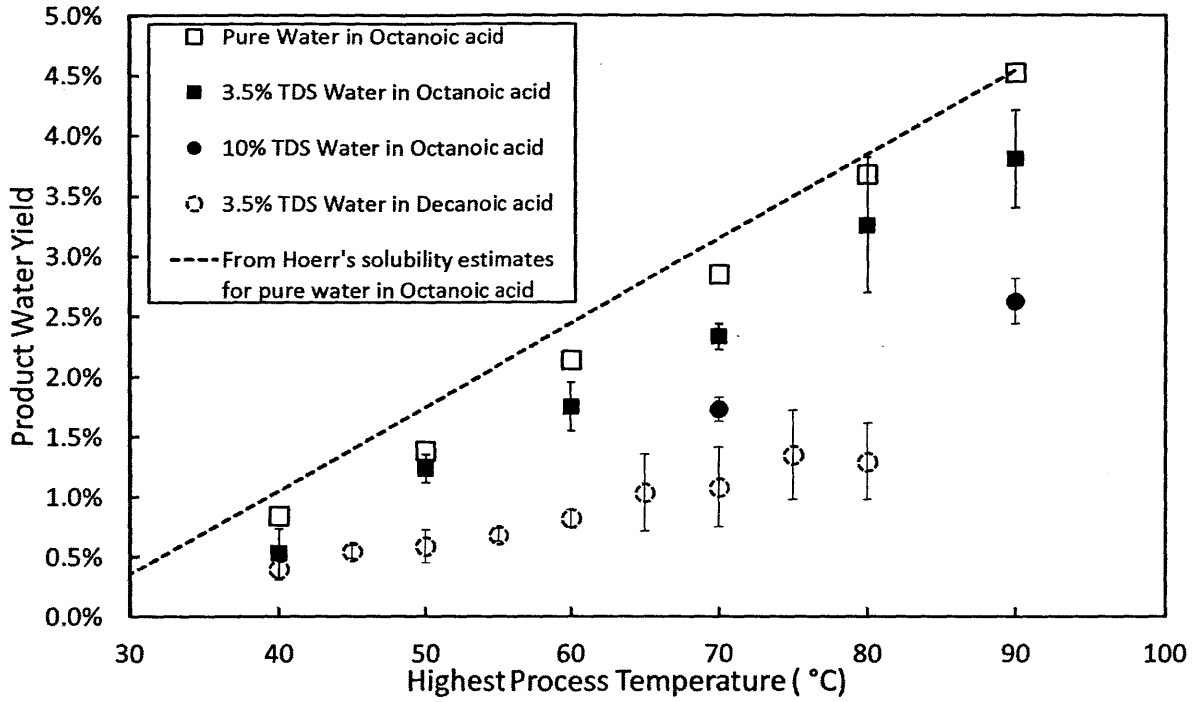

Figure 10. Product water yield as a function of temperature for when pure water is dissolved in octanoic acid and recovered upon cooling (open square), 3.5% TDS water is dissolved in octanoic acid and pure water is recovered (filled square), and calculated from Hoerr's solubility estimates [60] of pure water in octanoic acid (broken line). Broken circles are yields when 3.5% TDS water is dissolved in decanoic acid and fresh water recovered.

Saturated brines: Upon mixing the prepared saturated brine (>290,000 ppm NaCl) with octanoic acid maintained at 90 °C, solid salt was visually observed to crystallize out immediately. After stirring was stopped and the solvent decanted, the white residue of sodium chloride was observed at the bottom of the beaker as shown in Figure 11. DSE thus promises to be the only method other than phase change that can extract water from saturated brines. This is significant because certain oilfields, especially in the Bakken formation of North Dakota, do produce saturated brine.

Field produced water samples: The produced water samples obtained from Kennetcook, Nova Scotia were measured to have a starting TDS content of 58333 ppm (5.83%). The product water was recovered at a 72% recovery ratio and a final TDS content of 3667 (0.37%) ppm.

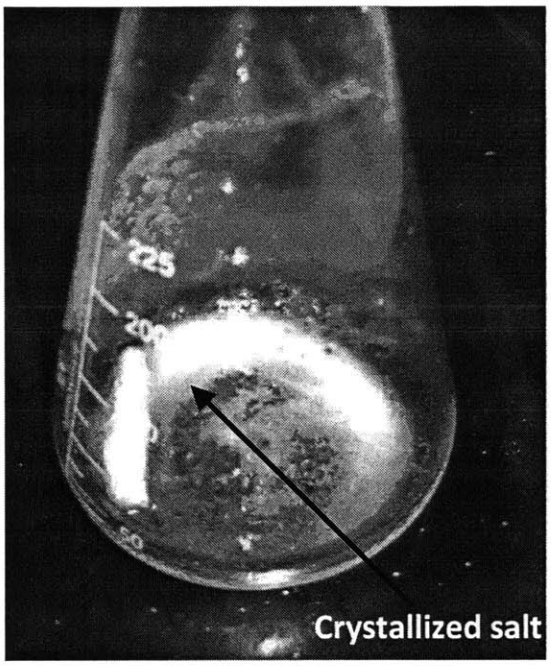

Figure 11. Salt crystallized out of saturated brine (29% NaCl in distilled water) upon mixing with Octanoic acid at 90 °C

Residual solvent: From a 137.595 mg sample of product water of 0.06% w/w sodium chloride content, 0.087 mg of residue was found to be left after boiling off the water. Since the salt (0.06%) is expected to be about 0.082 mg, the remaining residual weight of decanoic acid is equal to 0.005 mg. This gives a residual solvent concentration of 36 ppm by weight. This is in the experimentally reported range of 30 ppm [69] to 150 ppm [70].

Theoretically, the molarity of decanoic acid in a dilute solution of decanoic acid in water is given by the following expression [79],

$$S = \exp(-\Delta G/RT)/V_m \tag{3}$$

where ΔG is the difference in the free of decanoic acid in bulk and that of decanoic in water, R the ideal gas constant, T the temperature and V_m the molar volume of bulk amorphous decanoic acid. By taking $\Delta G = 16.04 - 9.82 = 6.22 Kcal/mol$, $V_m = 191.96 cc/mol$, and $T = 300K$, as calculated by Luo [64] it was found that $S = 1.6391 \times 10^{-7} mol/cc = 2.8192 \times 10^{-5} g/cc\_water = 28.192 ppm$. This theoretically predicted value of 28 ppm is also similar to the experimentally obtained value of 36 ppm.

A sample of water recovered from octanoic acid was similarly treated. From a 504 mg of sample product water of 0.13% w/w sodium chloride content, 0.95 mg of residue was found to be left after boiling off the water. Since salt (0.13%) is expected to be about 0.655 mg, the remaining residual weight of octanoic acid is 0.295 mg. This gives a residual octanoic acid concentration of 585 ppm by weight. This value is in reasonable agreement with reported solubility of octanoic acid in water of 680 ppm [68].

Energy and Exergy Analysis: The energy consumption of the batch process described above was calculated and then extrapolated to estimate the energy requirement of a continuous industrial process at a directional solvent desalination plant. The primary energy consumption is the heat required to elevate the temperature of the water-in-decanoic acid emulsion. It is assumed

that heat exchangers with a typical effectiveness of 0.8 will be used to recuperate energy [80] in the plant, thus the industrial energy requirement will be 20% of that in the laboratory.

To appreciate the benefit of using low temperature sources, it is imperative to calculate the exergy consumption, which is the maximum theoretical work that can be extracted, at Carnot efficiency, from the heat used to fuel the process and provides for fair comparison with the power requirements of reverse osmosis and multi-stage flash processes. The experiments were cycled between a lower temperature of T_o (34 °C for decanoic acid and 25 °C for octanoic acid) and a varying highest process temperature (T_H). Thus, the energy consumption of the process for heating up the decanoic-saline solution mixture per unit mass of recovered fresh water is simply given by:

$$Q_{lab} = (\frac{C_S}{Y_w} + C_W)(T_H - T_o) \tag{4}$$

where Y_w represents fresh water yield and C_S and C_w represent the specific heats of the directional solvent and water respectively.

In a continuous industrial process heat is exchanged between streams of decanoic acid, one of which is cooling down and the other is heating up. The amount of energy lost in this heat transfer will be determined by the effectiveness (η_{HE}) of the heat exchanger, and the energy requirement will then be given by:

$$Q_{ind} = Q_{lab}(1-\eta_{HE}) \tag{5}$$

In this case a practical heat exchanger effectiveness of 0.8 is assumed [80].

The theoretical energy consumption for when pure water is used as feed is expected to remain relatively constant. This becomes evident if equations (4) and (5) are modified for pure water. In this case, since the solubility of water in the solvent is a linear function of temperature, the yield Y_w becomes a linear function of the difference between the highest and lowest process temperature, and may be expressed as

$$Y_w = K(T_H - T_O) \tag{6}$$

where K is a constant. Equation (4) may thus be written as,

$$Q_{lab} = \frac{C_S}{K} + C_W(T_H - T_o) \tag{7}$$

The energy consumption thus varies linearly with increasing highest process temperature, T_H, but, $\frac{C_S}{K} \gg C_W$, the variation is quite insignificant.

The calculated thermal energy consumption for directional solvent extraction with decanoic acid as solvent is depicted in Figure 12. The graph shows calculated energy consumption for the experimental yield obtained for pure water in decanoic acid and 3.5% TDS water in decanoic acid, as well for the theoretical expected yield from Hoerr's solubility estimates [60]. As may be noted the experimental thermal energy consumption lies in the range of 350 - 480 kWh_{th}/ m^3. The theoretically expected energy consumption varies linearly and only slightly between 250 kWh_{th}/ m^3 and 265 kWh_{th}/ m^3. The experimental results for pure water experiments conform to theory. The experimental energy consumption for 3.5% TDS water is higher than the theoretical value due to the reduced product water yield per unit weight of the solvent when salt is present in feed water. Thermal energy consumption values are higher than

other thermal desalination techniques such as multi-stage flash distillation (MSF) which lie in the range of 60 – 90 kWh_{th}/ m^3 [31], [33], [34], [41–43].

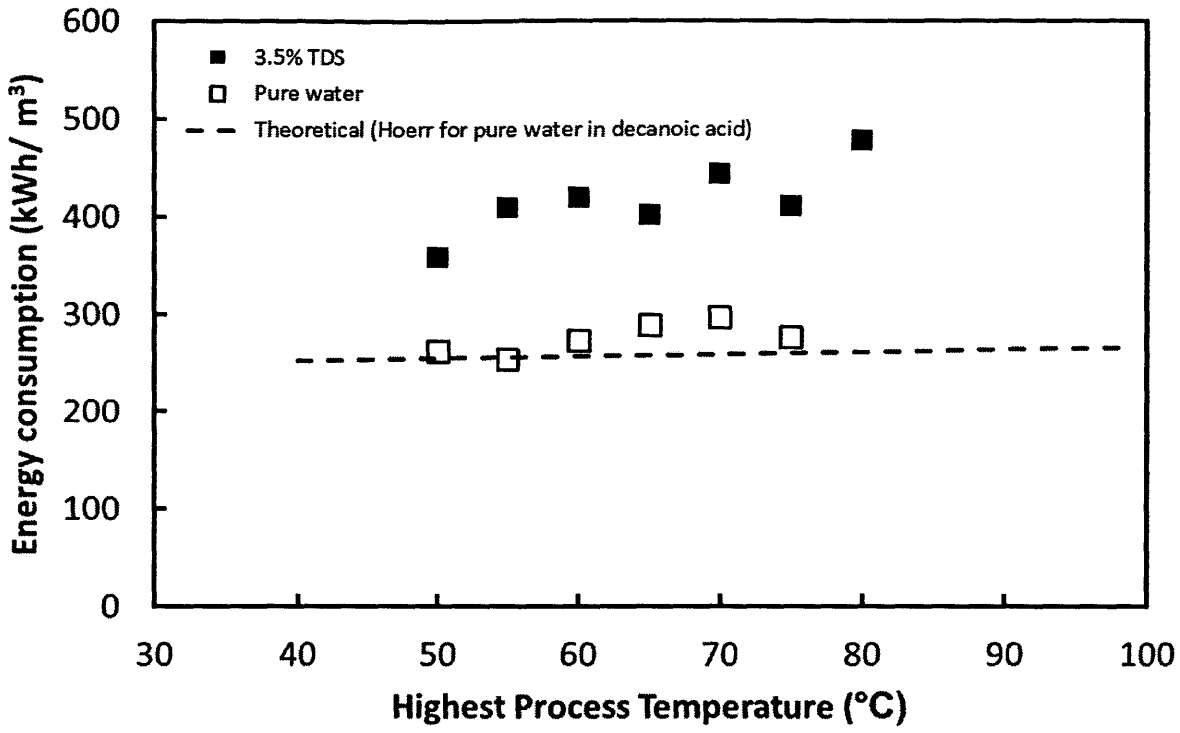

Figure 12. Thermal energy consumption as a function of the highest process temperature for directional solvent extraction (DSE) for when pure water is dissolved in decanoic acid and recovered upon cooling (open square), 3.5% TDS water is dissolved in decanoic acid and pure water is recovered (filled square), and calculated from Hoerr's solubility estimates [60] of pure water in decanoic acid (broken line). The lowest process temperature in these experiments was 34 °C; calculations assume a heat exchanger effectiveness of 80% [80]

Gained Output Ratio (GOR), defined by the following expression, is a parameter used for comparing the performance of thermal desalination technologies,

$$GOR = \frac{\dot{m}h_{fg}}{\dot{Q}} \tag{8}$$

where $\dot{m}$ is the water throughput rate of the desalination process, h_{fg} is the latent heat of vaporization of water and $\dot{Q}$ is the rate of thermal energy consumption. GOR indicates ratio of the latent heat of vaporization of water to the actual thermal energy required to produce a unit volume of desalinated water from a process. The experimental energy consumption for DSE with decanoic acid puts its GOR value between 1.3 and 1.8, which is lower than that for MSF generally expected in the range of 6 to 10.

To appreciate the benefit of using low temperature sources it is imperative is calculate the exergy consumption, i.e. the maximum work that can be derived from the energy consumed. This exergy consumption depends on the highest process temperature and is given by:

$$E = Q_{ind}(1-\frac{T_O}{T_H}) \tag{6a}$$

Equation (6a) may be re-written as

$$E = (\frac{C_S}{Y_w} + C_w)(1-\eta_{HE})(T_H - T_o)(1-\frac{T_O}{T_H}) \tag{6b}$$

This gives the maximum amount of work that may be extracted from the heat used to fuel the process and provides for fair comparison with the power requirements of RO and MSF processes.

The calculated exergy consumption as a function of the highest process temperature for decanoic acid as directional solvent is depicted in Figure 13, and compared with literature values for reverse osmosis [31–34] and multi-stage flash distillation [31], [33], [34], [41–43]. The

broken line represents the theoretically expected exergy consumption based on solubility of water in decanoic acid.

Note that reverse osmosis uses electrical power and the actual heat consumption from which this power is derived is also shown. Exergy is expressed in kWh/ m^3. Expression in kWh/ 1000 gal may be found in an externally published version of this work [73]. As may be noted, the exergy requirement of the directional solvent extraction with decanoic acid as solvent is similar or lower than that of multi-stage flash for highest process temperatures below 70 °C and similar or lower than that of reverse osmosis for highest process temperatures below 50 °C. It is important to emphasize that reverse osmosis uses electricity which is derived from a high temperature heat source as such by burning coal or natural gas or from nuclear power. The graph in Figure 13 also depicts the exergy of the actual heat consumed for electricity generation. Directional solvent extraction is thus the only membrane-less process that can be fueled by very low temperature energy sources.

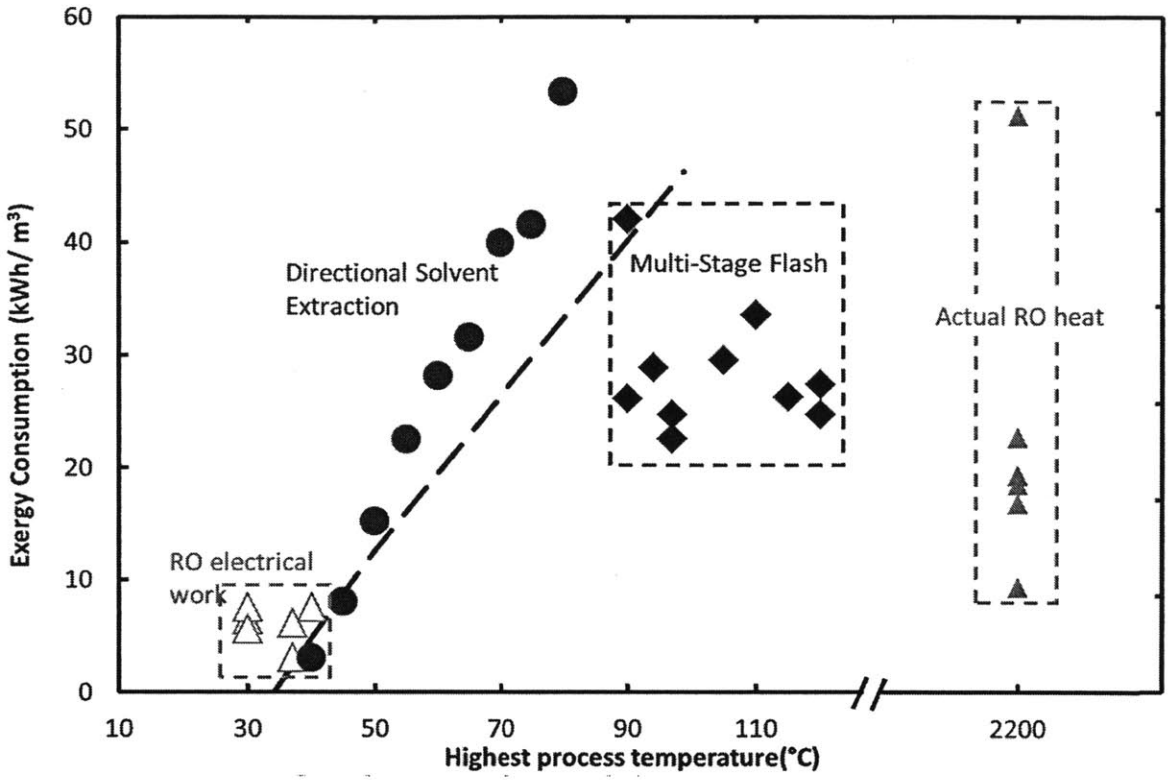

Figure 13. Exergy consumption as a function of the highest process temperature for directional solvent extraction (DSE) with decanoic acid compared with literature values for reverse osmosis (actual electricity consumption) [31–34], and multi-stage flash [31], [33], [34], [41–43]. Also shown is the theoretically expected exergy consumption for decanoic acid based Hoerr's solubility estimates (broken line) [60]. Note that reverse osmosis uses electrical power and the exergy of the actual heat consumption from which this power is derived is also shown

Thermal energy consumption was similarly calculated for octanoic acid as the directional solvent. Results are depicted in Figure 14. For octanoic acid as directional solvent the thermal energy consumption is seen to lie in the range of 220 – 260 kWh/ m^3 for 3.5% TDS feed, and in the range of 318 – 319 kWh/ m^3 for 10% TDS feed. The theoretically expected energy consumption varies linearly and only slightly between 178 kWh/ m^3 and 190 kWh/ m^3. As may be noted the calculated energy consumption values for experiments with pure water conform

well to the theory. For saline water the energy consumption, as stated above, is expected to be higher due to the reduced product water yield when salt is present in the feed. The energy consumption values are lower than those for decanoic acid but still higher than those for multi-stage flash.

The experimental GOR for seawater DSE with octanoic acid lies between 2.4 and 2.9, lower than MSF GOR of 6 to 10. However, given that directional solvent extraction can be run at lower temperatures and the equipment used for a continuous industrial process may be simpler and inexpensive, this technology promises to offer significant economic gains as is discussed in chapter 7.

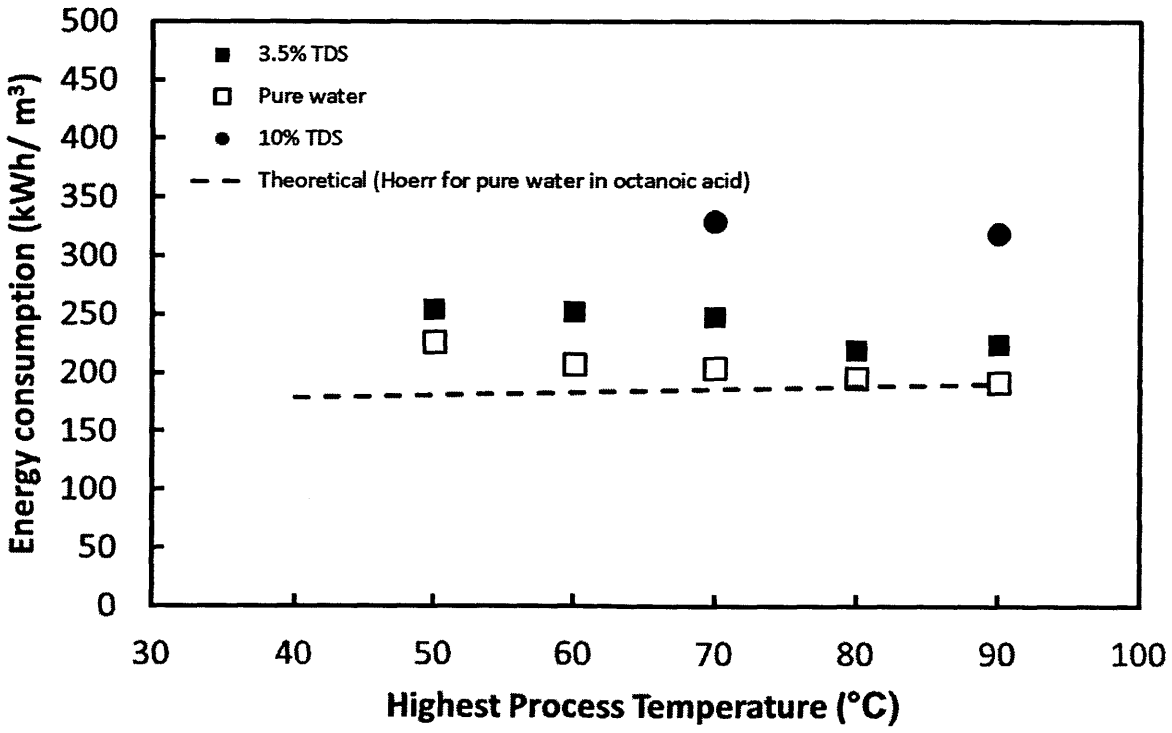

Figure 14. Thermal energy consumption as a function of the highest process temperature for directional solvent extraction (DSE) for when pure water is dissolved in octanoic acid and recovered upon cooling (open square), 3.5% TDS water is dissolved in octanoic acid and pure water is recovered (filled square), 10% TDS water is dissolved in octanoic acid and pure water is recovered (filled circle)

and calculated from Hoerr's solubility estimates [60] of pure water in octanoic acid (broken line). The lowest process temperature in these experiments was 25 °C; calculations assume a heat exchanger effectiveness of 80% [80]

To appreciate the benefit of operating at lower temperatures, exergy consumption is calculated for DSE with octanoic acid for 3.5% TDS feed as well and is represented in Figure 15. It may be noted that the experimental exergy consumption follows the same trend as the theoretical predictions as represented by the broken line on the plot. Here the exergy consumption for DSE with octanoic acid is lower than that for decanoic acid. Also the exergy consumption lies exclusively in or below the range of literature values for multi-stage flash (MSF) distillation for all highest process temperatures tested. The values approach those for reverse osmosis (RO) as the temperature approaches 50 °C and under. It is important, once again, to reiterate that RO is an electrical process and this electricity is derived from high temperature heat source often above 2000 °C.

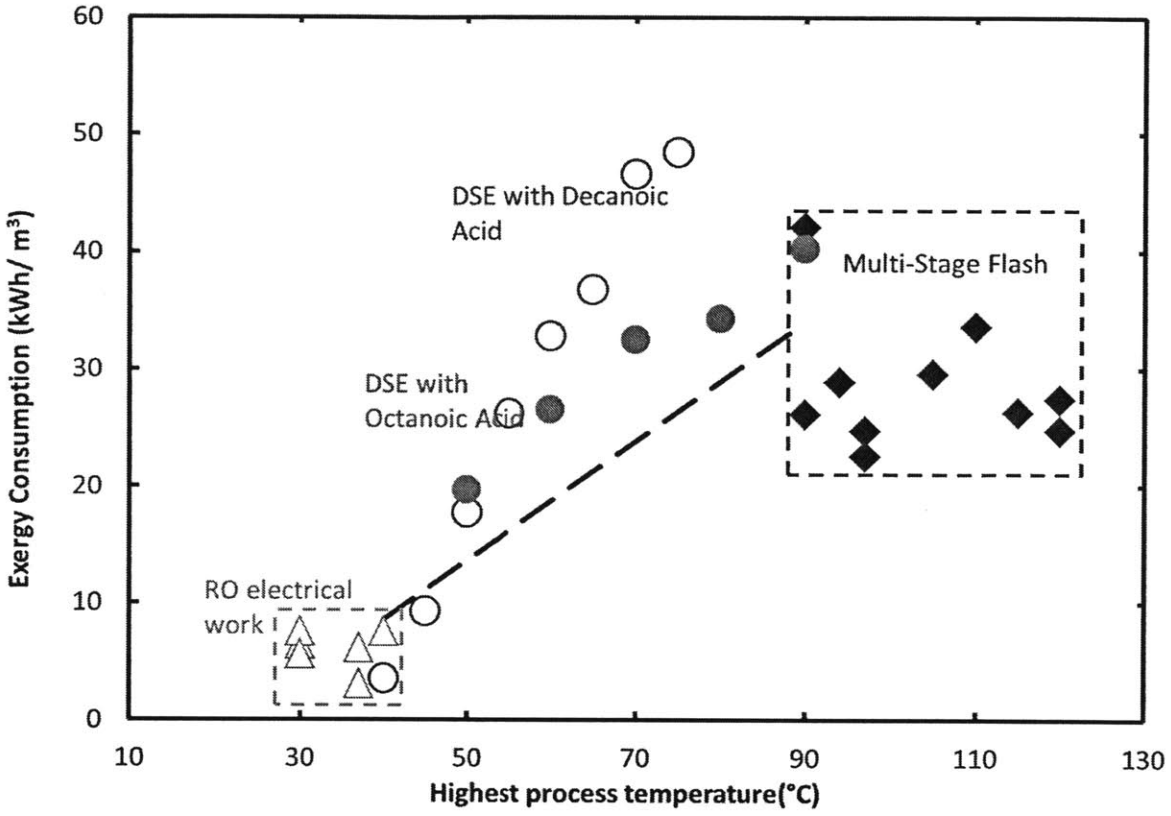

Figure 15. Exergy consumption as a function of the highest process temperature for directional solvent extraction (DSE) with octanoic acid compared with exergy consumption for DSE with decanoic acid and literature values for reverse osmosis (actual electricity consumption) [31–34], and multi-stage flash [31], [33], [34], [41–43]. Also shown is the theoretically expected exergy consumption for octanoic acid based Hoerr's solubility estimates (broken line) [60].

3.3 Summary & Discussion

First demonstration of directional solvent extraction as a novel desalination technology was completed in a benchtop batch process as describe above with decanoic acid and octanoic acid as the preferred directional solvents.

The basic DSE cycle as experimentally demonstrated consists of (1) mixing saline feed water with the directional solvent in a beaker using a magnetic stir bar (2) heating the beaker contents on a hot plate to a temperature between 40 °C and 90 °C so that pure water is dissolved into the solvent (3) allowing the un-dissolved brine-phase to settle gravitationally by stopping the stirring but maintaining the high temperature (4) decanting the clear solvent and water solution by pouring off into test tubes maintained at the lowest process temperature which may be room temperature or another convenient temperature (5) allowing the test tube contents to cool and the desalinated water to precipitate (6) separating the precipitated water from the solvent by allowing gravitational separation over several hours or by settling centrifugally in a lab centrifuge for 1-2 minutes and (7) finally collecting the recovered water from the bottom of the test tubes and (8) reusing the solvent.

Effective desalination was demonstrated with both decanoic acid and octanoic acid. Starting with a feed concentration of 3.5% w/w sodium chloride, the product water concentration was found to be between 0.07% and 0.11% w/w for decanoic acid and between 0.17% and 0.32% w/w for octanoic acid. The higher product TDS for octanoic acid was attributed to the shorter brine separation time employed. For a starting feed concentration of 10% w/w sodium

chloride the product water concentration was found to be between 0.37% and 0.51% w/w for desalination with octanoic acid.

Water yield is defined as the weight of product water obtained at the end of the cycle per unit weight of the directional solvent used. Due to the increase in solubility of water in the solvent with increasing temperature the yield also increases as the driving temperature difference, ΔT is increased. With a starting feed concentration of 3.5% decanoic acid was shown to give a yield of about 0.6% for ΔT of 16 °C which increases to about 1.3% for a ΔT of 46 °C. Octanoic acid, as expected, was shown to give higher yields than decanoic acid; for a ΔT of 25 °C, octanoic acid gives a yield of about 1% which increases to almost 4% for ΔT of 65°C. For starting feed concentration of 10% octanoic acid gives a yield of 1.73% for ΔT of 45 °C which increases to 2.62% for ΔT of 65 °C. Directional solvent extraction was also shown to be the only method other than phase that can extract water from and crystallize salt out of saturated brines.

Thermal energy consumption for the experiments was calculated. The experimental energy consumption for seawater concentrations (3.5%), translated to the scenario of a continuous industrial cycle with heat recovery, was found to vary between 350 kWh_{th}/ m^3 and 480 kWh_{th}/ m^3 for decanoic acid, and between 220 kWh_{th}/ m^3 and 260 kWh_{th}/ m^3 for octanoic acid. These energy consumption values are higher than other thermal processes such as MSF and MED. The benefit of using low temperature heat sources, however, is demonstrated by calculating the exergy consumption of DSE and comparing with other desalination technologies. It is noted that the exergy consumption for DSE with decanoic acid is less than that of MSF for temperature below 70 °C and in the same range as RO for temperatures below 50 °C. For DSE

with octanoic the exergy consumption is less than MSF for all tested temperatures and approaches that of RO for temperatures below 50 °C.

In addition, the experimental energy consumption for produced water concentrations (10%), translated to the scenario of a continuous industrial cycle with heat recovery, was found to vary between 318 kWh_{th}/ m^3 and 330 kWh_{th}/ m^3 for octanoic acid as the directional solvent.

Through this demonstration of concept it is shown that, by using directional solvents, it is possible to design thermal desalination processes that utilize very low to mid temperature energy sources. This process has been shown to operate with temperatures as low as 40 – 50 °C. Sources that could provide such temperatures are abundant and inexpensive. Although the absolute energy consumption is high, the exergy of this energy low thus utilizing energy that would otherwise be wasted. Further work on better understanding the phenomenon and characterizing the process parameters became important and is presented in the following sections.

Chapter 4 Characterization of DSE process parameters: Effect of process step times, varying feed TDS, and recovery analysis

4.1 Effect of process time parameters

The first demonstration of directional solvent extraction as a batch process involved very long mixing and brine separation times (60 minutes each) and focused primarily on testing the concept. The longer process times were used to eliminate any variability due to the kinetics of the dissolution of water in directional solvent and those of gravitational brine separation.

However, for the process to be practically feasible and economical, the process cycle time is critical. The faster the cycle the greater the product water throughput will be for the same amount of solvent and for the same system size. A shorter cycle will thus mean higher throughput rates, lower amounts of solvent in circulation, and smaller system sizes, all resulting in increased portability, lower on-site footprint, and lower capital costs.

The rate limiting steps are (1) mixing of feed water and the solvent, (2) brine separation, and (3) separation of the product water. The first two are experimentally characterized here and the third is discussed quantitatively and qualitatively.

Feed-solvent mixing time: In the mixing step, feed water droplets are formed within the solvent phase to facilitate quicker dissolution. The smaller the droplet size, i.e. the greater the droplet surface to volume ratio, the faster the dissolution will be. Shorter mixing time may

reduce the amount of water dissolved into the solvent and thus result in reduced yield. To investigate the effect of mixing time on the product water yield, droplets were formed using a stir bar rotating at 600 rpm in a 300 ml beaker and the mixing time was varied between 1 and 60 minutes. The feed water contained 3.5% TDS. Octanoic acid was used as the directional solvent and the highest process temperature was maintained at 90 ℃ for all the runs. All other process times were kept constant. Experiments for each case were carried out three times.

The product water yield was recorded for all mixing times and is depicted in Figure 16. As seen from the plot, the product water yield does not significantly change with changing mixing times except a slight decrease when the mixing time approaches one minute. This result suggests that it may be possible to reduce the time under the present experimental conditions to one minute without compromising on yield performance.

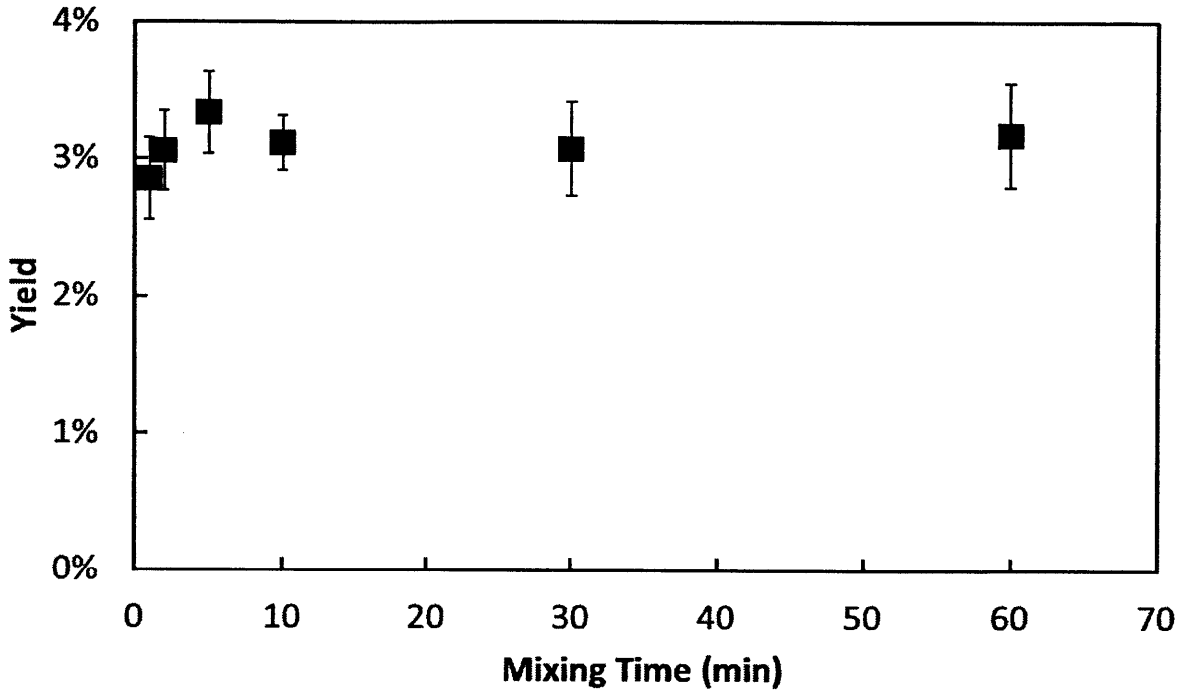

Figure 16. Product water yield as a function of feed-solvent mixing time for octanoic acid as solvent and 3.5% TDS feed water

Brine separation/ settling time: In the batch process experiments, brine is separated gravitationally once the stirring is stopped. Most of the brine droplets separated within a few seconds as was visually evidenced by the clearing up of the contents of the beaker. Some small droplets, however, seemed to separate slowly. Some droplets had likely not separated in the allowed separation time and mixed with the precipitated pure water, thus giving the product water a residual salt content. Shorter separations times may therefore lead to less ideal brine separation and higher product water TDS. To investigate this, the experimental process was repeated with varying brine separation/ settling time between 1 and 60 minutes. Octanoic acid was used as the directional solvent, the highest process temperature was maintained at 90 ℃, and the mixing time held constant at one minute. All other process times were kept constant.

The product water TDS content was measured in for each experimental run and the results are depicted in Figure 17. The plot shows that the product TDS does indeed increase with reducing separation times. The change is insignificant when the separation time is reduced from 60 minutes to 40 minutes for which the product TDS remain in the range of 0.1% w/w. As the separation time is reduced further the product water TDS increases to about 0.3% w/w for separation time of one minute. This reduction in performance, however, is outweighed by the gains due to reduction in separation time of 60 times. For produced water applications a TDS reduction of 90% (3.5% to 0.3%) would be acceptable for most reuse purposes. For seawater desalination applications a reduction to 0.3% TDS would make the water acceptable for certain agricultural and industrial application or for further treatment by RO or Electrodialysis (ED) which are extremely effective and economical at such low TDS levels. The separation kinetics of brine droplets are also discussed in more detail in the context of the continuous DSE process in chapter 6.

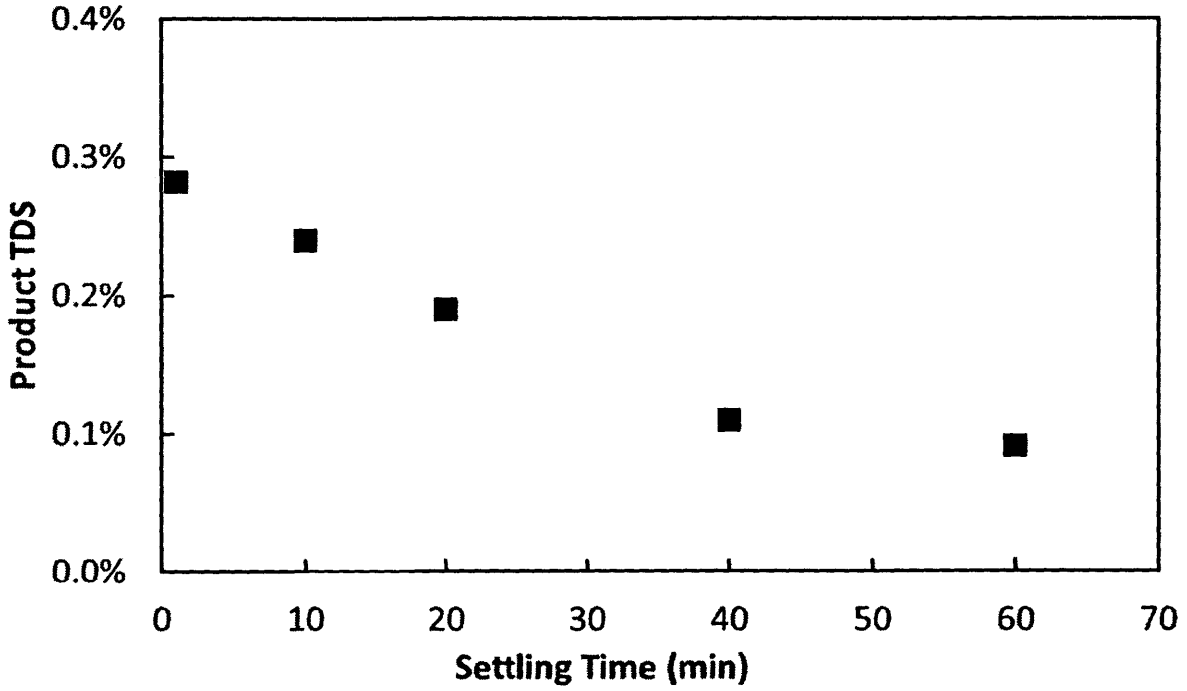

Figure 17. Product water TDS as a function of brine separation/ settling time for Octanoic acid as solvent and 3.5% TDS feed water

Separation of precipitated water: When the solvent is cooled back down the dissolved water droplets precipitate out by nucleating and then coalescing [81], [82]. Droplet formation has been investigated in detail by Kress [63]. Kress' experiments suggest that sizes of nucleating droplets increase with decreasing cooling rate. This may be because slower cooling rates result in primarily heterogeneous nucleation as there are existing precipitated droplets which form nucleation sites. The probability of homogeneous nucleation, i.e. the probability of smaller droplet sizes increases with increasing cooling rate.

For the cooling scenario in the experimental process, the solvent is cooled in test tubes by free convection in ambient air. A simple calculation suggests that the cooling rates are on the order of 1 – 10 ℃/ min, which would mean that the samples cool from 90 ℃ to ambient

temperature within an hour, as has been observed in the laboratory. For these cooling rates, Kress showed that water droplets precipitated in octanoic acid are in the size range of 10 μm in diameter. The gravitational settling of these droplets may be approximated as Stokes flow of a sphere (droplet) through a viscous fluid (solvent) [83]. The terminal velocity for such a flow is given by,

$$v = \frac{1}{18}\left(\frac{\rho g D^2}{\eta}\right) \tag{9}$$

where ρ is the density of water, η is the viscosity of the surrounding medium, in this case decanoic or octanoic acid, D is the droplet diameter, and g is gravitational acceleration. Taking density of water equal to 1000 kg/ m^3, gravitational acceleration 9.8 m/s^2, and viscosity of octanoic acid to be 5.5 cP [84], the terminal velocity for 10 μm diameter droplet is expected to be about 10^{-3} cm/s. For a 300 ml beaker, about 10 cm in height, used for the experiment, the maximum time that the droplets take to settle to the bottom is expected to be about 3 hours.

As can be seen from equation (9) the settling velocity is proportional to the square of the diameter. The settling time is therefore proportional to the inverse of the square of droplet diameter. For 5 μm droplets this settling time would increase to 12 hours, and for 2 μm droplets to about 75 hours. The fact that all brine droplets that not settled after 72 hours implies that a minor fraction (<3%) of the droplets were smaller than 2 μm in size.

4.2 Effect of feed TDS on DSE performance

DSE promises to be an effective desalination method for a wide range of feed TDS levels. Increasing TDS levels, however, do have an effect on its performance, primarily on the product water yield thus affecting the process energy consumption. To investigate this effect, the experimental procedure was repeated for varying feed TDS levels between pure water (0%) and 12% sodium chloride w/w, using octanoic acid as the directional solvent, and maintaining the highest process temperature at 90 °C. Learning from the above described process time investigations, the mixing and brine separation times were both reduced to one minute. For all the experimental runs, the product water yield was recorded and the results are depicted in Figure 18. As expected, the product water yield reduces with increasing feed TDS when the ratio of feed to the solvent is held constant (10% is this case), due to the increased difficulty of extracting water from a saline solution. As previously explained the strong salt-water interaction reduces the free energy of water in a saline solution which reduced with increasing salt content, and thus makes it energetically more difficult to transition to the state of being dissolved in the directional solvent.

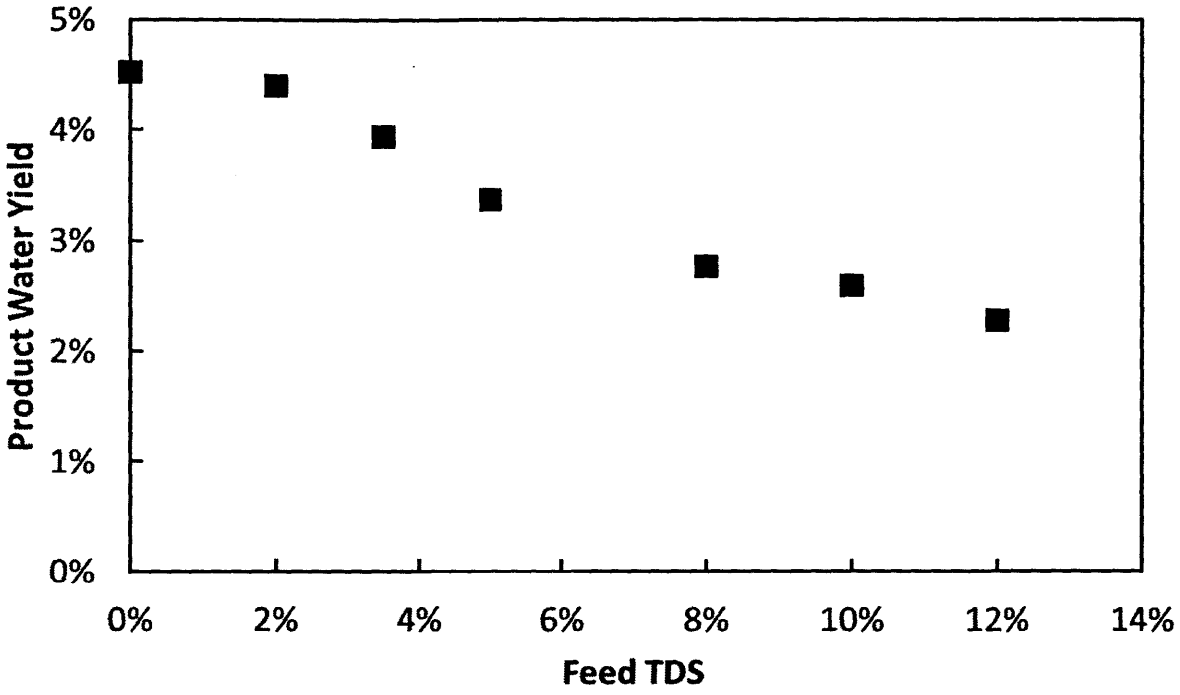

Figure 18. Product water yield as a function of feed TDS for Directional Solvent Extraction with Octanoic Acid, 10% feed to solvent ratio, and ΔT=65 ℃.

4.3 DSE Recovery ratio

The recovery ratio, an important performance parameter of any desalination process, has not been discussed so far in the context of directional solvent extraction. Recovery ratio is the ratio of the amount of desalinated product water recovered to the amount of feed water used as a process input. Any water that is not recovered as product is discharged as a waste brine stream. Recovery ratios of seawater reverse osmosis plants lie in the range of 30% to 50% [85–89], while representative seawater MSF recovery ratios are in the range of 15-50% [89].

Higher recoveries imply smaller amount of fluid passing through the system which translates to smaller system sizes and thus lower capital costs. Higher recoveries also imply

lower pumping energy consumption and costs as more of the feed pumped through the system is recovered as the desalinated product. High recoveries are thus desirable, and even more so in produced water applications, where the uncovered brine needs to be transported to a deep injection well as a very high cost. In fact, industry surveys suggest that an effective produced water desalination system would likely be required to demonstrate recoveries greater than 70%.

In the above described experiments, excess feed amounts were used to eliminate any variability due to increasing salt concentration in the brine phase as water was dissolved into the solvent. To investigate potential recovery ratios, however, it became necessary to reduce the amount of input feed and record the resulting changes in product water yields. The experiments were repeated with octanoic acid, and the feed to solvent ratio was varied over different experimental runs. For example, a first run was conducted with the above described 10% feed to solvent ratio (10g feed water in 100g solvent), and thereafter the feed amount was reduced to 9g, 8g and so on while keeping the solvent amount the same. To reiterate the product water yield is the ratio of the weight of product water recovered to the weight of the solvent used.

Recovery, therefore, can be calculated as,

$$RR = \frac{Y}{FSR} \tag{10}$$

where Y is the product water yield and FSR is the feed to solvent ratio. The recovery ratios were thus calculated from results for varying feed to solvent ratios and are depicted in Figure 19. As expected the recovery is seen to increase with decreasing feed/solvent ratio. The highest reported recovery in this single stage batch process was about 78% for 3% feed to

solvent ratio. This recovery is higher than any reported recoveries from seawater reverse osmosis, MSF, MED, MVC or ED processes.

The broken line represents the theoretically expected recovery for pure water in octanoic acid. It may be noted that for a feed to solvent ratio of less than 4.54%, which is the change in solubility of water in decanoic for the used ΔT of 65 °C, the recovery for pure water should be 100%. However, the presence of salt makes it more difficult to extract water as the salt concentration in the brine phase increases. With higher recoveries, this brine salinity increases, thus leading to the greater observable deviation from the pure water curve.

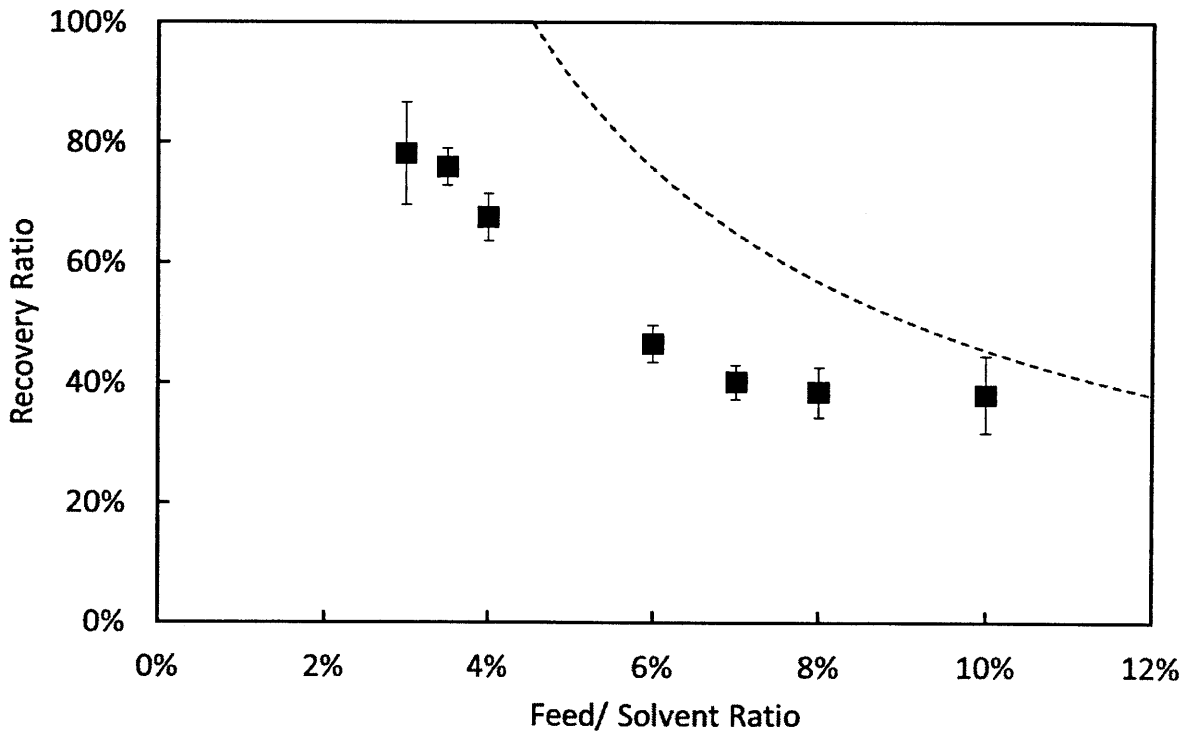

Figure 19. DSE Recovery Ratio as a function of feed to solvent ratio with Octanoic Acid as directional solvent, with ΔT=65 ℃, for 3.5% TDS feed water. The broken line represents the theoretical recovery based on Hoerr's solubility estimates of pure water in octanoic acid [60]

This deviation from the ideal pure water curve becomes more evident when the data is presented in terms of product water yield as a function of feed to solvent ratio. Interestingly, while the recoveries increase with decreasing feed/ solvent ratio the absolute product water yields tend to decrease with decreasing feed/ solvent ratio. The yield decreases, again, due to the increasing salinity as more water is pulled out into the solvent from the brine phase. The recorded yield are depicted in and compared with the pure water yield for the given ΔT (65 ℃) which is expected to remain constant at 4.54%, for any feed to solvent ratio greater than 4.54%. For any feed to solvent ratio less than 4.54%, the yield will be equal to the feed to solvent ratio, since in that case the solvent will dissolve all the pure feed water.

The implication of this decreasing yield is that for lower feed to solvent ratios, while the recovery increases, the energy consumption per unit amount of product water also increases. For example, while the energy consumption for 38% with a 10% feed to solvent ratio is 224 kWh/ m^3, it increases to 353 kWh/ m^3 when 78% recovery is realized with a 3% feed to solvent ratio. However, even with the increased energy consumption, higher recoveries may be desirable depending on the application, for example in produced water treatment, and depending on the availability of thermal energy, for example if waste heat is readily available or in scenarios where resources such as natural gas as a combustible fuel are inexpensive and plentiful.

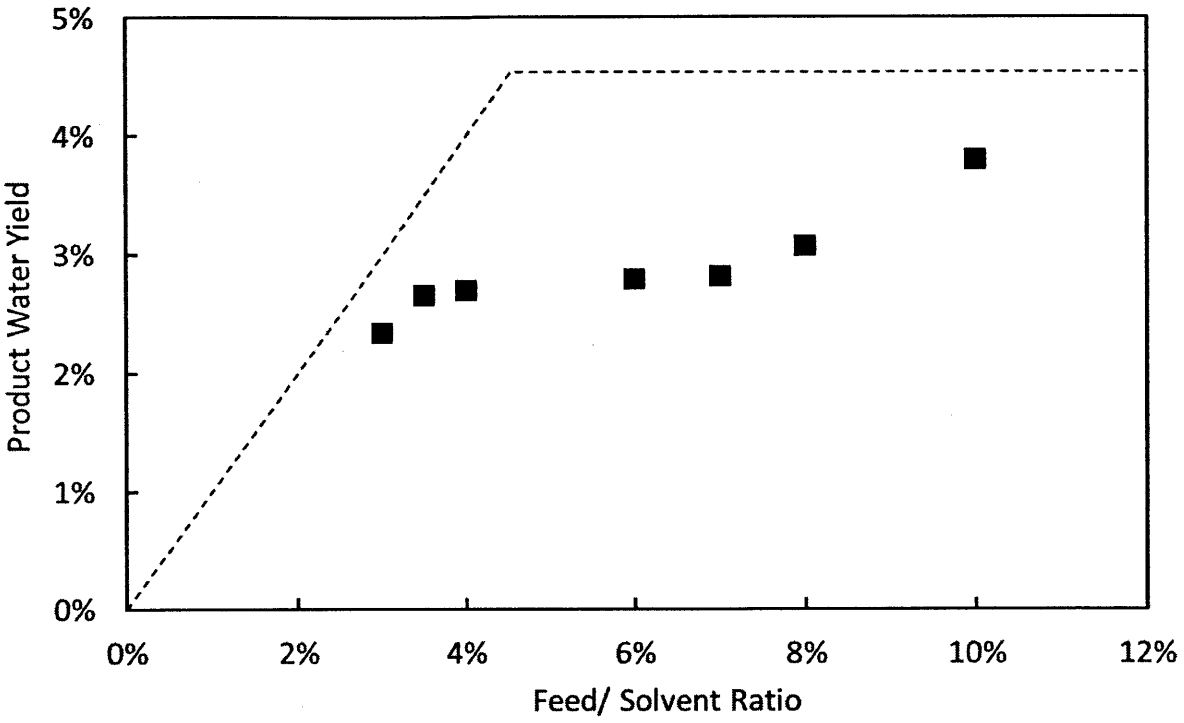

Figure 20. DSE product water yield as a function of feed to solvent ratio with octanoic Acid as directional solvent, with ΔT=65 °C, for 3.5% TDS feed water. The broken line represents the theoretically expected yield for pure water in octanoic acid based on Hoerr's solubility estimates [60]

4.4 Summary

The effects of process time parameters, the solvent-feed mixing time, the brine separation time, and the precipitated water separation were investigated with octanoic acid as the solvent. It was shown that the solvent-feed mixing can be reduced to 60 seconds without compromising performance, i.e. without reducing the product water yield.

Brine separation is gravitationally driven and it was observed that the product water salinity did not significantly change between this separation time was reduced from 60 minutes

to 40 minutes but a slight increase was noticed upon reducing the time further to 20, 10 and 1 minute. It was, however, noted that the gains from reducing brine separation time to 60 seconds outweigh the losses due to product water salinity increase to just 0.3% from 0.1%.

The separation of precipitated water from the solvent was modeled as Stokes flow of a sphere through a viscous medium and the required separation times based on droplet sizes were calculated. It was shown that 10 μm droplets are expected to settle to the bottom of a 10 cm tall experimental beaker in 3 hours, and that this time would increase to 12 hours and 75 hours for droplets 5 μm and 2 μm respectively.

The effect of varying feed TDS was investigated and it was shown that DSE may be used effectively for treating high TDS waters including saturated brines. It was, however, found that higher feed TDS resulted in lower product water yield. Upon increasing the feed TDS from 2% to 12% the product water yield halved from about 4.4% to about 2.3%.

Recovery ratio of the DSE process, i.e. the ratio of the mass of product water to the mass of the feed water, was shown to vary with the feed to solvent ratio. Recoveries as high as 78% were demonstrated for a 3.5% TDS, higher than any reported recoveries from seawater reverse osmosis, MSF, MED, MVC or ED processes. It was, however, noted that higher recoveries also require higher energy consumption. Thermal energy consumption increases from 224 kWh_{th}/ m^3 for 38% recovery to 353 kWh_{th}/ m^3 for 78% recovery. This increased energy consumption may, however, be acceptable in scenarios such as produced water treatment where a high value is placed on recovery.

Chapter 5 Multistage Direction Solvent Extraction

5.1 Introduction

Thus far, in this work, we have discussed the concept, demonstration, and characterization of directional solvent extraction as a single stage batch process where the feed water is fed into the system and a product water phase and a brine phase are removed as outputs. The waste brine phase from the process naturally has a higher salinity than the feed water. DSE, however, has been shown to be effective for higher TDS feed waters all the way up to saturated brines. This ability opens up the possibility of reusing the brine from one process cycle as feed for a subsequent cycle, with a view to recover even more desalinated product water. This modification to the DSE cycle is referred to as multi-stage directional solvent extraction. A multi-stage process may involve two or more stages, i.e. the brine from first stage is used as feed for a second stage and the brine by-product from the second stage is used as feed for a third and so on, until any more stages become impractical or the salt begins to crystallize out of solution.

In multi-stage flash distillation, subsequent stages are used to recover energy from evaporated water from the previous stage, thus reducing the energy consumption of the process. In a multi-stage DSE, the energy recovery from reusing the brine as feed in a subsequent stage, would not be significant as the feed forms a very small fraction (<10%) of the circulating fluid, most of which is the solvent. A minor amount of energy would still be recovered and may serve to reduce energy consumption slightly.

The major advantage of a multi-stage process is that it promises even higher recoveries than those already demonstrated using single stage DSE. This could be very significant in the produced water treatment scenario or another application where greater value is placed on high recoveries. A multi-stage process was therefore investigated experimentally and is described below.

5.2 Experimental procedure

Octanoic acid was used as the directional solvent to investigate multi-stage stage directional solvent extraction. Feed water samples were making 3.5% w/w sodium chloride in distilled water solution to simulate seawater, and 10% w/w sodium chloride solution to simulate produced water. The octanoic acid was first saturated with water at ambient temperature (25 ºC) as explained before. Similar to the earlier experiments, 100 g of octanoic acid were taken in a conical flask and heated on a heating and stirring plate. The acid was heated and maintained at 90 ℃ in all experimental runs. Both feed water samples (3.5% and 10%) were added to octanoic acid while stirring in varying amounts between 4g and 10g (4% and 10% FSR) over different experimental runs. Stirring was continued for one minute to allow for dissolution of the water into the solvent. Stirring was then stopped, the flask contents were maintained at 90 ℃, and un-dissolved brine droplets were allowed to settle gravitationally for one minute. Thereafter, two clear layers of solvent with dissolved water (top) and brine (bottom, as described in section 3) were observed to form in the flask. The solvent-water solution was carefully decanted into conical tubes maintained at room temperature of 25 ℃.

The remaining brine at the bottom of the beaker was then poured off into another test tube, its weight recorded, and saved for use in the next stage. The experimental cycle was then repeated except that the brine from the previous stage was used as feed. The second stage brine was also collected and used as feed for a third stage.

The decanted solvent-water solution from all three stages was allowed to cool in ambient air for about 60 minutes to room temperature (25 ℃). As described earlier, the clear solution turned cloudy indicating the precipitation of water from the solvent. These samples were transferred to a centrifuge and centrifuged at relative centrifugal force of 5000 g for about 60 seconds. The test tubes were observed to have two clear layers of settled water (bottom) and the solvent (top). The water was recovered by piercing a hole in the bottom of the test tubes and the solvent saved for reuse.

The recovered water samples from all three stages were measured for weight and salinity, and the resulting yield, product TDS, and recoveries were recorded. In most experimental runs, except for the one with 10% first stage feed to solvent ratio, no brine was left was the end of the third stage. Instead, salt was observed to crystallize out and was left behind at the bottom of the beaker as a white precipitated residue.

5.3 Results & Analysis

The obtained recoveries are depicted in Figure 21. As can be seen the achieved recoveries for seawater concentrations are in the range of 65% to 85% and those for produced water concentration are in the range of 56% to 82%, much greater than representative RO recoveries for seawater desalination. 3-stage recoveries are significantly greater than single stage recoveries

and for feed to solvent ratios of over 6% the 3-stage recoveries for 3.5% TDS and 10% TDS feed water are even greater than the theoretically expected single stage recoveries for pure water.

As noted, in most experimental runs expect for the one with 10% first stage feed to solvent ratio, no brine was left at the end of the third stage and salt was observed to crystallize out and precipitate. This might seem to indicate 100% recovery; yet the maximum apparent recovery was 85%. The additional water was lost due to evaporation, lost due to the crude recovery method of piercing a hole in the test tube, or remained bound with the hydrated salt. Sodium chloride sometimes crystallizes as a dehydrate ($NaCl.2H_2O$) [90] in which case about 2.16% water will remain bound to it for 3.5% TDS feed and 6.17% water will remain bound for 10% TDS feed. The likelihood of this happening is extremely low as sodium chloride has negligible probability of forming a hydrate at 25 °C and atmospheric pressure [91]. This suggests that most of the water loss is due to evaporation or experimental oversight.

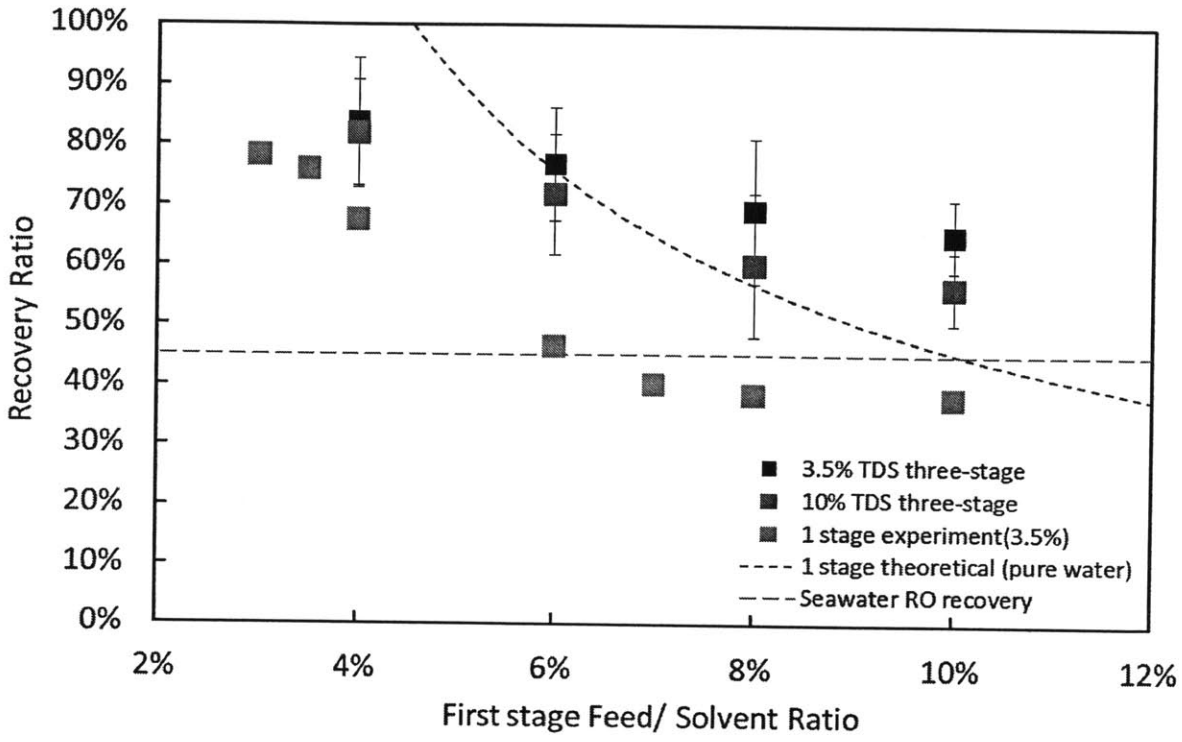

Figure 21. Three-stage Directional Solvent Extraction recovery ratio as a function of first stage feed to solvent ratio for 3.5% (black solid square) and 10% TDS (red solid square) feed water with Octanoic acid as solvent and ΔT=65 ℃. The results are compared with experimental recoveries for single stage 3.5% TDS water (green solid square) and also with theoretically expected recoveries based on Hoerr's solubility estimates [60] for pure water in octanoic acid (black broken line); representative seawater RO recovery [85] (blue broken line) is also superimposed for comparison

As mentioned earlier, however, the greater recoveries come at a greater energy price. The experimental energy consumption translated to energy consumption in an industrial scenario where heat recovery is used, is depicted in Figure 22. As may be seen the energy consumption range, 320 – 450 kWh/ m^3 for seawater concentrations and 370 – 630 kWh/ m^3 for produced water concentration, is much higher than single stage DSE or for other thermal processes. This higher energy consumption is a result of the diminishing product water yield in every successive stage due to reduced feed amounts and increased salinity. Actual inputs and data for one experimental run are shown below in Table 2 to illustrate this point.

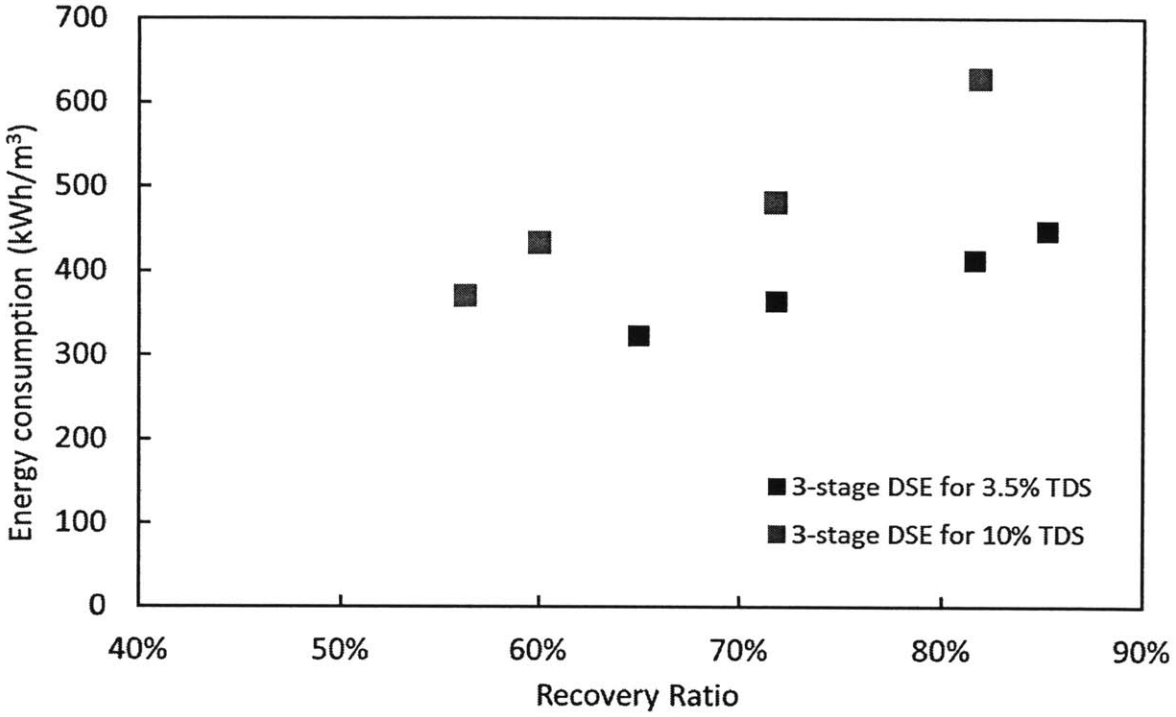

Figure 22. Thermal Energy consumption of a 3-stage Directional Solvent Extraction process for varying experimental recoveries with Octanoic acid as solvent and driving temperature difference ΔT=65°C; calculations assume a heat exchanger effectiveness of 80% [80]

Table 2. Experimental scenario for a three-stage DSE process with 3.5% starting feed TDS

	FSR	TDS	Recovery
Stage 1	6%	3.50%	52%
Stage 2	2.21%	7.29%	54%
Stage 3	1.14%	16.02%	65%
Overall	6%	3.50%	**84%**

5.4 Discussion & Improvements

Multi-stage directional solvent extraction has been demonstrated as a desalination method that can achieve higher recoveries than any conventional desalination method. Recoveries as high as 85% have been demonstrated for 3.5% TDs feed water and those as high as 82% have been demonstrated for 10% TDS feed water. However, the high recoveries are, as shown, as achieved at much higher energy consumption than a single stage process. Such higher energy consumptions may be acceptable in situations where high recoveries imply significantly higher economic values. In fact, for produced water treatment a key requirement for the treatment method is very high recoveries or zero liquid discharge.

A better method of achieving high recoveries, without significantly losing on the energy consumption, may be to mix the brine from one stage with the source feed water and use the mixture as feed for another stage, or in other words, recirculating the brine a prescribed number of times depending upon the initial salinity and the maximum allowable specific energy consumption.

An example of this scenario, with octanoic acid as directional solvent and a driving temperature difference of 65 ℃, is presented in Table 3. A feed to solvent ratio of 10% and a starting feed salinity of 3.5% are considered. The feed salinity for subsequent stages is calculated based on the recovery of the preceding stage and the additional feed water added to maintain the 10% feed to solvent ratio. Recoveries for different salinities are obtained from experimental results shown in Figure 18. As shown in Table 3, over 79% recovery is achieved when the brine is recirculated 10 times with a specific energy consumption of 291 kWh_{th}/ m^3. In contrast, the

experimental energy consumption, without mixing the brine with additional feed, was about 400 kWh_{th}/m^3 for 80% recovery (see Figure 22).

Table 3. Calculated illustration of a multi-stage DSE process where the un-recovered brine is recirculated and mixed with additional feed water such that the feed to solvent ratio remains constant at 10%. Calculations are for 3.5% starting feed salinity, octanoic acid as directional solvent, and a driving temperature ΔT=65 ℃

	FSR	TDS	Recovery	Specific energy consumption (kWh/ m^3)
Stage 1	10%	3.50%	40%	214
Stage 2	10%	4.90%	34%	249
Stage 3	10%	6.09%	32%	263
Stage 4	10%	7.21%	29%	289
Stage 5	10%	8.23%	28%	299
Stage 6	10%	9.21%	27%	309
Stage 7	10%	10.15%	26%	321
Stage 8	10%	11.06%	25%	333
Stage 9	10%	11.94%	24%	346
Stage 10	10%	12.78%	23%	361
Overall	**10%**	**3.50%**	**79%**	**291**

Another scenario for a starting feed salinity of 10% is presented in Table 4. The calculations are similar to those of Table 3. As calculated, a recovery ratio of 76% is achieved at a specific energy consumption of 367 kWh/ m^3 when brine is recirculated 10 times. In contrast, the experimental energy consumption, without mixing the brine with additional feed was about 480 kWh/m^3 for 72% recovery (see Figure 22). These are experimentally derived predictions for the designed recirculating multi-stage directional solvent extraction process.

Table 4. Calculated illustration of a multi-stage DSE process where the un-recovered brine is recirculated and mixed with additional feed water such that the feed to solvent ratio remains constant at 10%. Calculations are for 10% starting feed salinity, octanoic acid as directional solvent, and a driving temperature ΔT=65 ℃

	FSR	TDS	Recovery	Specific energy consumption (kWh/ m3)
Stage 1	10%	10.00%	27%	309
Stage 2	10%	10.95%	26%	321
Stage 3	10%	11.86%	24%	346
Stage 4	10%	12.70%	23%	361
Stage 5	10%	13.50%	23%	368
Stage 6	10%	14.29%	22%	376
Stage 7	10%	15.06%	21%	393
Stage 8	10%	15.79%	21%	393
Stage 9	10%	16.53%	20%	412
Stage 10	10%	17.23%	19%	433
Overall	**10%**	**10.00%**	**76%**	**367**

Chapter 6 Continuous DSE process

After demonstrating a proof of concept of DSE as a laboratory batch process, it became imperative to design a continuously operating process and develop a prototype device to take the project closer to field application. On-site treatment of produced water was identified as the primary field application, given the immediate needs of the industry and the current environmental concern surrounding them. Industry surveys suggested that unconventional oil and gas well operators require on-site systems to treat 1-15 m^3 (6 to 100 barrels) of produced water per day. This section presents a design for a 1 m^3/ day system and describes the construction of a system with a goal of treating 1 bbl./ day (0.16 m^3/ day).

6.1 Process design

A schematic diagram of the design for the continuous directional solvent extraction process is depicted in Figure 23. The continuous desalination process must accomplish the following tasks in the given order with the solvent flowing is a closed look and the water in an open loop:

1. Heating of the directional solvent to the highest process temperature: This may be accomplished by running the solvent through any heat source, which in the case on-site oilfield operation could be a tank-less natural gas furnace. On-site gas is readily available at oil and gas well sites and is currently used for heating other processes. Furthermore, it would be difficult to recover waste heat from well site operations at the first system demonstration stage.

2. Feed water addition and mixing with the solvent: The mixing of feed water with the solvent at high temperatures facilitates water dissolution. This may be accomplished by a paddle wheel or a stirrer in the mixing chamber, by spraying the incoming feed water into the solvent, or simply by using a specific flow pattern that facilitates formation of water droplets in the solvent.
3. Dissolution of water into the directional solvent: The system must allow a short flow time during which the water is dissolved into the solvent, while maintaining the high process temperature. As shown earlier, a dissolution time of 60 seconds is sufficient and a more detailed analysis is presented later in this chapter.
4. Separation of un-dissolved brine: Following the dissolution of water the un-dissolved brine must be separated from the solvent-water solution in a first-stage separation process. This may be accomplished gravitationally (as described in chapter 6.2) or by using an electrocoalescer [92–96], which are widely used in the oil industry to separate water from crude oil.
5. Cooling of the solvent and heat recovery: After the brine is removed, the solvent stream is cooled down to facilitate the precipitation of pure water. It is important that energy from this stream be recovered. As such the solvent stream is cooled by exchanging heat with the returning solvent stream, preferably in a liquid-liquid plate heat exchanger [97]. Following the heat exchanger the solvent is further cooled using a radiator.
6. Separation of precipitated water from the solvent: This is the step where pure water is recovered in a second stage separation process. This may be done by using an

electrocoalescer or an in-line centrifuge, although the latter would involve high electrical energy consumption.

7. Pre-heating: After the water is separated and recovered, the solvent stream returns to the gas furnace via a heat exchanger where it gets pre-heated as mentioned in Step (5), and is conveniently recycled.

Figure 23 represents a continuous directional solvent extraction system with listed energy consumptions for a unit processing 1 m^3/ day of feed-water. Based on experiments, a recovery ratio of 70%, a product water yield of 3.3%, and thermal energy consumption of 200 kWh are shown. The calculations assume a heat exchanger effectiveness of 80% which is reasonable for a balanced liquid-liquid cross flow heat exchanger [97]. More specific discussion of the components of the continuous process may be found in an associated US patent application [98].

The continuous process will eliminate the manual processing involved in a batch, reduce energy consumption by recovering some energy from the cooling stream, and also significantly reduce cycle time by expediting the separation processes which are currently the rate limiting step in the system. It is expected that the continuous process will reduce the cycle time to less than 10 minutes, thus allowing about 150 cycles per 24 hour day.

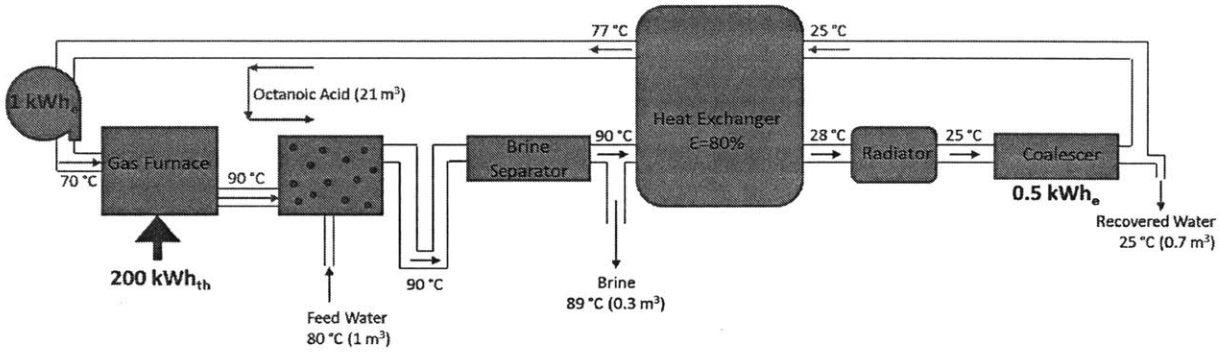

Figure 23. Schematic diagram of a 1m^3/day continuous DSE desalination system

6.2 Prototype design & construction

Figure 24 illustrates shows a schematic diagram of the laboratory prototype. The lab prototype is a simplified version of the designed continuous process such that it replaces proposed natural gas furnace with an electric heater and the electrocoalescer with an inline centrifuge. Electric heater is convenient and practical to operate in the laboratory environment and it was much easier to obtain a small scale in-line centrifuge than a small scale coalescer. Individual prototype component design is discussed as follows. Prototype construction was accomplished with the help of Michael Fowler [99] and testing was done with the help of Maximus St. John.

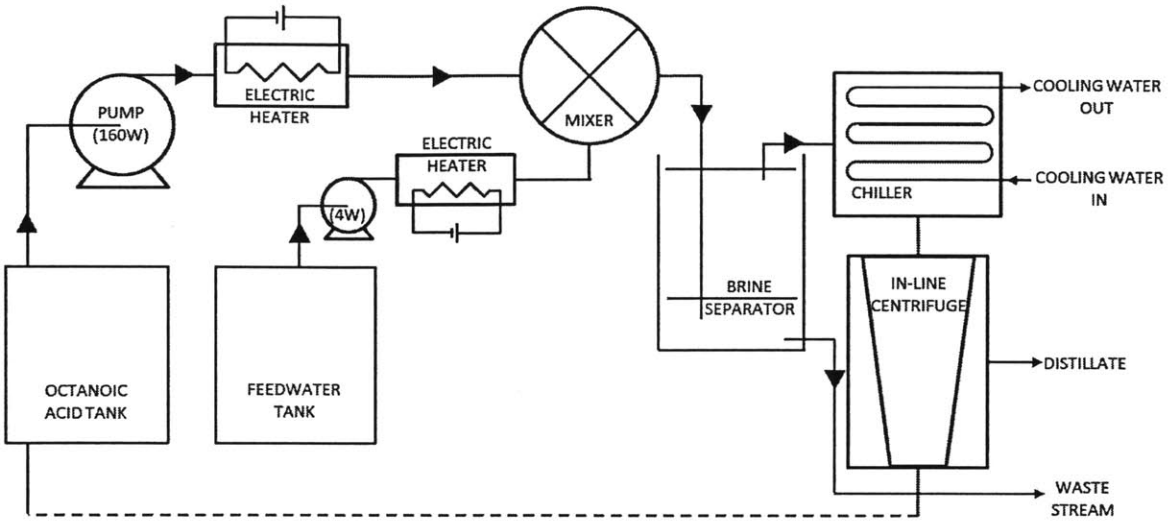

Figure 24. Schematic diagram of the constructed laboratory prototype system for the continuous Directional Solvent Extraction process

Solvent and feed water reservoir: Octanoic acid was used as the solvent to test the continuous process. Two five gallon high temperature plastic buckets were used as reservoir tanks for the solvent and feed water.

Pumps: An Omega® PHP-800 series 160W chemical metering pump was used to pump the solvent and Prominent® Solenoid 4W metering pump was used to pump the feed water. Metering pumps are highly controllable and allowed for flow variations over experimental runs.

Heaters: Electrical heaters are used to raise the temperature of the solvent and the feed water going to the process loop. Two Omega® Flow-through heaters with resistive heating elements of 5 kW and 1.5 kW respectively were used to heat the solvent and water respectively. A photograph of the heater is shown in Figure 25. The current input to the heaters may be regulated using the attached control unit.

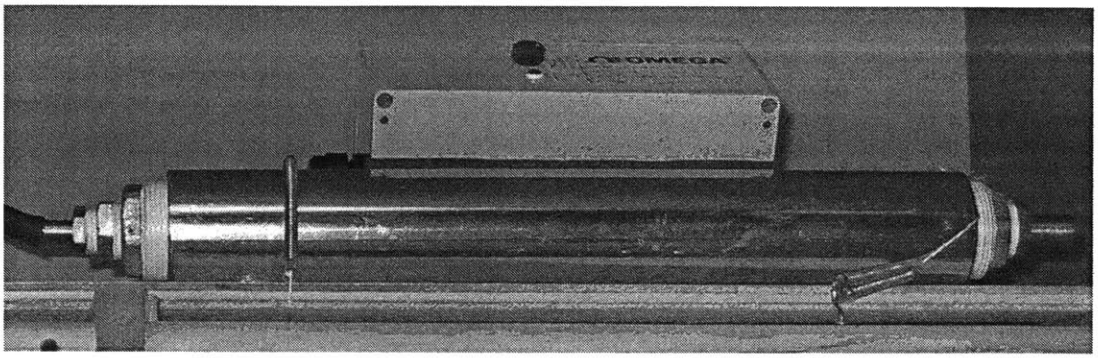

Figure 25. Omega flow-through heater with a 5kW electrical resistive heating element for heating the solvent; Water heater is identical except with a 1.5 kW resistive heating element

Mixer: After passing through the heater the solvent and feed water streams enter the mixer, which is the first component of the loop that required specific design and construction within the laboratory. The mixer consists of three major components, a cylindrical containment vessel, a stirrer, and a restraining stand.

The containment vessel is a capped cylinder, four inches in diameter and 45 cm in length is final version. Removable end caps provide access to the inside of the vessel, which allows proper cleaning and maintenance. The liquids enter and leave the containment vessel through barbed pipe fittings attached to the caps. The first version of the containment vessel was made out of polyvinyl chloride (PVC) plastic, as shown in Figure 26a. This was replaced by chlorinated polyvinyl chloride (CPVC) to be able to withstand temperatures higher than 65 °C (Figure 26b).

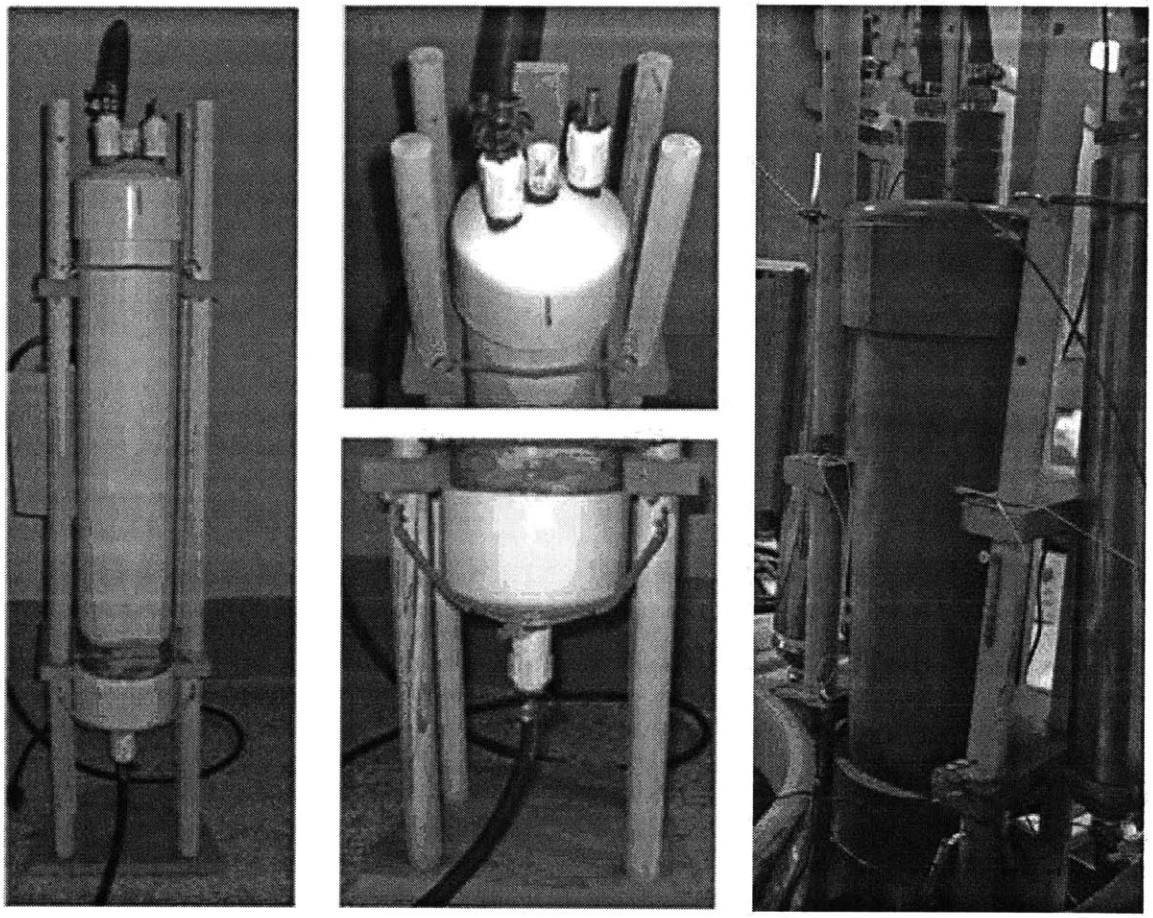

(a) (b)

Figure 26. (a) PVC mixer containment vessel and stand with close up views of the top and bottom caps; top cap has two ports for the solvent and contaminated water and a hole in the center for the stirrer rod; the bottom cap has one port for the mixture leading to the brine separator, and (b) CPVC mixer vessel to withstand higher temperatures with all other features remaining the same. The wooden stand uses springs to remove vibrations and to allow for thermal expansion and contraction of the vessel

The stirrer is a Caframo ® BDC^{TM} digital stirrer with a shaft connected to a three-inch diameter propeller blade at its end which facilitates the actual mixing. The stirrer speed is controllable between 40 and 2000 rpm. The shaft is long enough that the propeller is more than

half way down the containment vessel to ensure proper mixing. Figure 27 shows the propeller blade being lowered into the mixer containment vessel. Figure 28 shows a photograph of the completed mixer setup with labeled individual parts. Following construction the containment vessel was covered with insulation to minimize heat losses during prototype operation. Heaters were mounted on the mixer stand to minimize prototype footprint.

Figure 27. Stirring propeller blade being lowered into the mixer containment vessel

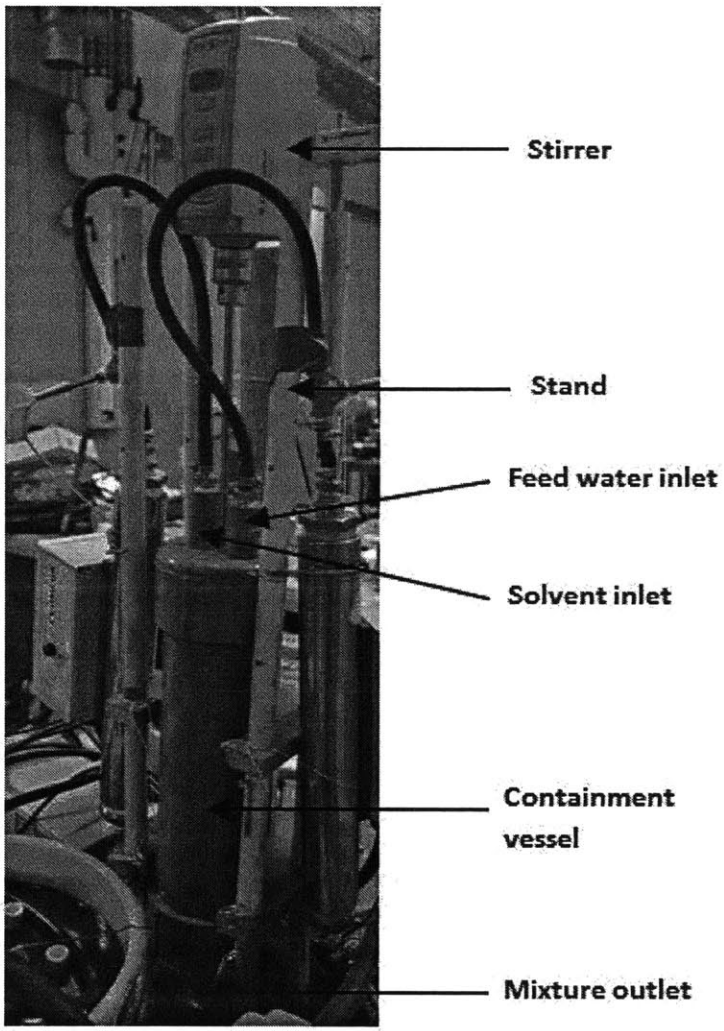

Figure 28. Completed mixer setup with labeled individual parts; solvent and feed water enter through fittings on the top cap, the stirrer runs a propeller blade used to mix the solvent and feed, and mixture exits through the fitting on the bottom cap.

It is important that the residence time of the water and solvent mixture in the mixer containment vessel be greater than the time required for water to dissolve into the solvent. The rate of dissolution of water from the droplet into the solvent is given by [100],

$$N_w = \frac{D_{w/OA}(C_{w/w} - C_{w/OA})}{r} \quad (10)$$

where, N_w is the molar flux of water from the droplets into octanoic acid, $D_{w/OA}$ is the diffusion coefficient of water in octanoic acid, $C_{w/w}$ is the molar concentration of water in the feedwater droplets, $C_{w/OA}$ is the molar concentration of water in the octanoic acid, and r is the feed water droplet size. This model assumes quasi-steady state diffusion from a sphere into an infinite medium.

The diffusion coefficient of water in octanoic acid was not measured but based on literature values of self-diffusion coefficients of water [101] and octanoic acid [102], its value is expected to be $D_{w/OA} \sim 10^{-10}$ m^2/s. This value is also expected from our previously reported calculations for the diffusion coefficient of water in decanoic acid which was found to be about 0.5×10^{-10} m^2/s [64]. The larger the feed water droplets in the octanoic acid, the slower the diffusion will be. As discussed in detail in the next section, it is reasonable to expect feed water droplets of diameter on the order of 100 μm. According to equation (10), then a water droplet of 100 μm in size should dissolve completely in octanoic acid in about 0.6 seconds. This extremely short time scale suggests that the water dissolves into the solvent almost instantly compared to the process time scales.

Brine Separator: After leaving the mixer, the feed water in solvent emulsion reaches the first separation step where the un-dissolved brine is separated. In the laboratory prototype, a gravitational separator was found to be sufficient for brine separation, thus minimizing the energy consumption of this separation process. A schematic diagram of the separator design is

shown in Figure 29. The separator housing is a five gallon high temperature plastic bucket about 33 cm in height and having top diameter of 30 cm, tapering to about 25 cm at the bottom.

Two separator discs, made of acrylonitrile butadiene styrene (ABS) are placed into the housing. The liquid mixture enters the housing through a pipe below the bottom separator disc. This disc serves to minimize turbulence from the flow and any mixing of the brine with the contents above the plate. This disc has notches, as shown in the photographs in Figure 30, around its circumference to allow for the liquid to flow up, rise, and fill the separator bucket. As the mixture enters, the brine droplets, being heavier than the solvent, begin to settle gravitationally. Brine accumulates at the bottom of the separator and is discharged periodically into a waste tank from the brine outlet using a siphon pump. The solvent containing the pure water reaches the top and is extracted from the top solution outlet. The height difference between the mixture inlet and the top solution outlet is 20 cm. The top cover disc serves to contain the liquids within the housing and prevent splashing. This design is put into practice by constructing an insert, as shown in Figure 30(a), which is placed inside the separator bucket to completer the setup as shown in Figure 30(b).

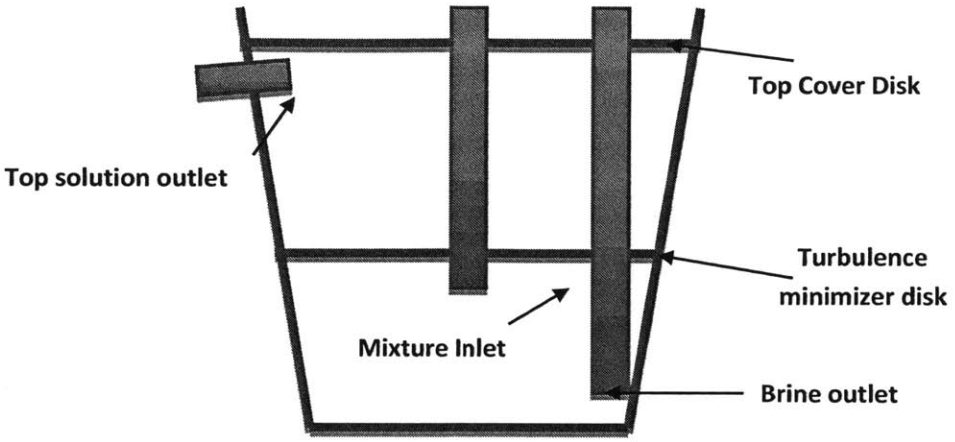

Figure 29. Schematic diagram of brine separator design; the solvent/ brine mixture from the mixer setup enters through the mixture inlet in the center, the solvent rises through notches in the turbulence minimizer disc and is extracted from the top solution outlet; the brine collects at the bottom and is discharged via the brine outlet using a siphon pump

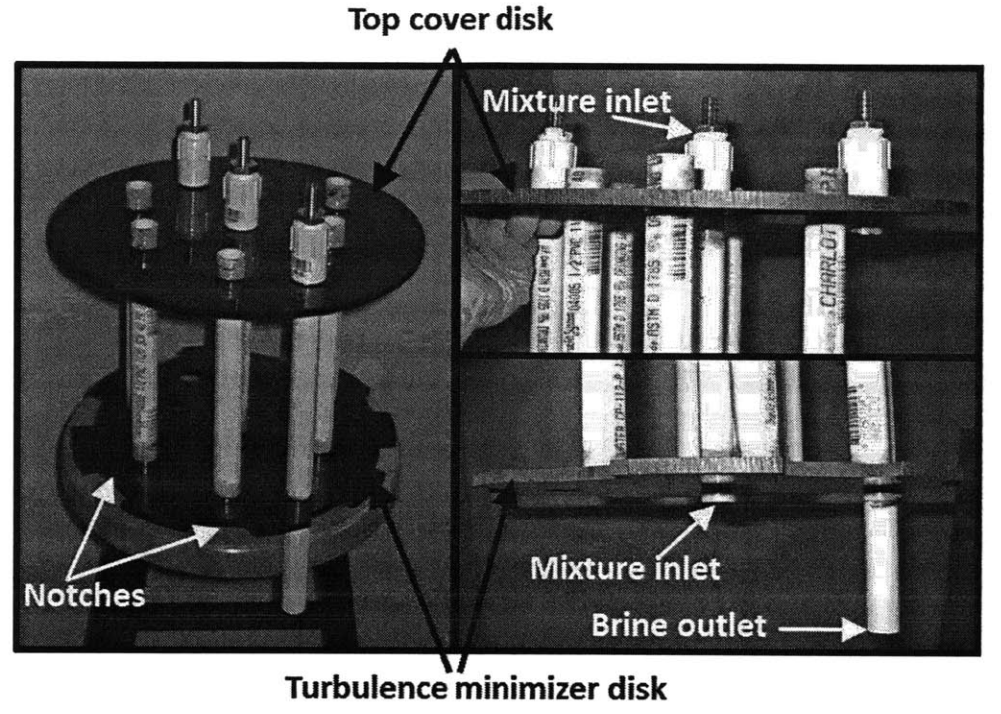

(a)

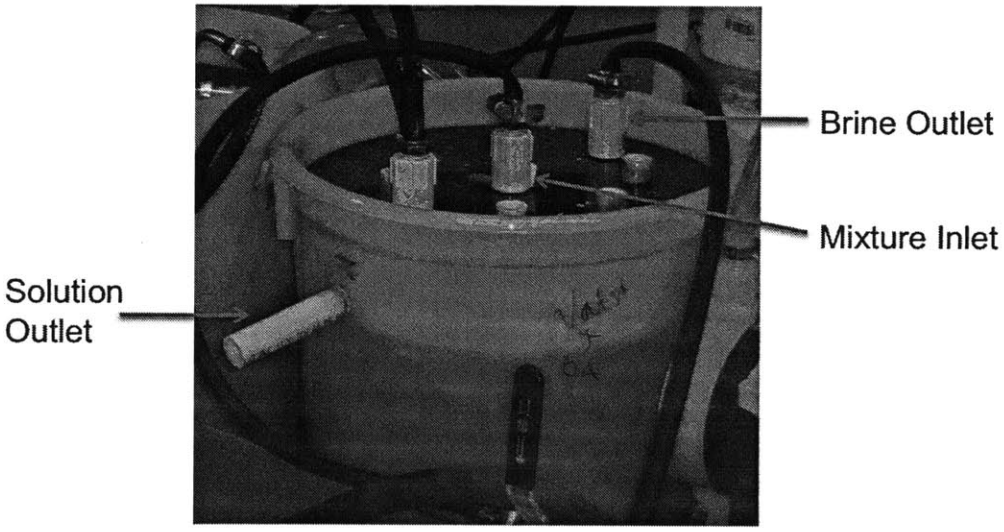

(b)

Figure 30. (a) Photographs of brine separator insert during construction; this insert is placed in a five gallon high temperature plastic bucket to complete the separator setup, and (b) external view of the completed brine separator

As previously discussed the gravitational settling of the droplets may be approximated as Stokes flow of a sphere (droplet) through a viscous fluid (solvent). The terminal velocity of the falling droplets is expressed as shown in equation (9), reprinted here for convenience:

$$v = \frac{1}{18}\left(\frac{\rho g D^2}{\eta}\right) \tag{9}$$

While the droplets are settling the bulk of the liquid, the solvent, rises at it fills up the separator bucket. The solvent containing the dissolved water is extracted at the top of this bucket. To ensure that the brine droplets do not reach the top outlet the residence time of the solvent in the brine separator must be greater than the time required for the brine droplets to settle through the height of the separator,

$$t_{res} > \frac{H}{v} \tag{11}$$

where, H is the height of the separator and v is the droplet terminal velocity.

The terminal velocity depends on the size of the brine droplets. The droplet size is expected to change with the mixing speeds and the resulting agitation. The droplet sizes should be smaller for higher mixing speeds. To investigate this, the droplet sizes were measured during prototype construction by taking samples of the solvent/ brine mixture from the mixer outlet. By the time of reaching the mixer outlet the dissolution of water is likely to have already happened and the remaining droplets would represent the un-dissolved brine.

The mixer stirrer was run at three different speeds, 500 rpm, 1000 rpm, and 1500 rpm. About 0.5 ml of the sample was taken, placed on a glass slide, and observed under a Nikon®

Eclipse LV100 microscope. Photographs were taken under bright field and at 40X magnification. Representative microscope photographs are shown in Figure 31(a) for 500 rpm and (b) for 1500 rpm. For a stirrer speed of 500 rpm, the brine droplet diameters were found to be in the range 30 to 195 μm with about 97% of the volume contained in droplets greater than 104 μm in diameter. For a separator height, H of 20 cm (as constructed), a residence time of greater than 169 seconds is required to separate 97% of the brine droplets. Similarly, for a stirrer speed of 1000 rpm, the brine droplet diameters were in the range of 11 to 59 μm with about 97% of the volume contained in droplets greater than 50 μm in diameter. Therefore to separate 97% of the brine droplets, a residence time of greater than 12 minutes is required. Finally, for a stirrer speed of 1500 rpm, the brine droplet diameters were in the range of 7 to 50 μm, with about 97% of the volume contained in droplets greater than 37 μm. Therefore to separate 97% of the brine droplets, a residence time of greater than 21 minutes is required.

The separator volume is 5 gallons (0.019 m^3), which allows for calculation of the maximum allowable flow rate depending on the required residence time for each stirrer speed,

$$\dot{Q}_{max} = \frac{V}{t_{res}} \tag{12}$$

where, V is the separator volume. Therefore the maximum allowable total liquid flow rates, to ensure that 97% of the brine droplets are separated, are 0.11 liters/ s, 0.026 liters/ s, and 0.015 liters/ s for 500 rpm, 1000 rpm, and 1500 rpm stirrer speeds respectively. These calculations are summarized in Table 5.

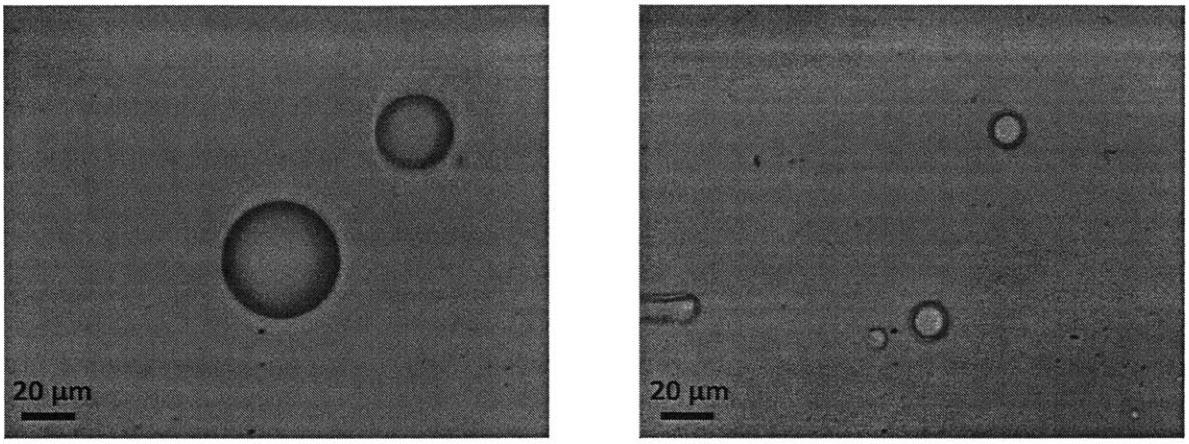

(a) (b)

Figure 31. Representative microscope photographs of water droplets in octanoic acid formed in the mixer at 500 rpm (a) and 1500 rpm (b) respectively. The photographs are taken at 40X magnification using a Nikon Eclipse LV100 microscope

Table 5. Droplet size distribution for different mixing speeds and the associated required residence times and maximum allowable flow rates

Mixing speed (rpm)	Drop size range (µm)	97% vol. cutoff size (µm)	Required residence time (min)	Max. allowable flow rate (L/s)
500	30 - 195	104	3	0.11
1000	11 - 59	50	12	0.026
1500	7 - 50	37	21	0.015

Chiller: After exiting the brine separator, the solvent – water solution must be cooled to precipitate out the desalinated water. In the original continuous process design this was accomplished in a heat exchanger. To simplify construction, heat recovery was not employed in the prototype device, and a chiller was used instead. This component is a simple design with a stainless steel immersion "wort" chiller placed inside a five-gallon plastic bucket as shown in Figure 32. Stainless steel is used as octanoic acid can be corrosive to copper which would

otherwise provide better heat transfer. Tap water is circulated through the chiller coils and used as the heat transfer fluid. The solvent-water solution begins cooling as soon as it enters the chiller bucket. The cooled liquid is expected to sink to the bottom of the bucket, where it is extracted using an Omega ® PHP-800 chemical metering pump similar to the one described earlier. It was observed that a clear liquid entered the chiller where it became cloudy upon cooling, due to water precipitation, as was also seen in the batch process experiments.

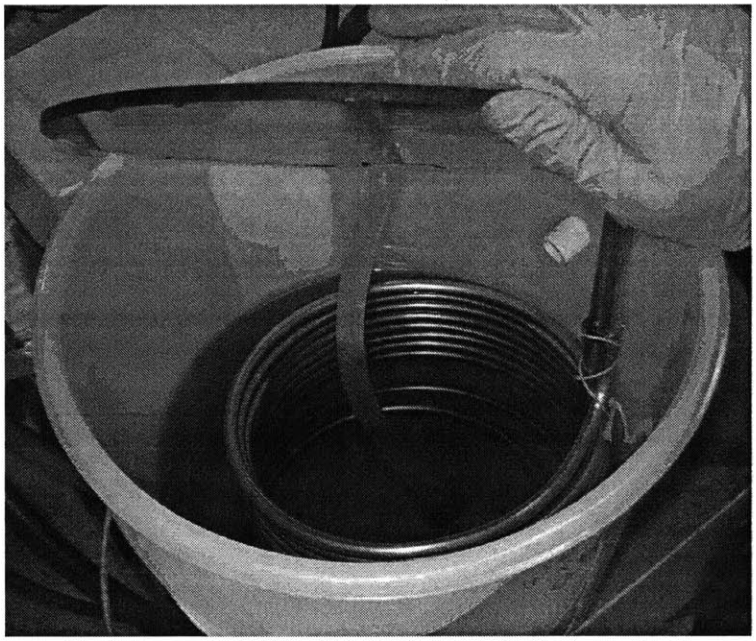

Figure 32. A stainless steel "wort" chiller placed inside a plastic bucket to cool the solvent-water solution; tap water is circulated through the coil and used as the heat transfer fluid

After cooling down in the chiller, the precipitated water must be separated from the directional solvent. This separation, as discussed earlier, may be accomplished through passive gravitational separation or accelerated through centrifugation, which increases the gravitational force, or by using an electrocoalescer which increases the size of water droplets by coalescing them so that they may settle faster under gravity. In every scenario, and much like the separation

of the brine from the solvent described earlier, the separation kinetics here also depend on the size of the water droplets suspended in the octanoic acid phase.

Samples of the solvent-water emulsion exiting the chiller were taken and observed under the microscope to measure the sizes of the water droplets. A representative microscope image is shown in Figure 33. The distinguishable droplets varied between 1 μm and 30 μm in diameter with over 97% of the volume contained within droplets larger than 5 μm. This droplet size range is in reasonable agreement with Kress' experiments [63] on water droplet formation in octanoic acid.

Again, treating the droplets as spheres settling under Stokes' flow through a viscous fluid, according to equations (9-11), 5 μm droplets would take over 30 hours to settle through a 30 cm height of a five-gallon bucket like the ones used as solvent and feed water reservoir. It is therefore desirable to accelerate this separation process.

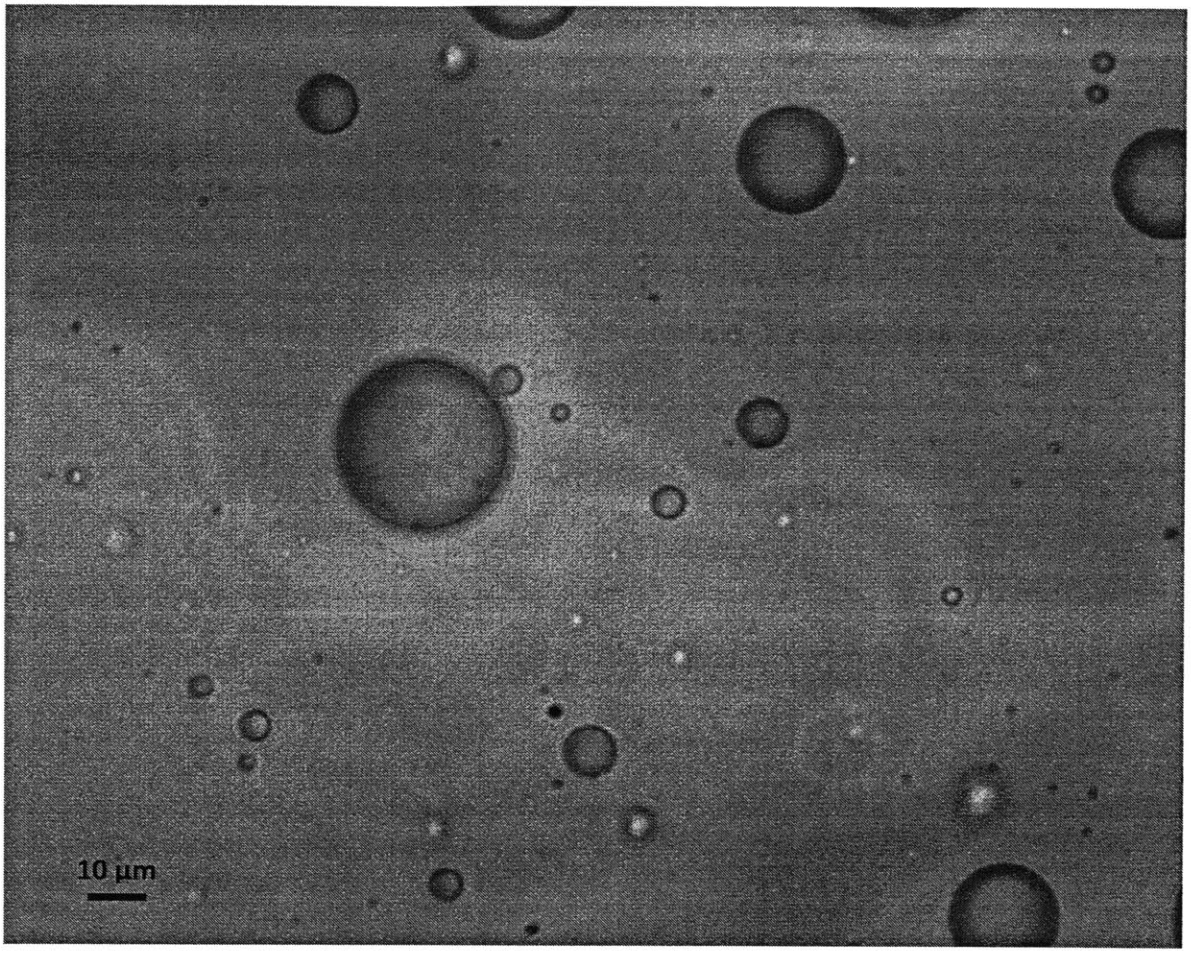

Figure 33. Microscopic image of precipitated pure water droplets in octanoic acid from samples collected after passing through the chiller in the continuous process prototype; images taken at 40X magnification using a Nikon ® Eclipse LV100 microscope

Centrifugal separator: A commercial in-line centrifuge, CINC® Model V02, was obtained from CINC industries, Carson City, NV. A detailed description of in-line centrifuge operation may be found in the equipment manual available on the internet [103]. According to manufacture specifications, this centrifuge is able to provide a maximum a relative centrifugal force of 1600g. The rotor diameter for this model is 5.1 cm, which is the distance that the water

droplets need to move through to get separated from the octanoic acid. According to equations (9-11), at the maximum force and to separate droplets larger than 5 μm the required residence time of the emulsion within the centrifuge is about 12 seconds. A residence time chart [103] from the equipment manual suggests that the residence time would be greater than 12 seconds for flow rates lower than 0.01 L/s, which also becomes the upper limit for the process flow rate. This serves to reduce the achievable throughput rates significantly.

Instrumentation: Temperature measurements were taken all along the process loop using installed in-line thermocouples as shown in Figure 34. These in-line thermocouples are inserted into the path of flow using T-adapters and thus provide continuous temperature readout in a clean, automatic way without manual intervention. Temperature readouts were obtained through an Agilent ® 34901A 20 Channel Multiplexer Module installed on an Agilent ® 34970A Data Acquisition Unit.

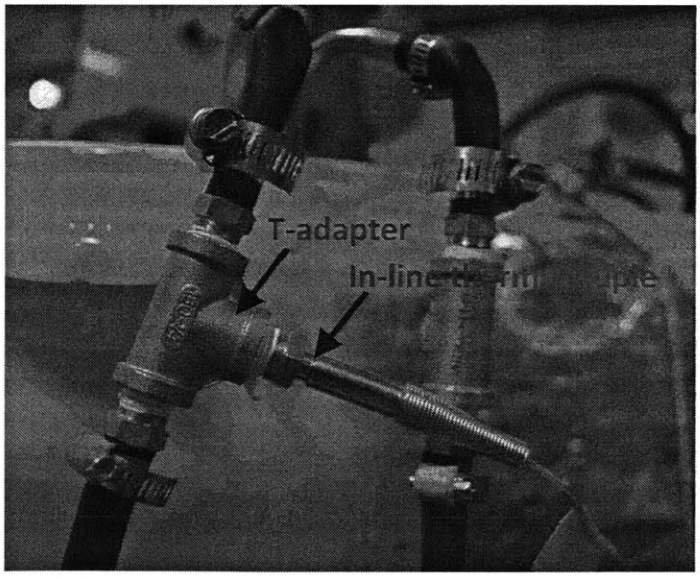

Figure 34. In-line thermocouples inserted in the flow path for continuous temperature read-out

The completed DSE continuous process prototype is depicted below in Figure 35. The unit's footprint is 90 cm x 60 cm and the total height is 190 cm including the mixer setup.

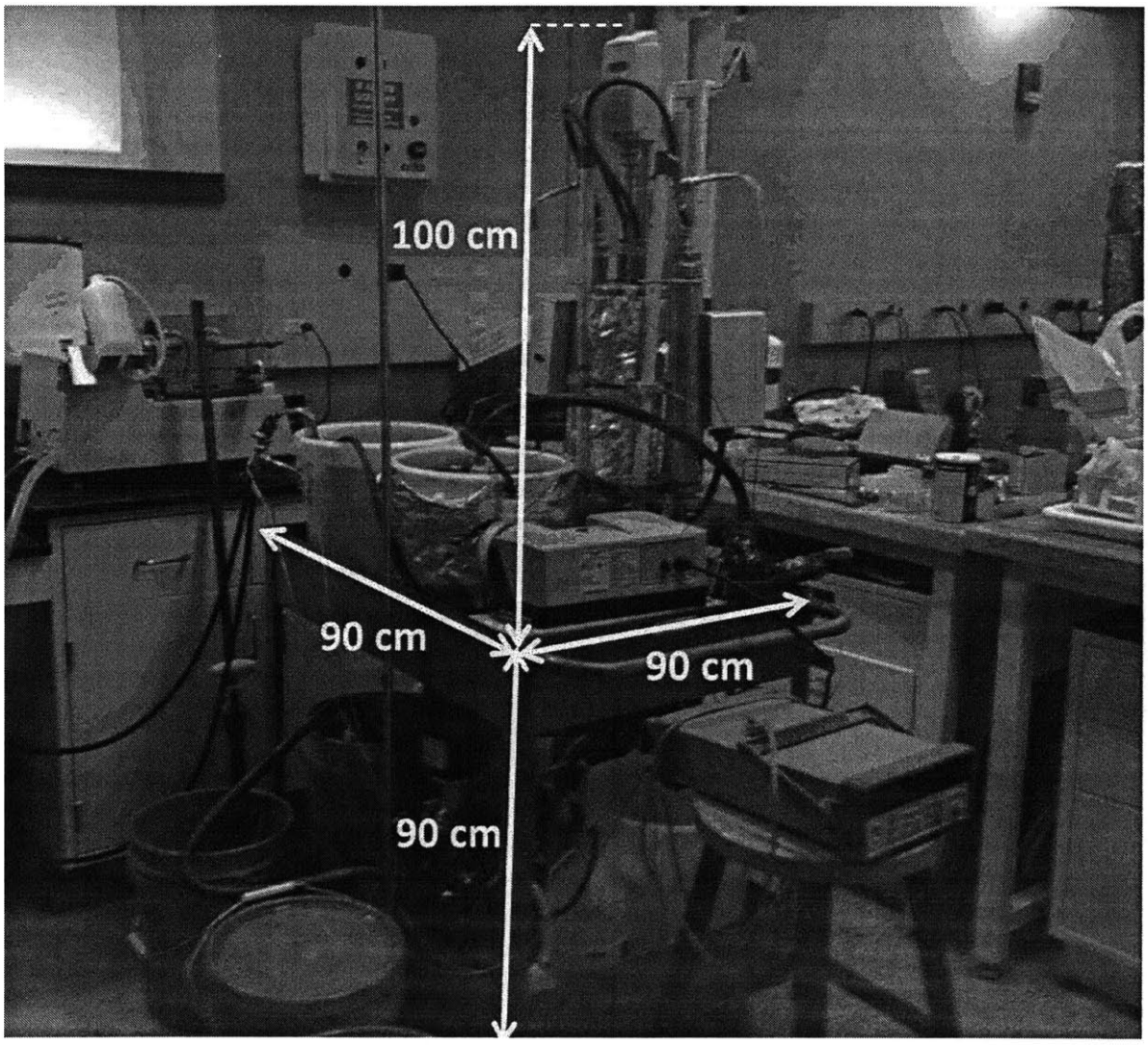

Figure 35. Completed Directional solvent extraction continuous process prototype mounted on a movable cart

6.3 Prototype testing & analysis

The DSE prototype was run with octanoic acid as the directional solvent and a 3.5% w/w aqueous solution of sodium chloride as feed. After significant troubleshooting all prototype components functioned as planned and expected in the design with reasonable variation, except the in-line centrifuge. The heaters were controllable and achieved high temperatures between 85 °C and 90 °C. The mixer met the desired performance metrics as discussed in section 6.2. The brine separator performed extremely well at the experimental flow rates with the product water containing very low salinities as discussed in the following text. The chiller functioned reasonably well.

The in-line centrifuge did not perform well in separating the precipitated water from the octanoic acid. The inlet and outlet of the centrifuge both appeared cloudy indicating the presence of water droplets emulsified in the octanoic acid. The centrifuge did not function as expected even at flow rates lower than 0.01 L/s, suggesting that the relative centrifugal forces provided were lower than those specified in the equipment manual. As an alternative, the samples of the water in octanoic acid emulsion from the chiller outlet were collected, placed in conical tubes and centrifuged in the already introduced laboratory centrifuge (Fisher Scientific ® Marathon 21000) at 5000 g for 60 seconds. This procedure was found to be sufficient for separating the water from octanoic acid. The weights of the recovered water and the chiller outlet samples were recorded and the yield and recovery calculated from these values. The salinities of the product water were also measured. Thus, while the entire process loop was not demonstrated, the performance of the continuous process was tested. The in-line centrifuge is a commercially available component and not critical to demonstration of the concept.

A representative once-through experimental run is depicted by the process diagram in Figure 36. The last connection in the cycle is represented by a broken line since it was not completed at the time of this compilation. The measured flow rates and temperatures at each step and for each inlet and outlet are also depicted. In addition, the calculated energy inputs from the electric heaters are shown.

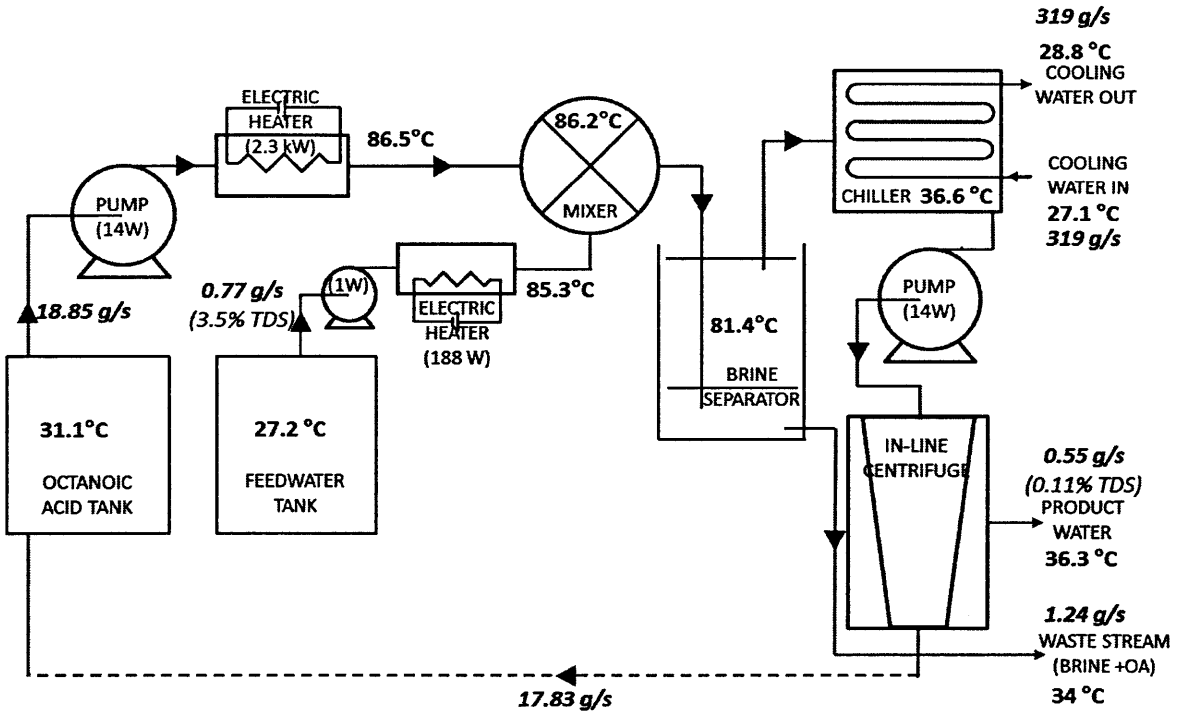

Figure 36. Process diagram for a representative semi-continuous once through DSE process with measured flow rates and temperatures listed for each step

As can be seen the prototype, in this run, operated with a feed water input of 0.77 g/s (66.5 liters/ day) which is about 0.42 bbl./ day, containing 3.5% starting TDS. The prototype produced desalinated water with 0.11% TDS at a rate of 0.55 g/s (47.5 liters/ day) which is about 0.3 bbl./ day, thus achieving about 71% recovery. The thermal energy consumption for this run is about 1251 kWh/ m^3. It must be noted that this prototype does not employ heat recuperation and

with an 80% heat recovery, as discussed in the process design, this run would have an energy consumption of 250 kWh/ m^3.

The actual electrical energy consumption for this process, due to pumping, was about 14.5 kWh_e/ m^3. It must be noted that the metering pumps used, while highly controllable, are energy inefficient and in this case a large part of the electricity is used by the display and the control module. In addition, the process flow path is not optimized and significant pressure losses exist that could be avoided with better flow path design. Typical pumping energy consumptions of industrial liquid pumping and solvent extraction processes are on the order of 0.01 - 0.04 kWh/ m^3 of fluid pumped [104–106]. In DSE, however, since the product water is only about 3% of the total flow volume, it is expected that the pumping energy consumption of the process, after optimizing the flow path and with using industrial centrifugal pumps, would be about 0.3 - 1.2 kWh/ m^3 of water desalinated.

The electrical energy consumption of the centrifugal separator, even if it had functioned as expected, would be about 30 kWh_e/ m^3, indicating that this may not be a viable separation technique in a commercial operation.

This experimental run also produced a waste stream at 1.24 g/s of which about 1.02 g/s is octanoic acid and 0.22 g/s is water. The process, therefore, resulted in 5.4% solvent loss. This solvent loss is a consequence of the position of the brine extraction outlet and the resulting entrainment of the solvent with the brine. This is a major challenge that must be addressed and potential ways of doing so are discussed in chapter 6.4. Performance parameters are summarized in Table 6.

Table 6. Performance summary of representative once-through DSE prototype run

Water production (bbl./day)	**0.42**
Recovery ratio	**71%**
Feed TDS	**35,000**
Product TDS	**1100**
Thermal Energy consumption (actual, kWh/ m^3)	**1251**
Thermal Energy consumption (with heat recovery)	**250**
Electrical Energy consumption (pumping, actual, kWh/ m^3)	**14.5**
Solvent loss	**5.40%**

A thermal energy balance analysis was conducted on the above described experimental run to verify the measurements and to estimate the heat losses. The total power input to the cycle is about 2.49 kW as represented by the electric heaters.

The two main sources of thermal losses are (1) the piping between the mixer and the brine separator, (2) the brine discharge piping and the brine collection tank. The losses in these sections may be calculated by doing a simple energy balance between the inlet streams and the outlets steam as depicted in Figure 36,

$$\Delta H = \dot{m}_{OA} C_{OA} (T_{in} - T_{out})_{OA} + \dot{m}_w C_w (T_{in} - T_{out})_w \tag{13}$$

where, $\dot{m}$ is the mass flow rate, C is specific heat, and T_{in} and T_{out} are the section inlet and outlet temperatures respectively. The subscript OA stands for octanoic acid, and w stands for water.

The heat losses were thus calculated and found to be about 215W for the piping between the mixer and the separator and 151W for the brine discharge piping and tank, which add up to about 15% of the thermal power input.

Drawing a control volume around the entire system, as shown in Figure 37, a complete systemic energy balance analysis was conducted. The enthalpy input comes from the octanoic acid, feed water, and cooling water inlets, the heat supplied by the electric heaters, and the work supplied by the pumps. The enthalpy output is via the product water, returning octanoic acid, and the waste stream outlets and the heat losses as already identified. At steady state, when the measurements were taken, the enthalpy input and output must be the same. Using the experimentally measured values as depicted in Figure 36, and the reference state of 0.01 ℃, the total calculated enthalpy input rate was 40,011 W and the total calculated output rate was 40,362 W; the two values are within an error of less than 1%, which most likely arises from measurement errors, especially in the chiller water flow rates which are much higher than all other inputs and outputs.

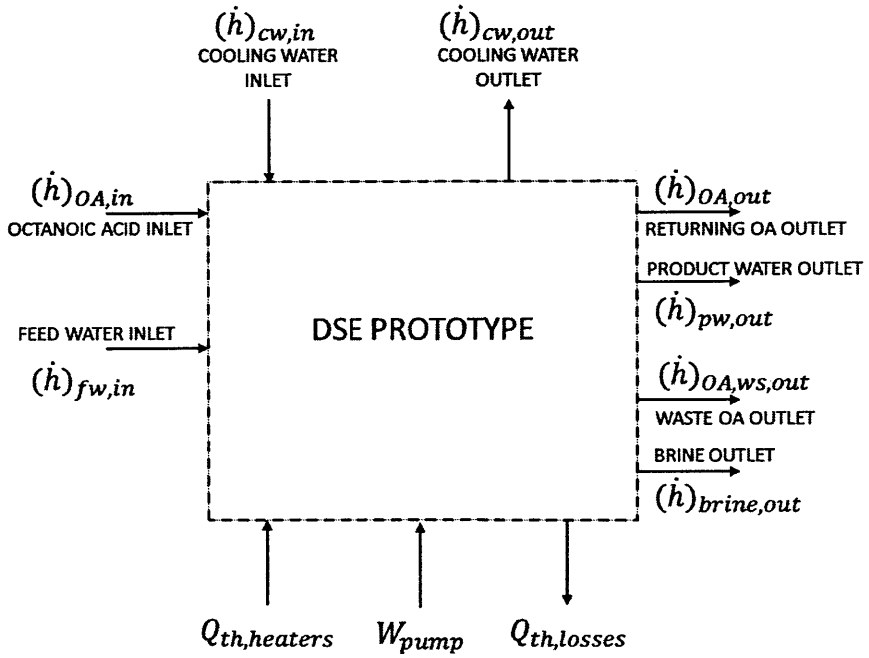

Figure 37. Energy balance around a control volume for the DSE prototype system

The prototype device was similarly tested over additional experimental runs with varying temperatures, flow rates, and feed to solvent ratios. The mixer stirring speed was kept constant at 1000 rpm through all experimental runs. The prototype experimental results are depicted graphically.

Figure 38 depicts product water salinity as a function of total liquid flow rates, which includes the solvent and the water. As calculated in chapter 6.2 the maximum allowable total liquid flow rate, for the brine separator to achieve 97% brine rejection give a 1000 rpm mixer stirring speed, is 0.026 L/s. Higher product salinity is therefore expected when flow rates are higher as may be seen from the plot.

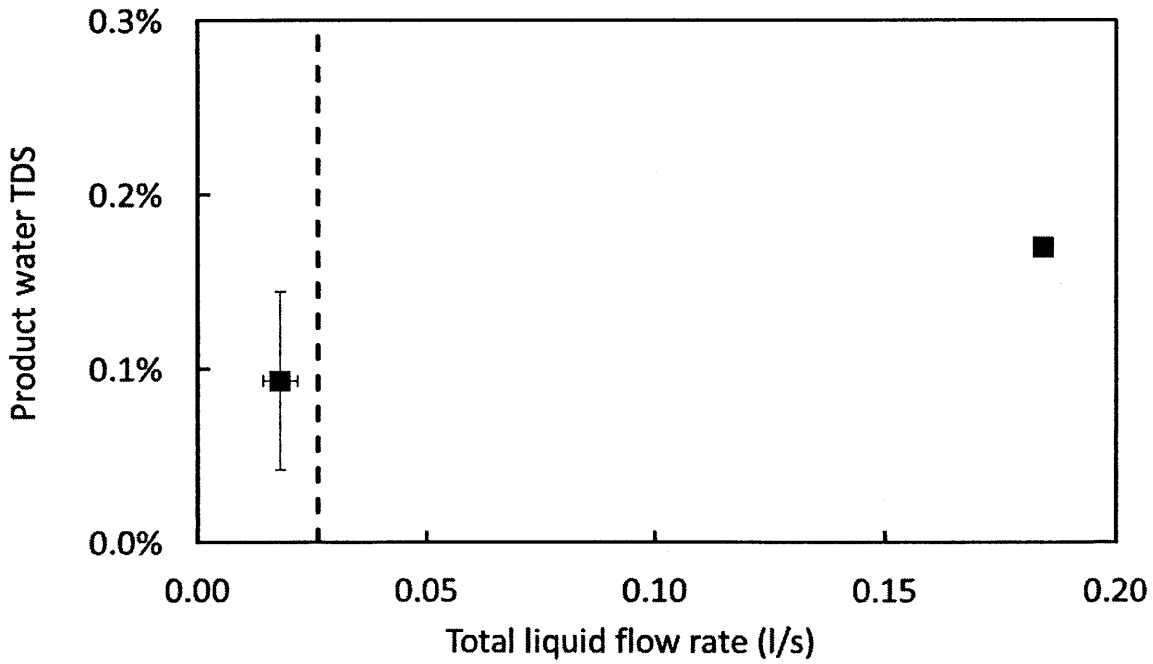

Figure 38. Product water TDS as a function of total liquid flow rate (both solvent and water) with feed TDS of 3.5%; the maximum allowable flow rate for at least 97% of the brine to separate with 1000 rpm mixer stirring speed is depicted by the broken line

Figure 39 shows the product water yield as a function of the driving temperature difference compared with the experimental yields obtained from the batch process. Also superimposed is the theoretically expected yield for pure water from Hoerr's solubility estimates [60]. As may be the prototype yields are similar to those obtained from the batch process and follow the same trend as the theoretically expected yields for pure water. This observation suggests that batch process experiments may be used to effectively predict yields from the continuous process and for a real industrial scenario.

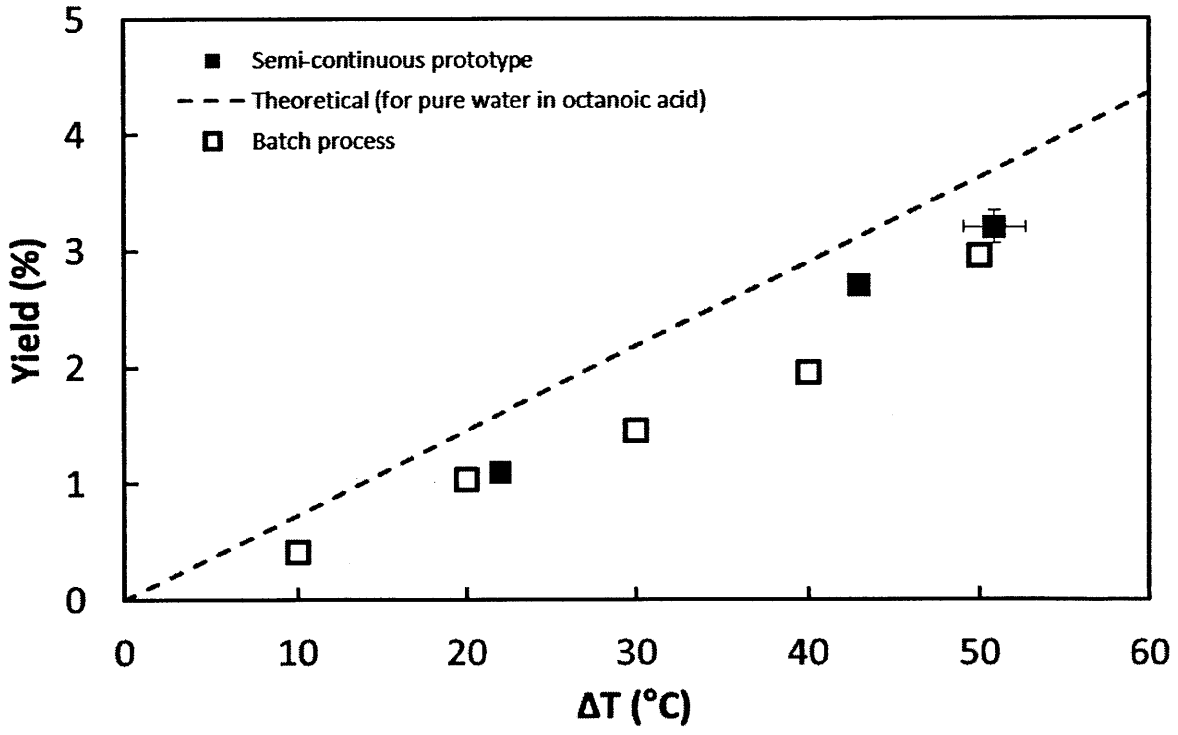

Figure 39. Product water yield for the semi-continuous DSE process prototype, as a function of temperature for when 3.5% TDS water is dissolved in octanoic acid and desalinated water is recovered (filled square), compared with batch process results for 3.5% TDS water in octanoic acid (open square) and with theoretically expected yield as calculated from Hoerr's solubility estimates [60] of pure water in octanoic acid (broken line).

Figure 40 depicts the obtained recovery ratios as a function of feed to solvent ratio and for two different driving temperature differentials (50 °C and 22 °C). It must be noted that some recoverable water was lost with the solvent loss in the waste stream. Recovery ratios adjusted for this solvent are also depicted to give an estimate of achievable recoveries when solvent loss is minimized. The batch process recovery ratios are depicted for comparison. Calculated theoretically expected recoveries for pure water using Hoerr's solubility estimates [60] are shown as well.

As seen from the plot, recoveries of over 70% were achieved for desalination of 3.5% TDS water using a driving temperature differential of 50 °C and recoveries of about 20% were achieved using a driving temperature differential of 22 °C. The recoveries obtained from the prototype are similar to those obtained from the batch process experiments and follow a similar trend to those theoretically expected for pure water.

These observations suggest that batch process experiments may also be used for effectively predicting expected recoveries from a continuous process and for varying temperatures.

Greater than 70% demonstrated recovery from the prototype further confirm this significant advantage of DSE over existing desalination techniques, especially for produced water applications.

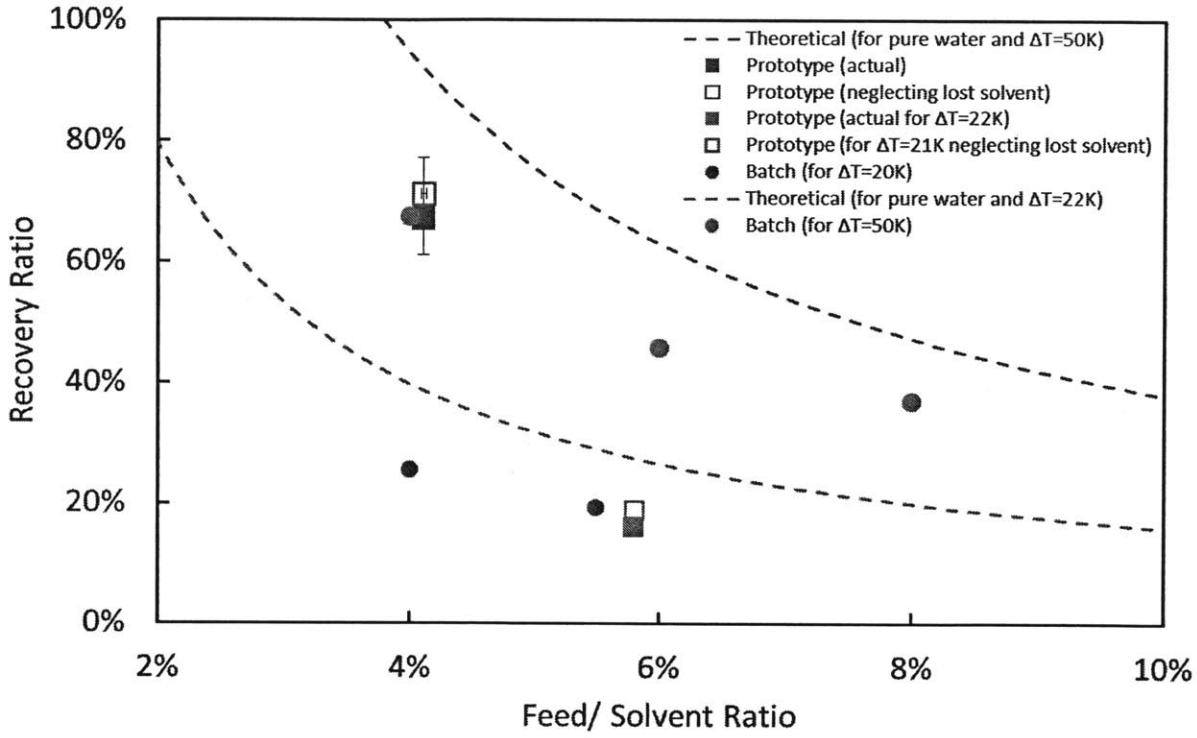

Figure 40. Recovery ratios for the semi-continuous DSE prototype as a function of feed to solvent ratio for starting feed TDS of 3.5% and for driving temperature differential of 50 ℃ (blue filled square) and 22 ℃ (orange filled square) and corrected for recoverable water lost with solvent loss in the waste stream (open squares); the results are compared with recoveries obtained from the batch process experiments for varying feed to solvent ratio and for driving temperature differential of 50 ℃ (green filled circle) and 22 ℃ (red filled circle); also shown are theoretically expected recoveries for pure water from Hoerr's solubility estimates [60] for driving temperature differential of 50 ℃ (blue broken line) and 22 ℃ (orange broken line)

Finally, an important process parameter, the cycle time was estimated. Cycle time may be estimated by measuring the total functional volume of the prototype device and dividing that by the volumetric flow rate,

$$t_{cycle} = \frac{V_{functional}}{Q_{total}} \tag{14}$$

To measure the functional prototype volume the system was purged of liquids and the cycle loop was closed, i.e. the chiller outlet was connected to the solvent reservoir as an input. This ensured that any liquid going into the cycle returned to the solvent reservoir. The water reservoir was taken out of the process loop since it is a minor volume. The solvent reservoir was then filled with octanoic acid and the solvent pumps were run at 0.01 liters/ second. As the octanoic acid level in the solvent reservoir fell more octanoic acid was added to maintain the level. This was continued until the octanoic acid level became steady, i.e. the inflow was equal to the outflow, which implied that the functional system volume was then full. The pump power was then gradually increased to 0.03 liters/ second to ensure that this increase did not change the solvent level. The total volume of octanoic acid added then gave the functional system volume. This volume was found to be about 32 liters.

Therefore at the flow rate of 0.018 liters/ second as demonstrated in the representative run the cycle time was about 30 minutes and that at the maximum allowable flow rate of 0.026 liters/ second was about 20 minutes. Adding 30 to 60 seconds for centrifugal or coalescer separation would not change these times significantly. With improved process design it is likely that this process time would be reduced to half or less. Possible modifications to reduce this time are discussed in the following section.

6.4 Discussion and Improvements

The design and construction of the continuous DSE prototype is discussed and its successful operation is demonstrated. The system is shown to be most effective in producing desalinated water up to 0.5 bbl. / day at a greater than 70% recovery ratio. For a starting feed

TDS of 3.5% w/w, the product water was found to contain about 0.1% TDS indicating greater than 97% salt rejection. It was shown that once heat recovery can be employed the constructed laboratory prototype would have a thermal energy consumption of 250 kWh/ m^3 which translates to a GOR of 2.5. This thermal energy consumption is for operation between a heat source temperature of 90 ℃ and an ambient temperature of 25 ℃. The effect of certain process parameters such as flow rate, driving temperature difference, and feed-solvent mixing time is analyzed and an energy balance was conducted to verify the accuracy of temperature and flow measurements.

As also mentioned in the preceding text, a significant shortcoming of the continuous DSE prototype demonstration was the high solvent loss (>5%) due to entrainment which could serve to hurt the process performance and economics. Further process and device development should aim to minimize this solvent loss. One design modification to accomplish this could be to replace the manual siphon pump in the brine separator with an automatic pump placed below the brine-solvent interface and equipped with a liquid density sensor to prevent any solvent (lighter liquid) from being extracted along with the brine.

Another key area of improvement in prototype design is reduction of the process cycle time. A possible modification to reduce cycle time this may include optimal sizing of the brine separator such that the flow residence time in this component is just enough to allow the brine droplets to settle through its height; this may require the use of a shallower and wider brine separator. Another possible medication to reduce cycle time is to reduce the size of the mixer such the residence time in this component minimal, especially since it is observed that the water dissolves into the solvent almost instantaneously.

Chapter 7 Economic Analysis

An economic analysis is necessary to assess the commercial feasibility of the developed directional solvent process. Without the likelihood of commercial feasibility it may be difficult to finance the further development and field deployment of a DSE test facility. A detailed economic analysis was therefore conducted and is presented in the following chapter. The analysis was conducted for two scenarios: (1) the laboratory prototype with the actual lab costs incurred and no heat recovery employed, and (2) for the expected pilot prototype with reduced procurement costs and energy savings due to the use of heat exchangers. To reiterate, the current cost for large scale seawater desalination are in the range of $\$1/m^3$ and for small scale seawater desalination they can be between $\$3/ m^3$ to over $\$ 12/ m^3$. Costs of produced water handling may range from $\$12/ m^3$ to over $\$60/ m^3$

7.1 Laboratory prototype economics

A detailed cost estimate for the prototype raw materials, components, and construction costs is shown in Table 7. As may be seen the full constructed system cost $22,175, including labor, of which about 33% is the centrifuge alone and about 24% is the construction cost. This system was shown to operate most effectively (lowest product salinity) for water throughput rates of about 0.5 bbl. / day ($0.08 m^3$/ day).

A cost analysis worksheet is shown in Table 8. The thermal energy consumption without heat recovery was assumed to come from a natural gas heat source and the actual electricity consumption of the pumps was included in the worksheet. Natural gas price was assumed to be

at $2.28/ MMBtu, the average US wellhead price for 2012 [107], and electricity cost was assumed to be $0.07/kWh, the average industrial price for 2012 [108]. The octanoic acid price was assumed to be $3200/MT, the actual bulk pricing in February 2012 [109]. A typical estimate for fixed O&M costs of desalination plants is less than 2% of the capital cost [110]. However, since DSE is a new technology a higher annual fixed O&M of 5% of the capital cost is assumed. A physical plant life of 5 years, a capacity factor of 90%, and discount rate of 8% are used.

As may be seen from the worksheet the total levelized cost of water desalination is about $243/ m^3 or $40/ bbl. These costs are higher than current seawater desalination plants by two orders of magnitude but only about 4 times the cost of handling produced water in the Marcellus region of Pennsylvania. It must be noted that these costs are for a first ever demonstration unit in an un-optimized laboratory setting, where individual components were purchased from lab-scale suppliers at very high prices. Additionally the lack of heat recovery in the prototype contributes to about 5 times higher thermal energy costs as a field test unit would be expected to consume.

Table 7. Actual incurred cost of laboratory prototype raw-materials, components, and labor costs for construction and assembly

Component	Description	Supplier	Unit price	Qt.	Cost (USD)
Reservoir tanks	Polyethylene Buckets - 5 gallon	Mcmaster Carr	$18.00	4	$72.00
	Bucket lids	Mcmaster Carr	$3.00	4	$12.00
Pumps	Digital control Chemical Metering Pumps for solvent	Omega	$1,431.00	2	$2,862.00
	Solenoid metering pump for feed water	Prominent	$325.00	1	$325.00
Heaters	1 kW electric flow-through heater	Omega	$525.00	1	$525.00
	5 kW electric flow-through heater	Omega	$550.00	1	$550.00
Mixer	4" CPVC Pipe - 2'	US Plastics	$24.00	1	$24.00
	4" CPVC End caps	US Plastics	$25.00	2	$50.00
	Digital stirrer and stand	ESP Chemicals	$770.00	1	$770.00
	Stirrer shaft	ESP Chemicals	$189.00	1	$189.00
	Stirrer propeller blade	ESP Chemicals	$75.00	1	$75.00
Brine separator	Polyethylene bucket - 5 gallon	Mcmaster Carr	$18.00	1	$18.00
	2' x 2' x 1/8" ABS sheet	Mcmaster Carr	$25.00	2	$50.00
	1/2" PVC pipe - 4'	Mcmaster Carr	$8.00	1	$8.00
	Siphon pump	Mcmaster Carr	$4.00	1	$4.00
Chiller	Polyethylene bucket - 5 gallon	Mcmaster Carr	$18.00	1	$18.00
	Immersion 'wort' chiller	NY BrewSupply	$43.00	1	$43.00
Centrifuge	Model V02 centrifuge and accessories	CINC Industries	$6,452.00	1	$6,452.00
Piping, Valves & Fittings	1/2" Neoprene tubing (ft)	Mcmaster Carr	$1.28	100	$128.00
	SS Ball valves	Mcmaster Carr	$11.00	6	$66.00
	SS Hose clamps (100 pk)	Home depot	$10.00	100	$1,000.00
	Insulation	Home depot	$44.00	1	$44.00
	Other SS adapters and Plumbing fittings	Mcmaster Carr/ Home depot	$80.00	1	$80.00
Instrumentation	In-line thermocouples with adapters	Omega	$40.00	8	$320.00
	Data Acquisition Card	Agilent	$490.00	1	$490.00
Solvent	Octanoic acid (by kg)	Sigma Aldrich	$20.00	40	$800
Labor (Construction & Assembly)	**Hourly labor**		**40.00**	**120**	**4800.00**
TOTAL					**$19,775.00**

Table 8. Cost analysis worksheet for DSE laboratory prototype without heat recovery and natural gas as thermal energy source and including actual incurred costs for raw material, components, and labor

Levelized Cost Worksheet for DSE desalination plant			
Inputs in blue			
Capacity		**Solvent**	Octanoic
gpd	21	Product water yield	3.30%
m3/d	0.08	Solvent/ Water Loss Ratio	0.001
bbl/d	0.5	Solvent Density (kg/m3)	910
		Solvent cost ($/MT)	$3,200.00
Capital Cost		**Energy consumption**	
Total	$19,775	Thermal (kWh/m3)	1251
$/g/d	**$ 942**	Electrical (kWh/m3)	42
$/m3/d	**$ 264**	NG price (@/MMBTU)	$2.28
		Elec. Price ($/kWh)	$0.070
Line		Capital Cost (CC)	
1		Capital Cost	$19,775.00
		Yearly Operating Cost	
2		Annual Fixed O&M - (% of Line 1- CC)	5.00%
3		Variable O&M - Energy cost ($/m3)	$12.64
4		Variable Consumable - Solvent loss ($/m3)	$2.91
		Capital Recovery Computation	
5		Physical Life of Plant (Years)	5
6		Interest Rate (%)	8.00%
7		Capital Amortization Factor (CAF)	0.250
		Capacity	
8		Water recovered per day (m3)	0.08
9		Capacity Factor	90.00%
10		Water Recovered per Year (m3)	26.11
		Levelized Annual Cost	
11		Annual Amortization	$4,952.78
12		Annual Fixed O&M	$988.75
13		Annual Levelized Cost ($/m3)	$227.52
		Total Cost Calculated	
14		Annual Levelized Cost ($/m3)	$227.52
15		Variable O&M ($/m3)	$15.55
16		**Total Levelized Cost ($/m3)**	**$243.07**
17		**Total Levelized Cost ($/barrel)**	**$40.51**

7.2 Projected field economics

The analysis conducted for the laboratory prototype was extrapolated to project the economics of a DSE field unit for produced water treatment. A 25 bbl. / day (4 m^3/ day) unit is sized and analyzed for economic performance. This size means that the unit takes 25 bbl. / day as input and at a 70% recovery ratio, produces about 18 bbl. / day of treated water and 7 bbl. / day of highly concentrated brine. A product water yield of 2.5% for high TDS water (100,000 ppm) with a 65 ℃ temperature differential, as demonstrated earlier, is assumed. For a 100,000 ppm feed this plant is expected to produce desalinated water of 4000 ppm as demonstrated by the batch process experiments.

Heat exchanger and thermal energy consumption: There is a trade-off between the heat exchanger cost and lifetime and its effectiveness which relates directly to the energy consumption of the process. The heat exchanger is also likely to be the most expensive component of the system. Plate heat exchangers, due to their superior performance to other types, are the preferred configuration in desalination applications [111]. A plate heat exchanger for the given flow rates and fluid properties was designed in Aspen Exchanger Design & Rating (EDR) software. Its cost was estimated using specifications from manufacturer Alfa Laval (Plate M-6) and Titanium as the material of construction. Titanium has excellent resistivity in saline water environments and is the preferred construction material for heat transfer surfaces in desalination plants [111–113]. It is difficult to develop a mathematical relationship between heat exchanger cost and effectiveness as these vary significantly on a case by case basis. The optimal effectiveness was thus found iteratively by changing designs in Aspen EDR. For this scenario a

heat exchanger effectiveness of 77% was found to be optimal. This results in thermal energy consumption of about 340 kWh/m^3 for treating 100,000 ppm feed water.

Electrical energy consumption: The electrical energy consumption for pumping depends upon the pressure drop across the flow path of the system. Most of this pressure is expected to be within the heat exchanger which has the narrowest flow channels and thus the maximum flow restricting surface area. The pumping electricity consumption will therefore depend upon the heat exchanger design. From the Aspen EDR heat exchanger design the total pressure drop across it was found to be about 97 kPa. For this pressure drop and the given flow rates the pumping energy consumption is found to be about 2.37 kWh/ m^3. Electricity consumption for the electrocoalescer separation is estimated to be 0.06 – 0.6 kWh/ m^3 [114]. A value of 2.75 kWh/ m^3 is therefore used for total electrical energy consumption. This, however, does not have a significant effect on the overall system economics.

A cycle time of 10 minutes, half of the prototype cycle time is assumed, which implies that 144 cycles can be run in a 24 hour day. It was assumed that some solvent will get lost due to dissolving in the desalinated water and brine. This is estimated to be about 0.6% (600 ppm, slightly higher than the estimated solubility of octanoic acid in water) of the feed water flow rate. These plant specifications are summarized in Table 9.

Table 9. Specifications for a 25 bbl. / day DSE produced water desalination plant

Water production	**17.5 bbl./ day**
Product water flow rate	**0.033 kg/s**
Octanoic acid flow rate	**1.34 kg/s**
Recovery ratio	**70%**
High process temp	**90 ºC**
Ambient temp	**25 ºC**
Feed TDS	**100,000 ppm**
Product TDS	**4000 ppm**
Product water yield	**2.50%**
Heat recovery	**77%**
Energy Consumption	**340 kWh_{th}/m^3, 2.75 kWh_e/m^3**
Cycle time	**10 minutes**
Solvent loss	**0.6% of feed**

Capital costs: Costs of manufacturing the DSE desalination plant were estimated as follows.

The Aspen EDR generated diagram of the heat exchanger is depicted in Figure 41. The empty weight of this heat exchanger was estimated to be 23.4 kg and the cost was estimated to be USD 11,739.

Electrocoalescers are employed for separation of the precipitated water from the octanoic acid at the end of the process cycle. Due to the lack of electrocoalescer use for small scale application, it was difficult to obtain a product quote, but a price estimate from Ecofine® Filtration Products Co. Ltd, China , suggested that a small scale coalescer could be obtained for USD 1000 – 2000 [115]. A cost of USD 1500 was therefore used for the economic model.

Brine separator and mixer assembly costs were estimated by using a multiple of the laboratory prototype costs. For a system size of about 35 times the most effective range of the laboratory prototype (17.5 bbl. / day vs. 0.5 bbl. / day desalinated water), it is assumed that the brine separator will cost about 10-15 times more. The lab prototype mixer, however, was demonstrated to operate effectively even for over 10 times the most effective limit (see Figure 38). It is therefore assumed that the mixer cost for the field prototype will be less than twice of that for the lab prototype.

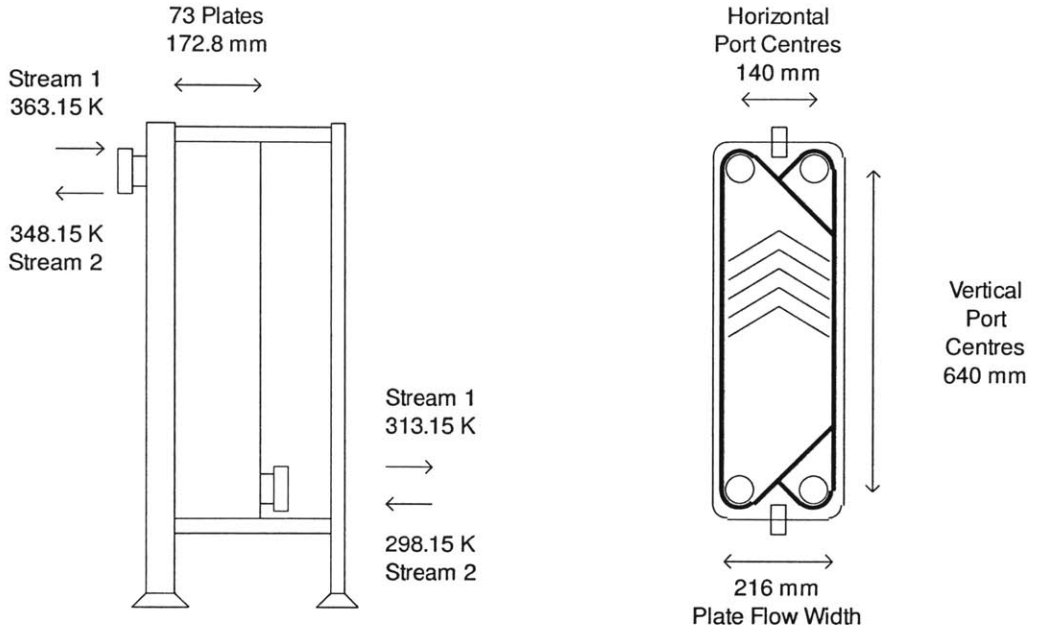

		Plate thickness	0.4 mm
Actual surface area	10950000. mm2	Compressed plate pitch	2.4 mm
Number of passes Stream 1 / 2	3 /3	Area of each plate	150000. mm2
Effective channels Stream 1 / 2	36 / 36	Chevron angle (to horizontal)	31
Number of exchangers	1	Material type	Titanium
		Port diameter	60 mm

Figure 41. Plate heat exchanger design from Aspen Exchanger Design & Rating software for the 10 bbl. / day DSE produced water desalination plant; heat exchanger effectiveness is 0.8

Costs of fluid containers/ reservoirs are estimated to be 7 times more than those for the laboratory prototype. The cost of the octanoic acid pump is assessed from the specifications of a Dayton ® 10 GPM, 1 HP, chemical resistant pump, that may be obtained from Grainger for USD 805 [116]. The cost of piping was estimated to be 20% of the heat exchanger cost. The housing, instrumentation, and control were estimated to be about 25% of purchased equipment cost [117]

and construction and assembly costs were estimated to be about 20% of the total cost of all materials and components [118].

In addition to the components and materials, the initial batch of octanoic acid also comprises a capital cost. At the desalinated water throughput rate of 17.5 bbl. / day (0.0128 kg/s), 2.5% recovery, and 144 cycles per day, as discussed earlier, the system will require about 809 kg of octanoic acid in circulation which would cost USD 2589. Capital cost estimates are summarized in Table 10. The total capital costs for a 25 bbl. / day DSE produced water desalination plant are estimated to about USD 33,000.

Using these capital costs, the specifications in Table 9, a system lifetime of 10 years, fixed O&M of 5%, capacity factor of 90%, and, discount rate of 8%, the total levelized costs were calculated as depicted in Table 11. The levelized cost of water desalination was found to be \$12.20 / m^3 or about \$2.03 / bbl. for 100,000 ppm feed water. It is observed that while the estimated costs may not make this economical for seawater desalination, the economics look extremely promising for produced water treatment.

Table 10. Capital cost estimate for a 25 bbl. / day DSE produced water desalination plant

Tanks/ fluid reservoirs	\$1,120
Pumps	\$805
Mixer assembly	\$2,200
Brine separator assembly	\$560
Heat exchanger	\$11,739
Electrocoalescer	\$1,500
Piping	\$2,348
Housing, instrumentation & control (25%)	\$5,068
Construction/ assembly (20%)	\$5,068
Octanoic acid	\$2,589
Total	**\$32,996**

Table 11. Projected cost analysis worksheet for a 25 bbl. / day DSE produced water desalination plant with heat recovery and natural gas as thermal energy source

Levelized Cost Worksheet for DSE desalination plant			
Inputs in blue			
Capacity		**Solvent**	Octanoic
gpd	769	Product water yield	2.50%
m3/d	2.91	Solvent/ Feed Water Loss Ratio	0.0006
bbl/d	17.5	Solvent Density (kg/m3)	910
Cycles/day	144	Solvent cost ($/MT)	$3,200.00
Capital Cost		**Energy consumption**	
Total	$ 32,996	Thermal (kWh/m3)	342
$/g/d	**$ 43**	Electrical (kWh/m3)	2.75
$/m3/d	**$ 264**	NG price (@/MMBTU)	$2.28
		Elec. Price ($/kWh)	$0.070
Line		Capital Cost (CC)	
1		Capital Cost	$32,996
		Yearly Operating Cost	
2		Annual Fixed O&M - (% of Line 1- CC)	5.00%
3		Variable O&M - Energy cost ($/m3)	$2.84
4		Variable Consumable - Solvent loss ($/m3)	$2.50
		Capital Recovery Computation	
5		Physical Life of Plant (Years)	10
6		Interest Rate (%)	8.00%
7		Capital Amortization Factor (CAF)	0.149
		Capacity	
8		Water recovered per day (m3)	2.91
9		Capacity Factor	90.00%
10		Water Recovered per Year (m3)	956.63
		Levelized Annual Cost	
11		Annual Amortization	$4,917.41
12		Annual Fixed O&M	$1,649.81
13		Annual Levelized Cost ($/m3)	$6.86
		Total Cost Calculated	
14		Annual Levelized Cost ($/m3)	$6.86
15		Variable O&M ($/m3)	$5.34
16		**Total Levelized Cost ($/m3)**	**$12.20**
17		**Total Levelized Cost ($/barrel)**	**$2.03**

Critical process parameters that affect the overall economics of DSE are product water yield per unit volume of the solvent and the total process cycle time. A higher product water yield (for example that with octanoic acid as compared to decanoic acid) would result in the use of smaller solvent volumes and, consequentially, smaller system sizes and lower energy consumption. Shorter cycle time would reduce the total solvent volume in the system, thus also reducing the size of some components such as the solvent reservoirs but without affecting any major components such as the heat exchanger or the energy consumption. The economic sensitivity to product water yield and cycle time was analyzed and the observed trends are depicted in Figure 42.

As can be seen the cost reduces rapidly as number of cycles are increased but the economic gains diminish significantly beyond 100 cycles per day or when the cycle is shorter than 14 minutes. As demonstrated earlier the experimental cycle is already about 20-30 minutes. When designing a DSE device it is important to ensure that cycle time is shorter than 20 minutes. Cycle times longer than 30 minutes may render the process uneconomical.

Additionally the plot shows that increasing product water yield can have the most significant impact on lowering the cost of desalination. This may be achieved by discovering new solvents. With a solvent that can provide 10% product water yield, it may be possible to achieve costs of less than \$1 / bbl. (< \$6/m^3) at which level DSE may become economical even for small scale seawater desalination.

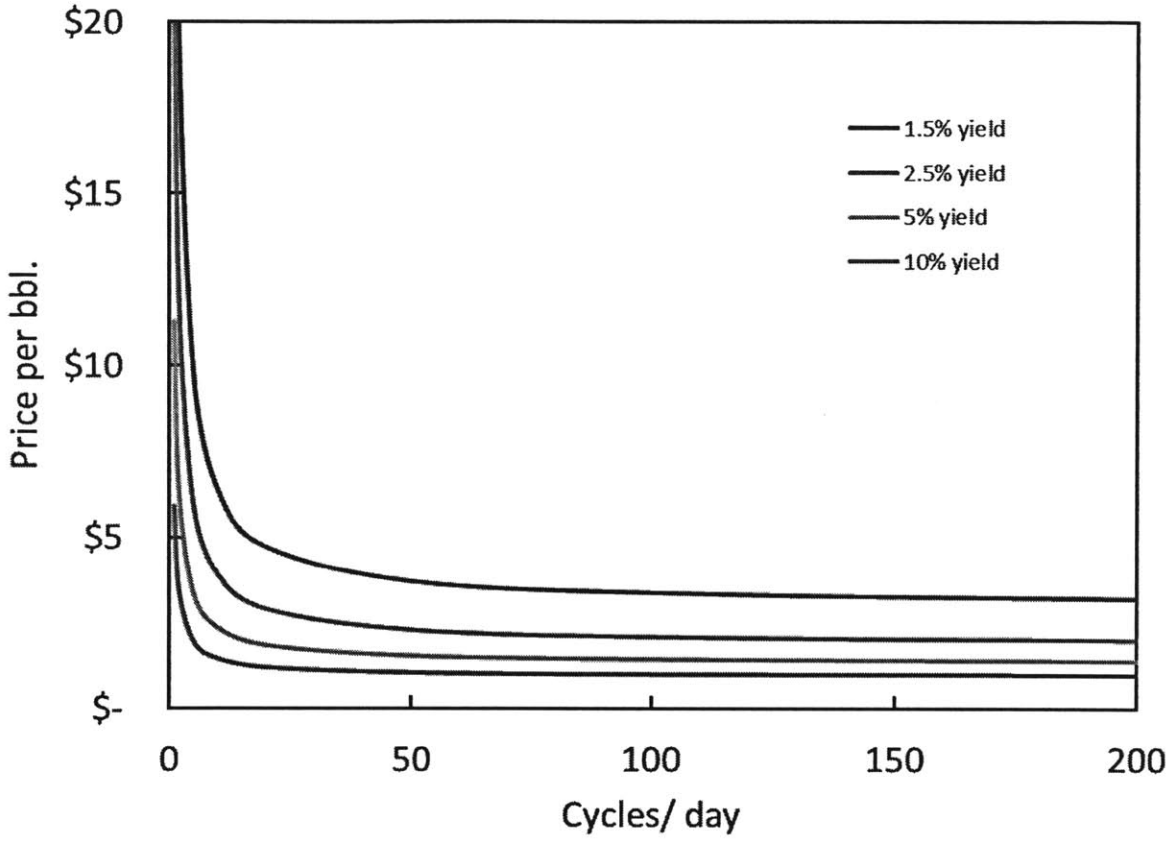

Figure 42. Price per barrel of treating produced water as a function of product water yield and number of cycles per day

Chapter 8 Summary and future directions

Here, we demonstrate Directional Solvent Extraction (DSE) as a new membrane free, low temperature method for desalination of water with applications in production of drinking water from the oceans as well in treatment of flowback and produced water from unconventional oil and gas extraction. DSE is demonstrated to deliver >97% salt rejection for samples of salinity similar to seawater and >95% for salinity similar to produced water. For seawater concentrations DSE is demonstrated to achieve recovery ratios of over 70% with a single stage process and almost 85% with a three-stage process. It is shown that DSE could operate at low temperatures and therefore may become an effective way of utilizing abundant and inexpensive waste heat. In addition, it is shown that DSE has the potential of being effective and economical as a process for desalination of high TDS waters.

Directional solvents dissolve water while rejecting water soluble salts, and, and are themselves insoluble in water. DSE works by dissolving water from a saline solution into a directional solvent by increasing its temperature. The directional solvents extract the water phase but reject salts and other contaminants. These salts are then separated and removed. Upon cooling back down the water precipitates out of the solvent, is recovered as purified water, and the solvent is reused. Importantly the solvent does not itself dissolve into water and the recovered water therefore contains a negligible amount of residual solvent. The directional solvents discussed in this work are hexanoic acid, octanoic acid, decanoic, and soybean oil. These fatty acids and oils dissolve water due to the presence of the carboxylic acid group (COOH) at their chain ends. The highly polar C=O and O-H groups facilitate the formation of hydrogen bonds with water molecules. While this chain end is hydrophilic the rest of the fatty acid molecule is

hydrophobic. The lowest fatty acids are miscible with water but as the chain length increases the solubility of both substances in each other decreases significantly. Octanoic acid and decanoic acid lie in the optimal chain length range and were found to be the most effective.

A proof of concept of the DSE technology is demonstrated through a bench-top batch process which shows that the process can be operated using low temperature energy sources. It is shown that starting with a feed solution of 35,000 ppm (to simulate seawater) DSE can deliver product water with concentrations in the range of 500 – 1000 ppm, which meets WHO drinking water salinity standards. DSE is also shown to be effective in desalination of high TDS water up to and including saturated brines. With starting feed solution of 100,000 ppm the process delivered product water with concentrations in the range of 3000 -6000 ppm, which is acceptable in the produced water treatment application. It is shown that the thermal energy consumption of DSE, with heat recovery, to desalt seawater would lie in the range of 350 kWh_{th}/m^3 and 480 kWh_{th}/m^3 with decanoic acid as solvent, and between 220 kWh_{th}/m^3 and 260 kWh_{th}/m^3 with octanoic acid. These energy consumption values translate to a GOR in the ranges of 1.3 – 1.8 and 2.4 – 2.9 respectively.

In addition to demonstrating the concept, the batch process is used to characterize the effect of parameters such as feed-solvent mixing time, brine separation time, feed to solvent ratio, and feed salinity, on the performance of the process. Higher feed salinities result in reduced product water yield per unit weight of solvent used and higher product salinities. An analysis of recovery ratios reveals that DSE can achieve greater than 70% recovery ratios for 35,000 ppm feed water in a single stage process.

A multi-stage DSE process which involves recirculation of the brine is introduced and demonstrated. In three circulation stages recovery ratios of almost 85% with 35,000 ppm feed and of 82% with 100,000 ppm feed are achieved. It is also observed that higher recoveries necessitate higher energy consumption but this ability may be applicable in applications such as produced water treatment where a significant economic value is placed on increasing recovery.

To bring this work closer to practical application a continuous process prototype is designed and constructed. The system is shown to be effective in producing desalinated water up to 0.5 bbl. / day at a greater than 70% recovery ratio. For a starting feed TDS of 35,000 ppm the product water was found to contain about 1000 ppm. The actual thermal energy consumption of the prototype was calculated to be 1251 kWh_{th}/ m^3. By incorporating heat recovery future versions of this prototype may be expected to have thermal energy consumption of about 250 kWh_{th}/ m^3 which translates to a GOR of about 2.5. The results from the continuous prototype device are shown to conform to those predicted by the batch process experiments. Finally, a detailed economic analysis is conducted which reveals that DSE can be used for produced water desalination at a cost of about $2/ bbl. with octanoic acid as directional solvent. With better solvents and improved process design this cost could potentially reduce to less than $1/ bbl. which might make DSE an economical choice even for small scale seawater desalination.

Clearly there remains much to be addressed before directional solvent extraction or related technologies can be brought to practical application. One major challenge remains the incorporation of appropriate ways to separate the product water from the solvent. Another critical shortcoming of the demonstrated prototype is the large solvent loss which must be minimized before the process can be put to practical application.

A logical next step is to scale up the continuous DSE prototype to achieve throughput capable of making an impact in the field. For produced water treatment it would be important to demonstrate operation at scale of 6 - 30 bbl./ day (1 – 5 m^3/ day). For small scale seawater desalination it may be critical to achieve effectiveness at scales of at least 10 m^3/ day. In addition, the demonstrated system is un-optimized and component and system optimization would be required for it to achieve better performance.

Combinatorial solvent searches could help identify new directional solvents and have a very significant impact on the performance and applicability of DSE. Key metrics for new directional solvents are likely to be directional solubility, salt rejection capability, product water yield, and cost. Molecular level modeling could also help further the understanding of directional solubility and potentially be used to computationally predict the performance of chemicals as directional solvents.

This work demonstrates a new type of desalination approach other than membrane and evaporative methods. DSE may be thought of as a molecular desalination process as it considers the interaction of water with salts and contaminants at the molecular bond levels and seeks to break those bonds by thermo-chemical means. It is our hope that this work will spur research activity in a new field of molecular desalination which will in turn find solutions to even greater challenges in water treatment that lie beyond the practical limits of current technology.

References

[1] *OECD Environmental Outlook to 2030*. OECD, 2008.

[2] S. Hoffmann, *Planet Water: Investing in the World's Most Valuable Resource*, 1st ed. Wiley, 2009.

[3] U. N. P. Fund, *Population and Sustainable Development: Five Years After Rio*. United Nations Pubns, 1998.

[4] International Water Management Institute (IWMI) and International Water Management Institute (IWMI), *Water for food, water for life: insights from the Comprehensive Assessment of Water Management in Agriculture [Electronic resource]*. Colombo: IWMI, 2006.

[5] Veolia Water, "Finding the Blue Path for a Sustainable Economy," Available online at http://www.veoliawaterna.com/north-america-water/ressources/documents/1/19979, IFPRI-White-Paper.pdf, [Accessed Aug 22, 2011]

[6] M. A. Shannon, P. W. Bohn, M. Elimelech, J. G. Georgiadis, B. J. Mariñas, and A. M. Mayes, "Science and technology for water purification in the coming decades," *Nature*, vol. 452, no. 7185, pp. 301–310, Mar. 2008.

[7] M. Elimelech and W. A. Phillip, "The Future of Seawater Desalination: Energy, Technology, and the Environment," *Science*, vol. 333, no. 6043, pp. 712–717, Aug. 2011.

[8] Y. Zhou and R. S. J. Tol, "Evaluating the costs of desalination and water transport," *Water Resour. Res.*, vol. 41, no. 3, p. W03003, Mar. 2005.

[9] "Review of the Desalination and Water Purification Technology Roadmap." Available online at http://www.nap.edu/openbook.php?isbn=0309091578. [Accessed: 11-Jul-2012].

[10] F. Banat and N. Jwaied, "Economic evaluation of desalination by small-scale autonomous solar-powered membrane distillation units," *Desalination*, vol. 220, no. 1–3, pp. 566–573, Mar. 2008.

[11] R. Pate, M. Hightower, C. Cameron, and W. Einfeld, "Overview of Energy-Water Interdependencies and the Emerging Energy Demands on Water Resources," Sandia National Laboratories, SAND 2007-1349C, 2007.

[12] D. Elcock, "Future U.S. Water Consumption: The Role of Energy Production1," *JAWRA Journal of the American Water Resources Association*, vol. 46, no. 3, pp. 447–460, 2010.

[13] H. J. Wiseman, "Untested Waters: The Rise of Hydraulic Fracturing in Oil and Gas Production and the Need to Revisit Regulation," *SSRN eLibrary*, Sep. 2008.

[14] E. Fjær, R. M. Holt, P. Horsrud, A. M. Raaen, and R. Risnes, "Chapter 11 Mechanics of hydraulic fracturing," in *Petroleum Related Rock Mechanics 2nd Edition*, vol. Volume 53, Elsevier, 2008, pp. 369–390.

[15] D. M. Kargbo, R. G. Wilhelm, and D. J. Campbell, "Natural Gas Plays in the Marcellus Shale: Challenges and Potential Opportunities," *Environ. Sci. Technol.*, vol. 44, no. 15, pp. 5679–5684, 2010.

[16] F. Verrastro, "The Role of Unconventional Oil and Gas: A New Paradigm for Energy," Center for Strategic & International Studies, 2012.

[17] K. Downey, "Fueling North America's Future," IHS CERA, Special Report, 2010.

[18] J. Deutch, "The Good News About Gas," *Foreign Policy*, vol. 90, no. 1, 2011.

[19] "Survey of Energy Resources: Focus on Shale Gas," World Energy Council, 2012.

[20] A. Jaffe, K. Medlock, and R. Soligo, "The Status of World Oil Reserves: Conventional and Unconventional Resources in the Future Supply Mix," Baker Institute of Public Policy at Rice University, Oct. 2011.
[21] "Countries - U.S. Energy Information Administration (EIA)." Available online at http://www.eia.gov/countries/index.cfm?view=consumption. [Accessed: 08-Aug-2012].
[22] "North Dakota Drilling and Production Statistics." Available online at https://www.dmr.nd.gov/oilgas/stats/statisticsvw.asp. [Accessed: 08-Aug-2012].
[23] "Water Management Associated with Hydraulic Fracturing," American Petroleum Institute, HF2, 2010.
[24] J. Veil and C. Clark, "Produced Water Volume Estimates and Management Practices," 2010.
[25] N. E. B. Government of Canada, "NEB - Energy Reports - Understanding Canadian Shale Gas - Energy Brief," 17-Nov-2009. Available online at http://www.neb.gc.ca/clf-nsi/rnrgynfmtn/nrgyrprt/ntrlgs/prmrndrstndngshlgs2009/prmrndrstndngshlgs2009nrgbrf-eng.html. [Accessed: 08-Aug-2012].
[26] R. F. Service, "Desalination Freshens Up," *Science*, vol. 313, no. 5790, pp. 1088–1090, Aug. 2006.
[27] U. Merten, Ed., *Desalination by Reverse Osmosis*. The MIT Press, 1967.
[28] H. K. et al Lonsdal, *REVERSE OSMOSIS FOR WATER DESALINATION*. 1965.
[29] L. F. Greenlee, D. F. Lawler, B. D. Freeman, B. Marrot, and P. Moulin, "Reverse osmosis desalination: Water sources, technology, and today's challenges," *Water Research*, vol. 43, no. 9, pp. 2317–2348, May 2009.
[30] K. P. Lee, T. C. Arnot, and D. Mattia, "A review of reverse osmosis membrane materials for desalination—Development to date and future potential," *Journal of Membrane Science*, vol. 370, no. 1–2, pp. 1–22, Mar. 2011.
[31] J. Miller, "Review of Water Resources and Desalination Technologies," Sandia National Laboratories, SAND 2003-0800, 2003.
[32] O. Buros, "The ABC's of Desalting," Topsfield, MA, 2000.
[33] A. K. Rajvanshi, "Large scale dew collection as a source of fresh water supply," *Desalination*, vol. 36, no. 3, pp. 299–306, Mar. 1981.
[34] K. E. Thomas, *Overview of village scale, renewable energy powered desalination.* National Renewable Energy Laboratory, 1997.
[35] J. Leinhard, "MIT OpenCourseWare 2.500 Desalination and Water Purification lecture 25." 2009.
[36] J. R. McCutcheon, R. L. McGinnis, and M. Elimelech, "A novel ammonia—carbon dioxide forward (direct) osmosis desalination process," *Desalination*, vol. 174, no. 1, pp. 1–11, Apr. 2005.
[37] T. Y. Cath, A. E. Childress, and M. Elimelech, "Forward osmosis: Principles, applications, and recent developments," *Journal of Membrane Science*, vol. 281, no. 1–2, pp. 70–87, Sep. 2006.
[38] J. K. Holt, H. G. Park, Y. Wang, M. Stadermann, A. B. Artyukhin, C. P. Grigoropoulos, A. Noy, and O. Bakajin, "Fast Mass Transport Through Sub-2-Nanometer Carbon Nanotubes," *Science*, vol. 312, no. 5776, pp. 1034–1037, May 2006.

[39] S. Kim, Y.-C. Wang, J. Lee, H. Jang, and J. Han, "Concentration Polarization and Nonlinear Electrokinetic Flow near a Nanofluidic Channel," *Physical Review Letters*, vol. 99, no. 4, Jul. 2007.
[40] K. S. Speigler and Y. M. El-Sayed, *A Desalination Primer*. Balaban Publishers, 1994.
[41] M. . Darwish and N. M. Al-Najem, "Energy consumption by multi-stage flash and reverse osmosis desalters," *Applied Thermal Engineering*, vol. 20, no. 5, pp. 399–416, Apr. 2000.
[42] O. A. Hamed, M. A. K. Al-Sofi, M. Imam, G. M. Mustafa, K. Ba Mardouf, and H. Al-Washmi, "Thermal performance of multi-stage flash distillation plants in Saudi Arabia," *Desalination*, vol. 128, no. 3, pp. 281–292, May 2000.
[43] T. Younos and K. E. Tulou, "Energy Needs, Consumption and Sources," *Journal of Contemporary Water Research & Education*, vol. 132, no. 1, pp. 27–38, 2005.
[44] A. Ophir and F. Lokiec, "Advanced MED process for most economical sea water desalination," *Desalination*, vol. 182, no. 1–3, pp. 187–198, Nov. 2005.
[45] M. Al-Shammiri and M. Safar, "Multi-effect distillation plants: state of the art," *Desalination*, vol. 126, no. 1–3, pp. 45–59, Nov. 1999.
[46] N. M. Wade, "Distillation plant development and cost update," *Desalination*, vol. 136, no. 1–3, pp. 3–12, May 2001.
[47] N. H. Aly and A. K. El-Figi, "Mechanical vapor compression desalination systems — A case study," *Desalination*, vol. 158, no. 1–3, pp. 143–150, Aug. 2003.
[48] G. P. Narayan, M. H. Sharqawy, E. K. Summers, J. H. Lienhard, S. M. Zubair, and M. A. Antar, "The potential of solar-driven humidification–dehumidification desalination for small-scale decentralized water production," *Renewable and Sustainable Energy Reviews*, vol. 14, no. 4, pp. 1187–1201, May 2010.
[49] G. P. Narayan, R. K. McGovern, S. M. Zubair, and J. H. Lienhard V, "High-temperature-steam-driven, varied-pressure, humidification-dehumidification system coupled with reverse osmosis for energy-efficient seawater desalination," *Energy*, vol. 37, no. 1, pp. 482–493, Jan. 2012.
[50] G. P. Narayan, "Thermal Design of Humidification Dehumidification Systems for Small-scale and Affordable Desalination," Doctoral, Massachusetts Institute of Technology, Cambridge, MA, 2012.
[51] R. R. Davidson, W. H. Smith, and D. W. Hood, "Structure and Amine-Water Solubility in Desalination by Solvent Extraction.," *J. Chem. Eng. Data*, vol. 5, no. 4, pp. 420–423, 1960.
[52] R. R. Davidson and D. W. Hood, "Thermodynamic Cycles for Recovery of Water by Solvent Extraction," *Ind. Eng. Chem. Process Des. Dev.*, vol. 3, no. 4, p. 399, 1964.
[53] C. B. Ellis and N. D. A., inc , White Plains N.Y, *Fresh water from the ocean for cities, industry, and irrigation*. Ronald Press Co., 1954.
[54] L. Lazare and L. Lazare, "Separating Water from Saline Solutions," U.S. Patent 327699604-Oct-1966.
[55] L. Lazare and L. Lazare, "Desalination of Sea Water," U.S. Patent 338691204-Jun-1968.
[56] L. Lazare, "The puraq seawater desalination process," *Desalination*, vol. 42, no. 1, pp. 11–16, Jul. 1982.
[57] L. Lazare, "The Puraq seawater desalination process — An update," *Desalination*, vol. 85, no. 3, pp. 345–360, Mar. 1992.
[58] "Lack of money to develop solvent extraction desalting plant," *Water Desalination Report*, vol. 6, no. 2, 1970.

[59] M. Hilder, "The solubility of water in edible oils and fats," *Journal of the American Oil Chemists' Society*, vol. 45, no. 10, pp. 703–707, 1968.
[60] C. Hoerr, W. Pool, and A. Ralston, "The effect of water on the solidification points of fatty acids. Solubility of water in fatty acids," *Journal of the American Oil Chemists' Society*, vol. 19, no. 7, pp. 126–128, 1942.
[61] M. He, C. Sun, and D. T. Chiu, "Concentrating Solutes and Nanoparticles within Individual Aqueous Microdroplets," *Anal. Chem.*, vol. 76, no. 5, pp. 1222–1227, 2004.
[62] A. Bajpayee, J. F. Edd, A. Chang, and M. Toner, "Concentration of Glycerol in Aqueous Microdroplets by Selective Removal of Water," *Anal. Chem.*, vol. 82, no. 4, pp. 1288–1291, 2010.
[63] S. Kress, "Droplet Formation in a Binary Water-Fatty Acid System," Masters thesis, Eidgenossische Technosche Hochschule Zurich and Massachusetts Institute of Technology, 2011.
[64] T. Luo, A. Bajpayee, and G. Chen, "Directional solvent for membrane-free water desalination—A molecular level study," *Journal of Applied Physics*, vol. 110, no. 5, pp. 054905–054905–6, Sep. 2011.
[65] T. P. Straatsma and J. A. McCammon, "Computational Alchemy," *Annual Review of Physical Chemistry*, vol. 43, no. 1, pp. 407–435, 1992.
[66] R. V. Stanton, D. S. Hartsough, and K. M. Merz, "Calculation of solvation free energies using a density functional/molecular dynamics coupled potential," *J. Phys. Chem.*, vol. 97, no. 46, pp. 11868–11870, 1993.
[67] D. R. Erickson, *Handbook of Soy Oil Processing & Utilization*. Amer Oil Chemists Society, 1980.
[68] C. L. Yaws, *The Yaws Handbook of Thermodynamic Properties for Hydrocarbons and Chemicals*. Gulf Publishing Company, 2006.
[69] R. H. Perry and D. W. Green, *Perry's Chemical Engineers' Handbook*, 7th ed. McGraw-Hill Professional, 1997.
[70] M. J. O'Neil and M. & Co, *The Merck Index: An Encyclopedia of Chemicals, Drugs, and Biologicals*. Merck, 2001.
[71] M Pesek, J. Spicka, and E. Samkova, "Comparison of fatty acid composition in milk fat of Czech Pied cattle and Holstein cattle," *Czech J. Anim. Sci*, vol. 50, no. 3, p. 122, 2005.
[72] K. Verschueren, *Handbook of Environmental Data on Organic Chemicals, 4th Edition, Two-Volume Set*, 4th ed. Wiley-Interscience, 2001.
[73] A. Bajpayee, T. Luo, A. Muto, and G. Chen, "Very low temperature membrane-free desalination by directional solvent extraction," *Energy & Environmental Science*, vol. 4, no. 5, p. 1672, 2011.
[74] A. Bajpayee, D. Kraemer, A. J. Muto, G. Chen, J. H. Lienhard, and B. B. Mikic, "Water desalination using directional solvent extraction," U.S. Patent 811900721-Feb-2012.
[75] D. R. Kester, I. W. Duedall, D. N. Connors, and R. M. Pytkowicz, "Preparation of artificial seawater," *Limnology and Oceanography*, vol. 12, no. 1, 1967.
[76] A. V. Bailey, J. A. Harris, and E. L. Skau, "Binary freezing point diagrams for a number of long-chain fatty acids in dimethyl sulfoxide," *J. Chem. Eng. Data*, vol. 13, no. 2, pp. 265–267, 1968.
[77] Maxam Analytics International Corp., "Certificate of Analysis for water from Kennetcook Brine Ponds," Halifax, NS, 07-8198, 2011.

[78] "Drinking Water Contaminants," US Environmental Protection Agency, 2011.
[79] M. W. Mahoney and W. L. Jorgensen, "A five-site model for liquid water and the reproduction of the density anomaly by rigid, nonpolarizable potential functions," *The Journal of Chemical Physics*, vol. 112, no. 20, pp. 8910–8922, May 2000.
[80] A. F. Mills, *Heat Transfer*, 2nd ed. Prentice Hall, 1998.
[81] D. W. Oxtoby, "Homogeneous nucleation: theory and experiment," *Journal of Physics: Condensed Matter*, vol. 4, no. 38, pp. 7627–7650, Sep. 1992.
[82] D. Kashchiev and G. M. van Rosmalen, "Review: Nucleation in solutions revisited," *Crystal Research and Technology*, vol. 38, no. 7–8, pp. 555–574, 2003.
[83] J. A. Fay, *Introduction to Fluid Mechanics*. The MIT Press, 1994.
[84] D. S. Viswanath, *Viscosity of Liquids: Theory, Estimation, Experiment, and Data*. Springer, 2007.
[85] B. Sauvet-Goichon, "Ashkelon desalination plant — A successful challenge," *Desalination*, vol. 203, no. 1–3, pp. 75–81, Feb. 2007.
[86] H. Zidouri, "Desalination of Morocco and presentation of design and operation of the Laayoune seawater reverse osmosis plant," *Desalination*, vol. 131, no. 1–3, pp. 137–145, Dec. 2000.
[87] B. Van der Bruggen and C. Vandecasteele, "Distillation vs. membrane filtration: overview of process evolutions in seawater desalination," *Desalination*, vol. 143, no. 3, pp. 207–218, Jun. 2002.
[88] A. D. Khawaji, I. K. Kutubkhanah, and J.-M. Wie, "Advances in seawater desalination technologies," *Desalination*, vol. 221, no. 1–3, pp. 47–69, Mar. 2008.
[89] T. Mezher, H. Fath, Z. Abbas, and A. Khaled, "Techno-economic assessment and environmental impacts of desalination technologies," *Desalination*, vol. 266, no. 1–3, pp. 263–273, Jan. 2011.
[90] B. Klewe and B. Pedersen, "The crystal structure of sodium chloride dihydrate," *Acta Crystallographica Section B Structural Crystallography and Crystal Chemistry*, vol. 30, no. 10, pp. 2363–2371, Oct. 1974.
[91] L. H. Adams and R. E. Gibson, "The melting curve od sodium chloride dihydrate: An experimental study of an incongruent melting at pressures up to twelve thousand atmospheres," *J. Am. Chem. Soc.*, vol. 52, no. 11, pp. 4252–4264, 1930.
[92] H. A. Pohl, *Dielectrophoresis: The Behavior of Neutral Matter in Nonuniform Electric Fields*. Cambridge University Press, 1978.
[93] J. Holto, G. Berg, and L. E. Lundgaard, "Electrocoalescence of drops in a water-in-oil emulsion," in *IEEE Conference on Electrical Insulation and Dielectric Phenomena, 2009. CEIDP '09*, 2009, pp. 196 –199.
[94] P. Atten, "Electrocoalescence of water droplets in an insulating liquid," *Journal of Electrostatics*, vol. 30, no. 0, pp. 259–269, May 1993.
[95] H. Aryafar and H. P. Kavehpour, "Electrocoalescence: Effects of DC Electric Fields on Coalescence of Drops at Planar Interfaces," *Langmuir*, vol. 25, no. 21, pp. 12460–12465, 2009.
[96] J. Sjoblom, *Emulsions and Emulsion Stability: Surfactant Science Series/61*. CRC Press, 2005.
[97] R. K. Shah, E. C. Subbarao, and R. A. Mashelkar, *Heat Transfer Equipment Design*. Taylor & Francis, 1988.

[98] A. Bajpayee, S. Kress, K. Kleinguetl, and G. Chen, "Continuous Water Desalination and Treatment Using Directional Solvent Extraction," .
[99] M. Fowler, "Construction of Prototype System for Directional Solvent Extraction Desalination," Massachusetts Institute of Technology, Cambridge, MA, 2012.
[100] C. J. Geankoplis, *Transport Processes and Unit Operations*, 3 Sub. Prentice Hall PTR, 1993.
[101] K. Tanaka, "Self-diffusion coefficients of water in pure water and in aqueous solutions of several electrolytes with 18O and 2H as tracers," *Journal of the Chemical Society, Faraday Transactions 1*, vol. 74, p. 1879, 1978.
[102] T. Ahlnäs and O. Söderman, "Aggregation, hydrocarbon-chain order and mobility in the system octanoic acid—sodium octanoate A 13C-NMR chemical shift, nuclear overhauser enhancement, spin—lattice relaxation and 1H-NMR self-diffusion study," *Colloids and Surfaces*, vol. 12, no. 0, pp. 125–135, 1984.
[103] "CINC V02 Operating and Maintenance Manual." .
[104] P. H. Gleick, "Water and Energy," *Annual Review of Energy and the Environment*, vol. 19, no. 1, pp. 267–299, 1994.
[105] L. J. Lefkoff and S. M. Gorelick, "Design and Cost Analysis of Rapid Aquifer Restoration Systems Using Flow Simulation and Quadratic Programming," *Ground Water*, vol. 24, no. 6, pp. 777–790, 1986.
[106] E. Frank, J. Han, I. Palou-Rivera, A. Elgowainy, and M. Wang, "Life-cycle analysis of Algal lipid fuels with the GREET model," Argonee National Laboratory, ANL/ESD/11-5, 2011.
[107] "U.S. Natural Gas Prices." [Online]. Available: http://www.eia.gov/dnav/ng/ng_pri_sum_dcu_nus_m.htm. [Accessed: 02-Aug-2012].
[108] "EIA - Electricity Data." [Online]. Available: http://www.eia.gov/electricity/monthly/epm_table_grapher.cfm?t=epmt_5_3. [Accessed: 02-Aug-2012].
[109] "Fatty Acids - Fractioned (Asia Pacific) Price Report - Chemical pricing information - ICIS Pricing." Available online at http://www.icispricing.com/il_shared/Samples/SubPage227.asp#. [Accessed: 02-Aug-2012].
[110] T. Younos, "The Economics of Desalination," *Journal of Contemporary Water Research & Education*, vol. 132, no. 1, pp. 39–45, 2005.
[111] J. B. Tonner, S. Hinge, and C. Legorreta, "Plate heat exchangers — the new trend in thermal desalination," *Desalination*, vol. 125, no. 1–3, pp. 243–249, Nov. 1999.
[112] A. U. Malik, P. C. M. Kutty, I. N. Andijani, and S. A. Al-Fozan, "Materials performance and failure evaluation in SWCC MSF plants," *Desalination*, vol. 97, no. 1–3, pp. 171–187, Aug. 1994.
[113] J. A. S. Green, B. W. Gamson, and W. F. Westerbaan, "Experience with desalination plants containing titanium heat exchange tubing," *Desalination*, vol. 22, no. 1–3, pp. 359–368, Dec. 1977.
[114] C.-M. Lee, G. . Sams, and J. . Wagner, "Power consumption measurements for ac and pulsed dc for electrostatic coalescence of water-in-oil emulsions," *Journal of Electrostatics*, vol. 53, no. 1, pp. 1–24, Jun. 2001.

[115] "China Stainless Steel Horizotal Coalescer Housings manufacturers - ECOFINE FILTRATION PRODUCTS CO., LTD." Available online at http://nb-filter.en.hisupplier.com/product-690278-Stainless-Steel-Horizotal-Coalescer-Housings.html. [Accessed: 03-Aug-2012].
[116] "Pump, 1 1/2 HP, 115/230V, 20/10 Amp - Chemical-Resistant Pumps - Centrifugal Pumps - 4JMV9 : Grainger Industrial Supply." Available online at http://www.grainger.com/Grainger/DAYTON-Centrifugal-Pump-4JMV9. [Accessed: 03-Aug-2012].
[117] M. Peters, K. Timmerhaus, R. West, and M. Peters, *Plant Design and Economics for Chemical Engineers*, 5th ed. McGraw-Hill Science/Engineering/Math, 2002.
[118] D. E. Whitney, *Mechanical Assemblies: Their Design, Manufacture, and Role in Product Development*. Oxford University Press, USA, 2004.